Regulation of proto-oncogenic Pim-1 kinase and miR-17-92 microRNA cluster in the human leukemia cell line K562

Dissertation
zur
Erlangung des Doktorgrades
der Naturwissenschaften
(Dr. rer. nat.)

dem

Fachbereich
der Philipps-Universität Marburg
vorgelegt von
Robert Prinz
aus Marburg

Marburg/Lahn 2009

Vom Fachbereich Pharmazie
der Philipps-Universität Marburg als Dissertation am 16.12.2009

angenommen.

Erstgutachter Prof. Dr. Roland K. Hartmann

Zweitgutachter Prof. Dr. Achim Aigner

Tag der mündlichen Prüfung am 27. Januar 2010

Regulation of proto-oncogenic Pim-1 kinase and miR-17-92 microRNA cluster in the human leukemia cell line K562

Summary

In this thesis the regulation of the oncogenic kinase Pim-1 and the microRNA cluster miR-17-92 has been investigated using the leukemia cell line K562 as a model system. Pim-1 and miR-17-92 have been reported to be highly expressed in the context of leukemia cells as well as in other cancer cell lines, albeit little is known about mechanisms leading to their overexpression. The aim of the work presented here was to evaluate the functions of Pim-1 in the promotion of tumorigenesis and to clarify its regulation, with the goal of exploring its potential for therapeutic interference. Several targets of the miR-17-92 encoded miRs have been identified in different cellular contexts, and probably more will be found in the future. Nevertheless, many open questions concerning the regulation of the cluster still remain unanswered. For those reasons, we focussed our efforts on transcriptional regulation of the cluster in K562 cells, as well as on the cluster's impact on one of its targets, the cell cycle regulator p21.

High expression levels of the Pim-1 kinase are characteristic for K562 cells. At the protein level, degradation of Pim-1 is promoted by the phosphatase PP2A. Inhibition of PP2A thus increases Pim-1 levels. Within the context of this work, it was shown by our group that inhibition of PP2A by ocadaic acid (OA) leads to a temporary increase of Pim-1 followed by a complete downregulation. This was accompanied by an upregulation of p21 which under normal growth conditions is not found at the protein level in this cell line. The cellular phenotype during OA-treatment changed from proliferation to apoptosis and siRNA-targeting of p21 delayed the onset of this apoptotic response, indicating that downregulation of p21 in K562 cells contributes to their anti-apoptotic and proliferative phenotype.

Interestingly, p21 protein is not found at normal growth in K562 cells, although substantial amounts of its mRNA can be detected. This implicates a posttranscriptional silencing mechanism. Here we found that p21 is a target of miR-17-5p and miR-20a, both miRs being encoded in the miR-17-92 cluster. We could prove this in two ways. First, we cloned the p21 3'-UTR into a reporter vector. Mutation of the two predicted miR-binding sites in the respective constructs revealed regulation by those miRs as inferred from an increase of reporter activity. Second, we interfered with microRNA target-binding by application of antisense molecules directed against mature miR-17-5p and miR-20a. For this, we used locked nucleic acids (LNAs), as those modified oligonucleotides bind with largely increased affinity to their complementary strands. Current AntimiR approaches

mostly rely on the use of 2´-O-Methyl-RNA molecules for targeting of mature miRs, as this modification stabilizes the molecules against nucleases compared to unmodified RNA. AntimiRs are designed to be complementary over the whole length of the targeted miR (22-24 nt). Here it was established in a proof of principle experiment that LNAs of only 14 nucleotides could efficiently abolish miR-function in vivo. For this, luciferase reporter constructs containing a let-7a binding site were generated. In K562 cells let-7a is abundantly expressed, so constructs were silenced when transfected, but not so in co-transfection experiments with respective LNAs targeting let-7a. LNA-AntimiRs, 8, 10, 12 or 14 nucleotides in length, were tested, and even the 8-mer showed some let-7a-specific derepression effect. With this tool at hand, we targeted miR-17-5p and miR-20a to evaluate the effects on cellular p21 protein levels. In Western blot analysis we found an induction of p21 protein upon transfection with LNA 14-mers against miR-17-5p and miR-20a. By this experimental approach, we were able to demonstrate the importance of translational downregulation of the p21 protein in K562 cells that in combination with Pim-1 overexpression is supposed to contribute to the observed proliferative phenotype.

In the same study, siRNA-targeting of Pim-1 revealed the dependency of K562 cells on this kinase to maintain proliferation. Pim-1 is thus an appealing target for therapeutic intervention. We asked if in addition to transcriptional regulation also posttranscriptional, i.e. translational regulation, may contribute to the high levels of Pim-1 protein in K562 cells. The browser tool TargetScanHuman (http://www.targetscan.org/) predicts several miR-binding sites in the Pim-1 3´-UTR. Among those with high confidence value was miR-33. A profiling of miRs revealed that in K562 cells miR-33 is expressed at low levels compared to miR-17-5p or miR-20a, and other miRs such as miR-16-1 or miR-214. This suggested that cellular miR-33 downregulation may contribute to the observed Pim-1 expression. To pinpoint this issue, construction of luciferase reporter vectors with Pim-1 3´-UTRs and mutated miR-33 binding sites was performed in order to determine the role of miR-33 target-interaction on Pim-1 levels. Those experiments confirmed the prediction that Pim-1 is targeted by miR-33 as mutated constructs showed increased reporter expression. The application of miR-33 Mimics (artificially synthesized double-stranded RNA molecules recapitulating mature miRNA structures) reduced respective reporter levels. Furthermore, it was shown by our group that miR-33 Mimic transfection also efficiently downregulates Pim-1 at the protein level. Additionally, miR-33 Mimics

reduced proliferation of K562 cells. Finally, LNA-AnitimiRs against miR-33 slightly increased reporter expression, suggesting that basal miR-33a levels in K562 cells are responsible for minor repression effects. Overall, we could clearly identify Pim-1 as the first experimentally validated target of miR-33.

Now that we had evaluated p21 as a target of the miR-17-92 cluster, we wanted to shed some light on the cluster regulation itself. The screening of several cancer cell lines confirmed the high expression of the cluster in K562 cells, as well as in lung cancer cell lines. We speculated on the coincidence of high miR-17-92 expression and Pim-1 expression. The miR-17-92 cluster is transcribed as part of a large locus on chromosome 13 (open reading frame 25), but also an internal promoter immediately in front of the cluster start site is predicted by an online promoter-browser (http://www.flybase.org). Furthermore a polyadenylation site at the end of the cluster was recently published, implicating that the cluster could be transcribed or regulated independently of the entire locus. We thus cloned segments 5´ the internal start site including the predicted promoter into a luciferase reporter vector to test the promoter activity of those segments. The tested segments were indeed shown to have promoter activity, and we were able to demonstrate that mutation of two non-consensus TATA-boxes located in the predicted promoter reduces activity of the respective construct. Furthermore, under Pim-1 knockdown conditions, expression of reporter constructs containing the internal promoter segments increased. Likewise, qRT-PCR experiments demonstrated increased miR-17-92 cluster expression under Pim-1 knockdown conditions. It is known that, among other targets, Pim-1 phosphorylates Heterochromatin Protein 1γ (HP1γ) thus modulating its effects on chromatin modification. Possibly, this is a mechanism how Pim-1 can regulate miR-17-92 expression. To evaluate this, our group conducted chromatin immunoprecipitation (CHIP) experiments that show decreased binding of HP1γ to the miR-17-92 cluster region under Pim-1 knockdown. Under normal growth conditions, Pim-1 itself is also associated with the cluster region, except for the subregion harbouring the inernal promoter. At this time point, the exact mechanism of Pim-1 dependent miR-17-92 regulation remains elusive, but it is surprising that silencing of Pim-1 even increases cluster expression.

Contents

Contents

1 Introduction

1.1 RNAi

RNA interference is a regulatory interaction between several classes of RNA molecules mediated by protein components. In general, short dsRNAs (21-24 nts) are generated from longer precursor molecules by the action of the enzyme Dicer (Du and Zamore 2005). Those so-called short interfering RNAs (siRNAs) are transferred to a protein complex named RISC. In this complex one of the two RNA strands is removed and degraded while the remaining strand is able to pair with a complementary sequence on a messenger RNA. This interaction facilitates degradation of the targeted mRNA. So-called microRNAs (miRNAs) are undistinguishable from siRNAs in their mature form but the way they are generated differs. In most cases, miRNAs can exhibit several effects, e.g. degradation or storage of targeted mRNAs, or translational repression due to interference with 5´ cap recognition (Mathonnet, Fabian et al. 2007). Also, transcriptional activation has been shown very recently (Place, Li et al. 2008). MiRNAs bind specifically to complementary sites in 3´-UTRs of mRNAs and thus modulate translation. Several miRNAs can be encoded in the same genomic region, a situation in which one speaks of a miRNA cluster. A prominent miRNA cluster is the miR-17-92 cluster encoding 7 miRNAs (see below).
RNAi has been regarded as an ancient defense mechanism against viral RNAs. Nowadays widespread regulation of transcriptome via RNAi is recognized as an intricate and extensive layer of cellular regulation. In animals, endogenously expressed microRNAs (miRNAs) are transcribed from introns (40%), exons (30%), or from intergenic regions (30%) by RNA polymerase II (Rodriguez, Griffiths-Jones et al. 2004). Those primary-miRNAs (pri-miRNAs) can be in the size of up to several hundred nucleotides and are capped at the 5´end as well as poly-adenylated at their 3´end in most cases. After this step, they enter a so-called microprocessor complex where they are processed to pre-miRNAs of 60-70 nucleotides containing a 5´phosphate and a 3´overhang of two nucleotides. Pre-miRNAs are exported from the nucleus to cytoplasm via exportin-5. The enzyme Dicer then cleaves the pre-miRNA to generate a mature miRNA that is transferred to the RNA-induced silencing complex (RISC). Within the complex the antisense strand can target and pair with respective mRNAs (Kutter and Svoboda 2008) (see figure 1.1). The most essential region for pairing with the target site is from nucleotides 2-8 of the miRNA´s

5´end (Doench and Sharp 2004; Brennecke, Stark et al. 2005). Further determinants of target specificity are base-pairing between bases 13-16 of the miRNA and the target region, so that a bulge can form (nucleotides 9-11) between two paired regions. Proximity to other microRNA target sites and a high AU-content near the target site also contribute to efficient targeting. A minimal distance (15nt) to the stop codon is required, and it could be shown that 5´ and 3´ ends of the 3´-UTR are more apt for efficient miRNA-target recognition (Grimson, Farh et al. 2007). Several other criteria such as sequence conservation of target sites in 3´-UTRs are used by different miRNA target prediction tools (e.g. TargetScan)(Yoon and De Micheli 2006; Maragkakis, Reczko et al. 2009). In general, integration of both, experimental and computational methods will lead to more accurate target prediction (Chaudhuri and Chatterjee 2007; Oulas, Boutla et al. 2009). The binding of proteins to uridine rich regions near miRNA target sites can also influence its accessibility. This shown was shown for the RNA-binding protein Dnd1that binds to an uridine rich sequence and thus blocks translational repression by the microRNA-RISC complex (Kedde, Strasser et al. 2007).

Many cellular processes are now known to be regulated by miRNAs and their functions can be found especially in development and cell cycle regulation, as well as in apoptosis or metabolic processes (Lee, Risom et al. 2006; Carleton, Cleary et al. 2007; Aumiller and Forstemann 2008; Wang and Blelloch 2009).

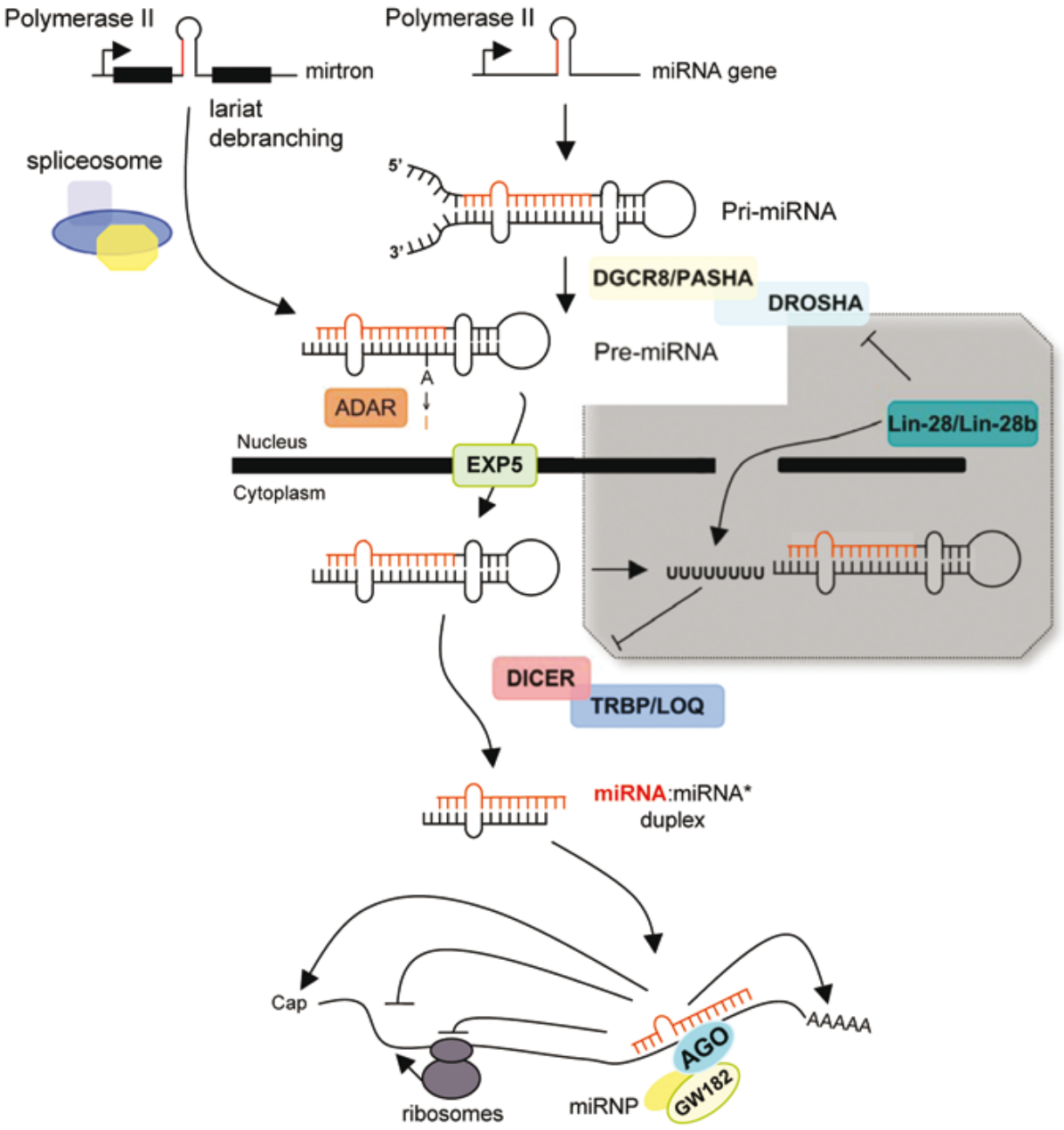

Figure 1.1 miRNA pathways in animals. Taken from reference" Kutter and Svoboda 2008". For details see text and reference.

1.2 miRNAs in cancer

In cancer cells several layers of regulation and signaling may be involved in malignant transformation. Since discovery of miRNAs, many studies have shown the role of miRNAs in cell cycle regulation and apoptosis (Cimmino, Calin et al. 2005; Linsley, Schelter et al. 2007) as well as in transformation and expression of metastatic phenotypes (Asangani, Rasheed et al. 2008; Valastyan, Reinhardt et al. 2009). One of the most prominent proto-oncogenes, c-Myc, was shown to be regulated by the let-7a microRNA

(Sampson, Rong et al. 2007). With respect to therapeutic approaches, transcriptomics of small RNAs may shift emphasis from small molecule inhibitors to small RNA inhibitors. Good known examples are miR-15 and miR-16 that were shown to induce apoptosis by targeting the mRNA of the anti-apoptotic protein BCL2 (B cell lymphoma 2) (Cimmino, Calin et al. 2005). Calin et al have evaluated the role of miR-15a and miR-16 as tumor-suppressor genes using in vivo models in mice (Calin, Cimmino et al. 2008). The same authors have shown the down-regulation of miR-15 and miR-16 in B cell chronic lymphocytic leukemia (B-CCL) samples from patients (Calin, Dumitru et al. 2002). In around 70 % of the samples the respective gene locus (13q14.3) was deleted or down-regulated. Linsley et al. (2007) show rather intricate regulation of a whole network of cell cycle regulators that are targeted by the miR-16 family and support the current view of expression fine tuning by miRNAs as proposed by Bartel and Chen (Bartel and Chen 2004). In this respect, the categorization of miRNAs into classical proto-oncogenes and tumor-suppressors may not be appropriate in many cases. Different or in some cases contradicting results may also arise from usage of different cell lines in those studies. At the same time, distinct expression patterns of miRNAs allow classification of cancer cell identities (Lu, Getz et al. 2005; Lee, Gusev et al. 2007; Gibcus, Tan et al. 2009). For example, miR-143 and miR-145 are downregulated in several B-cell malignancies (e.g. in chronic lymphocytic leukemia, CLL) (Akao, Nakagawa et al. 2007) and colon cancer (Cummins, He et al. 2006), as is miR-155 in some subtypes of Burkitt Lymphoma (Kluiver, Haralambieva et al. 2006). On the other hand, miR-155 is upregulated in distinct cases of pediatric Burkitt Lymphoma (Metzler, Wilda et al. 2004) obviating the difficulties in assigning phenotypes to the expression status of single microRNAs. To date emphasis is put on miRNA targets and their interaction with miRNAs, but for a better understanding of interactions between cellular regulatory layers (e.g. proteomics, transcriptomics, miROmics, metabolomics) and thus cell fate, the activation or transcriptional regulation of miRNAs itself needs detailed evaluation.

1.3 miR-17-92 cluster

MicroRNAs regulate a lot of cellular functions during normal cell cycle as well as in development and disease. It is thus interesting to find a cluster containing seven miRNAs (miR-17-3p/5p, miR18a, miR-20a, miR-19a, miR19b-1, and miR-92a-1) that seem to be

co-expressed and are involved in many cancer pathologies. Ota et al (Ota, Tagawa et al. 2004) showed that the miR-17-92 polycistron located on chromosome 13 ORF 25 is amplified in B cell lymphomas. He et al (He, Thomson et al. 2005) further investigated the role of this cluster and found that it accelerates tumor growth in cooperation with c-Myc in a mouse B cell lymphoma model. Interaction of the cluster with c-Myc was shown to modulate the expression of the transcription factor E2F1 (O'Donnell, Wentzel et al. 2005). The authors could show binding of c-Myc at the cluster locus via chromatin immunoprecipitation assays (CHIPs). Venturini et al. (Venturini, Battmer et al. 2007) confirmed the connection between c-Myc and the cluster. They showed that over-expression of the cluster compensates for reduced c-Myc levels. Tagawa et al (Tagawa, Karube et al. 2007) further strengthened this observation by parallel over-expression of c-Myc and the cluster which resulted in more aggressive phenotypes displaying the synergistic relationship of those players. E2F1 itself is regulated by c-Myc and at the same time targeted by miR-17-5p and miR-20a. There appears to be complex auto-regulation between the E2F transcription factor family members (E2F1, E2F2, E2F3) and the miR-17-92 cluster. Sylvestre et al (Sylvestre, De Guire et al. 2007) proved association of those transcription factors with the promoter region of the cluster, as well as their regulation via miR-20a binding sites in the respective 3´-UTRs of their mRNAs.

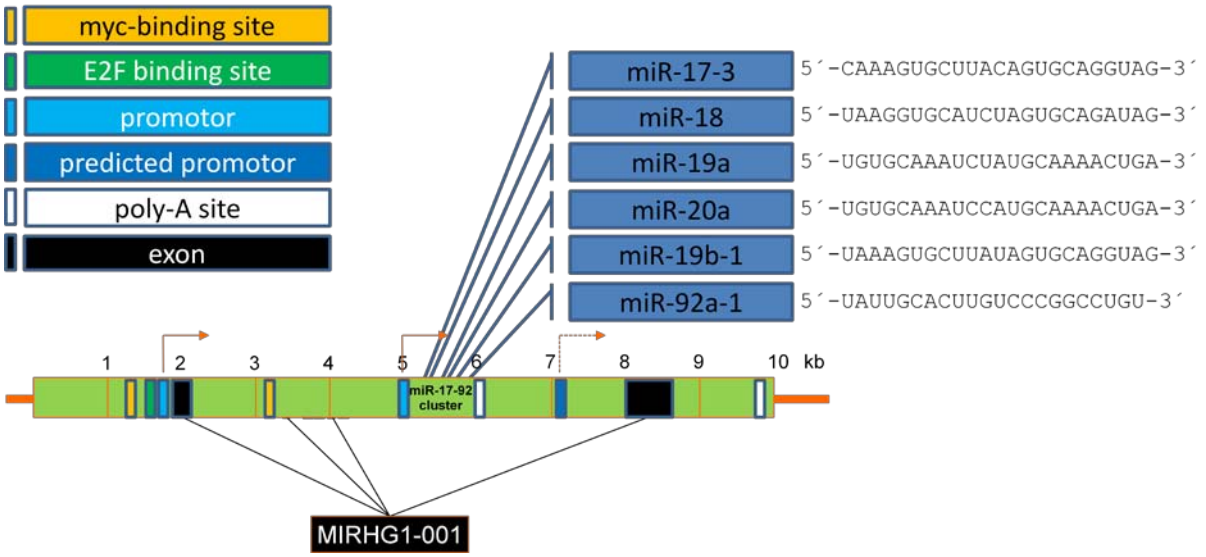

Figure 1.2 Organization of ORF 25 located on chromosome 13. The miR-17-92 cluster can be found ~3.5 kb downstream of the locus promoter (first arrow). In front of this promoter, a c-Myc binding site and a binding site for E2F3 are located. Four exons constitute a transcript called MIRHG1 (microRNA host gene 1), the function of which is

unknown. Between the locus promoter and the predicted promoter (second arrow) 4 c-Myc binding sites can be found. The cluster itself lies in the middle of the locus and is flanked by a polyadenylation site at its 3´ end. Further downstream another promoter element is predicted by NNPP v2.2 software (see text) followed by exon 4 of MIRHG1 and the polyadenylation sequence of the locus.

Very recently, p53 was found to negatively regulate cluster expression by binding next to the c-Myc site at the locus promoter and thus preventing c-Myc dependent activation of the cluster under hypoxic conditions (Yan, Xue et al. 2009).

miR-17-92 is involved in many cancer types and has been shown to be over-expressed in lung cancers (Hayashita, Osada et al. 2005). The same group could show that inhibition of miR17-5p and miR-20a by antisense oligonucleotides leads to apoptosis in the respective lung cancer cells (Matsubara, Takeuchi et al. 2007). In accordance with its pathologic role, Lu et al (Lu, Thomson et al. 2007) showed the cluster´s expression during normal lung development in mice where it is naturally expressed in early stages and declines in later stages. An over-expression in transgenic mice leads to elevated proliferation of lung epithelial cells and inhibition of differentiation. Carraro et al (Carraro, El-Hashash et al. 2009) showed the role of the cluster in branching and budding morphogenesis during lung development due to direct targeting of Mapk14 and Stat3 mRNAs. Foshay and Gallicano confirmed the regulation of Stat3 by miR-17 family members and elaborated their role for embryonic stem cell differentiation (Foshay and Gallicano 2007).

Further cancer types that have been shown to involve miR-17-92 cluster (dys)regulation are breast cancer (Hossain, Kuo et al. 2006; Yu, Wang et al. 2008), colon cancer (Diosdado, van de Wiel et al. 2009), and gastric cancer (Petrocca, Visone et al. 2008).

There are several other known targets of miR-17-92 members. Shan et al (Shan, Lee et al. 2009) showed targeting of fibronectin and fibronectin type-III domain containing 3A (FNDC3A) by miR-17, and targeting of thrombospondin-1 (Tsp1) and connective tissue growth factor (CTGF) was shown by Dews et al (Dews, Homayouni et al. 2006) who evaluated the miR cluster's role in tumor angiogenesis. Retinoblastoma protein 2 (Rb2) and p130 (another member of the same protein family) were shown to be targets of the cluster and implicate a role in adipocyte differentiation (Wang, Li et al. 2008). Regulation of cell cycle by miR-17 and miR-106b family members was shown by several groups. Cloonan et al (Cloonan, Brown et al. 2008) showed cell cycle-dependent expression of miR-17-92 in HeLa cells and increased proliferation of HEK293T cells after transfection

with plasmids overexpressing miR-17-5p. HEK293T cells show low endogenous expression of the cluster. Mitogen activated kinase 9 (MAPK9, aka JNK2) was one out of several targets the study confirmed. A more detailed study by Pickering et al (Pickering, Stadler et al. 2009) showed a role of the cluster in exact timing and integration of signaling events regulating the G1 checkpoint. Direct regulation of cell cycle regulator p21 (aka CDKN1A) was shown by Ivanovska et al (Ivanovska, Ball et al. 2008), Fontana et al (Fontana, Fiori et al. 2008), and could be confirmed by the author of this thesis in the cell line K562 (see manuscript 1).

A number of studies on miR-17-92 revealed its role in malignant lymphomas. Recently it could be shown that the tumor suppressor PTEN and the pro-apoptotic protein Bim are direct targets of miR-17-92 (Xiao, Srinivasan et al. 2008). TP53INP1and FOXP1, amongst others, were shown to be affected in different B-cell lymphoma subtypes (Inomata, Tagawa et al. 2009). AML1 (Acute myeloid leukaemia-1, aka Runx1) controls differentiation of leukemia cells and was also shown to be regulated via miR-17-5p, miR-20a and miR-106b (Fontana, Pelosi et al. 2007). A single study showed down-regulation of miR-17-5p in CLL (chronic lymphocytic leukemia) patients with TP53 abnormalities (Mraz, Malinova et al. 2009). Concerning the work presented here, we were interested in the relation of Pim-1 kinases (see below) that are over-expressed in several leukemia cell lines and the miR-17-92 cluster.

1.4 RNAi with modified oligonucleotides and mirMimics

RNA interference as a means of down-regulation of specific target mRNAs has been extensively used in recent years. Synthetic siRNAs and vector-based siRNA expression systems are available for efficient targeting approaches. A relatively new method for specific and efficient down-regulation is usage of so-called miRNA mimics (McLaughlin, Cheng et al. 2007; Xiao, Yang et al. 2007). These are synthetic microRNAs in their 22-24 nt dsRNA form, that are available commercially with (unspecified) modifications that are supposed by the manufacturers to confer increased metabolic stability on these molecules. In one of the studies mentioned above, miRNA mimics were encoded in triple combinations from a lentiviral vector and were used for targeting the Bcr-Abl oncoprotein. In the context of the work presented here, miRNA mimics were synthesized as single RNA strands and annealed in our lab. Compared to siRNAs, the annealed

miRNA duplexes are not fully base-paired, but rather contain the irregularities (bulges) of their natural counterparts. They were used here to mimic miR-33 expression in K562 cells for evaluating the miRNA´s role in targeting Pim-1 (see below).

RNA interference with miR mimics itself is an appealing approach to abrogate dysregulated miRNA function in cancer and other diseases associated with over-expression of microRNAs. In addition, so-called antagomirs were introduced by Krützfeld et al (Krutzfeldt, Rajewsky et al. 2005) who coupled cholesterol to ssRNA analogues (2´-OMe-modified) complentary to miRNAs. Those antagomirs were efficient in silencing miR-122 in in vivo models. Antagomirs are 100 percent complementary to the targeted miRNA and are supposed to act through permanent target-binding. Efficiency of this approach has also been proved by Cheng et al (Cheng, Byrom et al. 2005) in evaluating miRNAs involved in cell growth and apoptosis.

To further improve binding capacities and silencing efficiency, several oligonucleotide modifications have been introduced into anitimiRs. Most promising results have been shown for locked nucleic acids (LNAs). In those molecules a methylene bridge connects the 2´-oxygen of ribose with the 4´-carbon (see fig 1.2 for a comparison of different oligo modifications (taken from Ref. (Braasch and Corey 2001)). LNA-modified oligos are very stable against cleavage by endo- and exonucleases (Grünweller and Hartmann 2007). On the other hand it has been shown that so-called LNA gapmers (containing an unmodified DNA stretch in the middle) can recruit RNases. LNA gapmers cause cleavage of target molecules due to a recruitment of RNase H (Kurreck, Wyszko et al. 2002) in vitro, and it may be possible that other RNases are recruited in human cells.

LNA-antimiRs have already been used successfully in primate gene delivery approaches (Elmen, Lindow et al. 2008). It could be shown that miR-122 function was silenced, restoring normal aldolase A expression and respective cholesterol levels in African green monkeys without any associated toxicity. Yet another study claimed profound hepatotoxicity for LNAs, and the effects were shown to be independent of targets (Swayze, Siwkowski et al. 2007). Irrespective of those contradicting in vivo outcomes, LNAs offer a valuable tool for in vitro RNA interference and were used in this work for inhibition of miRNA function.

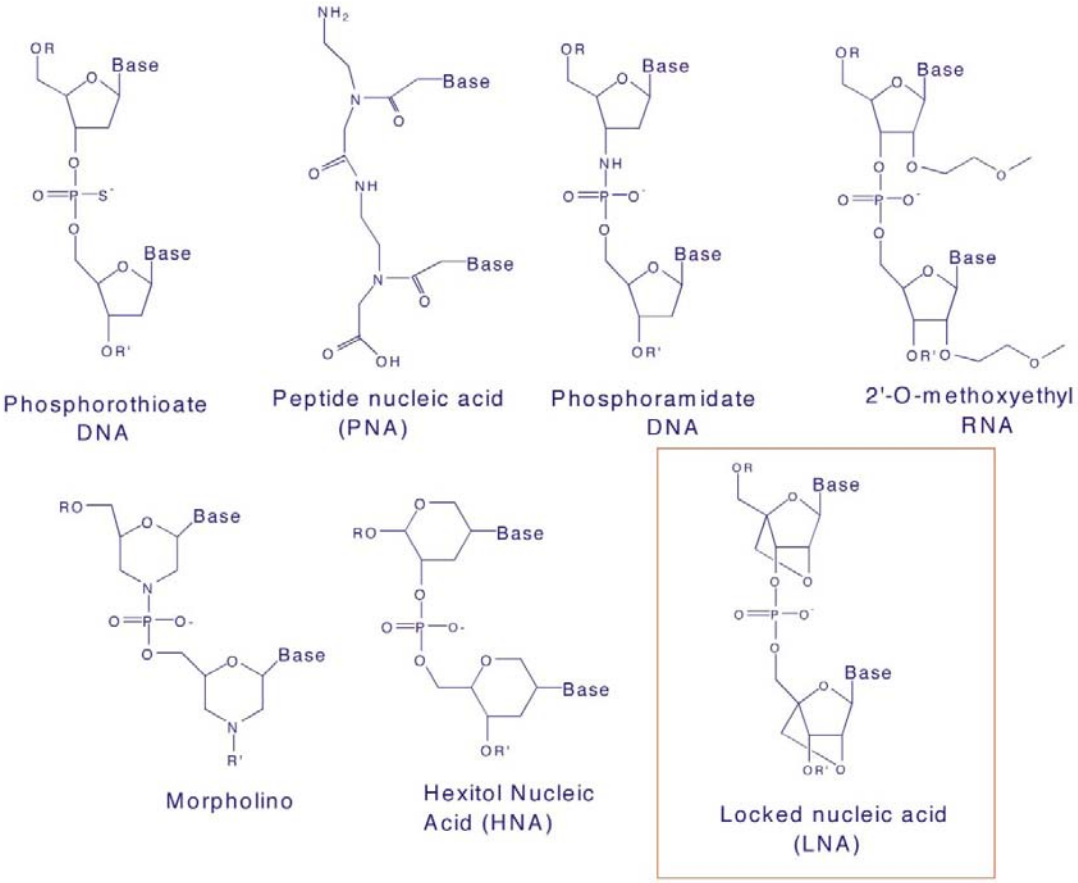

Figure 1.3 Different oligonucleotide modifications are shown that can be used in RNA interference applications. For this study, LNA modifications are relevant. Taken from Braasch and Corey, 2001.

1.5 Detection of microRNA expression

MicroRNAs can be detected by several means. On the one hand, high throughput methods such as micro-arrays or 454 sequencing are available (Hafner, Landgraf et al. 2008; Wark, Lee et al. 2008). Those methods are rather expensive and data analysis calls for respective resources and tools, albeit new tools that integrate databases were published very recently (Hackenberg, Sturm et al. 2009). On the other hand, classical methods such as Northern blot analysis are used to detect single microRNAs (e.g. in (Hayashita, Osada et al. 2005)) where no large scale profiling is necessary. Improvements to Northern blots were provided by introducing LNA (locked nucleic acid) modifications to probes (Valoczi, Hornyik et al. 2004; Varallyay, Burgyan et al. 2007). Northern blots require high amounts of starting material, so PCR-based methods may be more suitable. Chen et al. (Chen, Ridzon et al. 2005) introduced a technique that relies on intricate primer design and reverse transcription. A universal stem-loop primer for reverse transcription is used that

base pairs with its unique (complementary) 3´end to the mature miRNA 5´end. Reverse transcriptase can then elongate the looped primer over the whole length of the mature miRNA. A real time PCR follows where one primer is the sequence of the mature microRNA and a second universal reverse primer has the sequence of the 5' end of the stem-loop primer used for reverse transcription. The aim of this approach is to increase the length of the resulting PCR amplificate for easy detection with standard real time PCR settings (e.g. SYBR Green). Otherwise, a 20-30 bp segment cannot be amplified via PCR. At the same time the assay provides a specificity step due to the fact that the stem-loop with its 3´overhang only base pairs with an end of the respective miRNA and no other RNAs (i.e. because of steric hindrance). Chen´s approach has already been multiplexed for analysis in single cells (Tang, Hajkova et al. 2006) and can also be used in combination with detection of precursor miRNAs (Schmittgen, Jiang et al. 2004; Schmittgen, Lee et al. 2008). In the presented thesis, this approach was chosen because of easy, reliable and straightforward implementation.

Several other methods have been introduced to the field, such as splinted ligation that has no amplification step and is claimed to be more sensitive than Northern blot analysis, but nevertheless is based on usage of radioactively labeled probes (Maroney, Chamnongpol et al. 2007). Padlock probe rolling circle amplification and quantitative primer extension PCRs also rely on amplification steps (Raymond, Roberts et al. 2005; Jonstrup, Koch et al. 2006). The latter method is similar to the stem-loop approach, albeit here no loop is formed, but just a shorter universal sequence is added to a complementary sequence that pairs with mature miRNA 3´ end.

1.6 Pim-1 kinase

Pim kinases (Pim – proviral integration site for moloney murine leukemia virus; Pim-1, -2, -3) belong to the family of Serine/Threonine kinases. They are categorized as classical proto-oncogenes and have been shown to be over-expressed in several tumors, especially prostate cancers and hematopoietic disease (Chen, Chan et al. 2005; Dai, Li et al. 2005; Hammerman, Fox et al. 2005; Xu, Zhang et al. 2005; Chen, Limnander et al. 2008), and appear to be involved in malignant transformation. Their anti-apoptotic action can be assigned to phosphorylation and thus functional modulation of proteins like Bad or p21,

both molecules involved in cell-cycle regulation. In summary, they stimulate cell proliferation and inhibit apoptosis.

Pim-1 is the best known family member and involved in the development of B-cell lymphomas. Synergism between Pim-1 and the transcription factor c-Myc has been shown to play a role in this respect (Zippo, De Robertis et al. 2007; Zhang, Wang et al. 2008). Pim-1 kinases are constitutively active kinases and phosphorylate e.g. Cdc25A (Mochizuki, Kitanaka et al. 1999), and Cdc25C (Bachmann, Kosan et al. 2006), p21 (Wang, Bhattacharya et al. 2002), HP1γ (Koike, Maita et al. 2000), Bad (Aho, Sandholm et al. 2004), Tudor SN (Leverson, Koskinen et al. 1998) and others (for review see Bachmann and Möröy, 2005).

Interestingly a knockout of all three Pim kinases in parallel in mice caused no substantial effects in development and fertility of those animals. A reduction in body size at birth and throughout postnatal life and an impaired response to growth factors (Mikkers, Nawijn et al. 2004) were reported. This offers potential for therapeutic interventions in vivo, as side ("off-target") effects on healthy tissues and cells are expected to be low.

Pim-1 promotes polyploidy and leads to genomic instability as shown by Roh et al. (Roh, Gary et al. 2003; Roh, Franco et al. 2008). This is reflected in a mitotic spindle checkpoint defect and somehow mediated by posttranscriptional regulation of cyclin B1, as the protein levels of this cell cycle regulator follow Pim-1 levels. Effects of this Pim-1 dependent polyploidy on the expression of cell cycle regulators or microRNAs need further investigation. It is not clear, how this effect on polyploidy influences the differentiation of those cell lines and their long term existence as a distinct line.

The pro-apoptotic protein Bad is phosphorylated by Pim-1 and Pim-2 (Yan, Zemskova et al. 2003; Aho, Sandholm et al. 2004). Pim-dependent phosphorylation of serine 112 results in cytoplasmic sequestration of Bad by its binding to the 14-3-3 protein, which suppresses apoptosis by preventing interaction of Bad with Bcl-xL and thus cytochrome c release from mitochondria (Macdonald, Campbell et al. 2006). P21, another important target of Pim-1, can arrest the cell cycle at different stages by binding to several cyclin-dependent kinases (cdk) or to the proliferating cell nuclear antigen (PCNA) to block replication (Li, Waga et al. 1994; Waga, Hannon et al. 1994; Gartel 2005; Gartel and Radhakrishnan 2005). In human lung carcinoma cells Pim-1 was reported to phosphorylate p21 at Thr145 (Zhang, Wang et al. 2007). This phosphorylated form of p21

localizes to the nucleus, where it is thought to sterically interrupt the interaction of p21 with PCNA, which then relieves the p21-mediated blockage of the DNA synthesis machinery (Rossig, Jadidi et al. 2001; Zhang, Wang et al. 2007).

Expression of Pim-1 is mainly regulated at the transcriptional level by the action of several interleukins and growth factors that activate STAT3 and/or STAT5 via Janus kinases (Heinrich, Behrmann et al. 2003; Bachmann and Moroy 2005). In addition, the transcription factor Kruppel-like factor 5, which can be expressed after induction of DNA damage, represses Pim-1 expression in the p53-deficient cell line HCT116 by binding to the Pim-1 promoter, thus favoring apoptosis (Zhao, Hamza et al. 2008). In B cells CD40 signaling regulates the expression of Pim-1 kinase via the NF-kappaB pathway (Zhu, Ramirez et al. 2002).

Pim-1 protein stability is controlled by the heat shock proteins Hsp90 and Hsp70 as well as the phosphatase PP2A (Losman, Chen et al. 2003; Shay, Wang et al. 2005; Ma, Arnold et al. 2007). Hsp90 increases the half-life of Pim-1 by protecting it from proteasomal degradation, whereas Hsp70 can mediate Pim-1 degradation (Shay, Wang et al. 2005). The prolyl-isomerase Pin1 is thought to mediate binding of phosphorylated Pim-1 to the regulatory subunit B56-beta of PP2A, leading to dephosphorylation by the catalytic subunit of PP2A followed by ubiquitinylation and degradation of Pim-1 via the proteasome (Ma, Arnold et al. 2007). Pin1 is thus redundant with Hsp70´s function in reducing Pim-1 half-life.

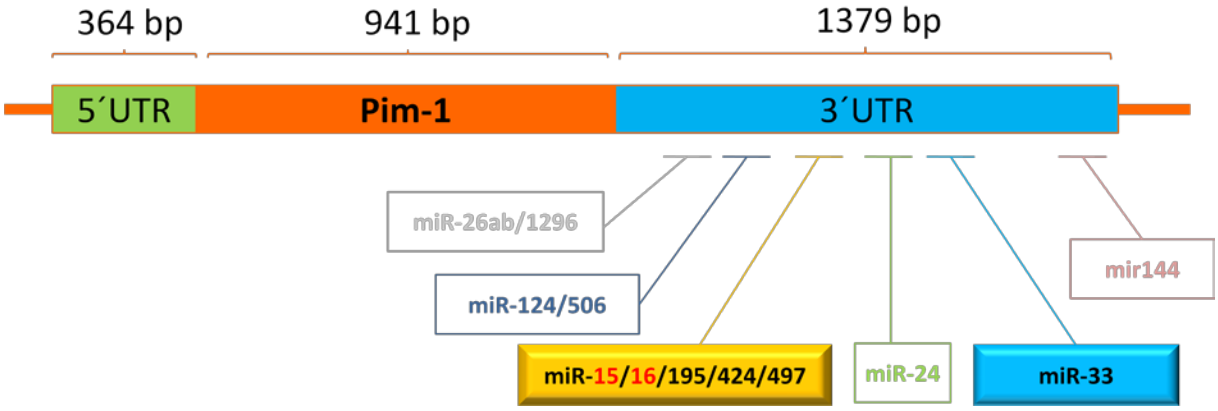

Figure 1.4 Pim-1 mRNA. MicroRNA binding sites as predicted by TargetScanHuman 5.1 are shown. Those binding sites relevant to the thesis presented are highlighted.

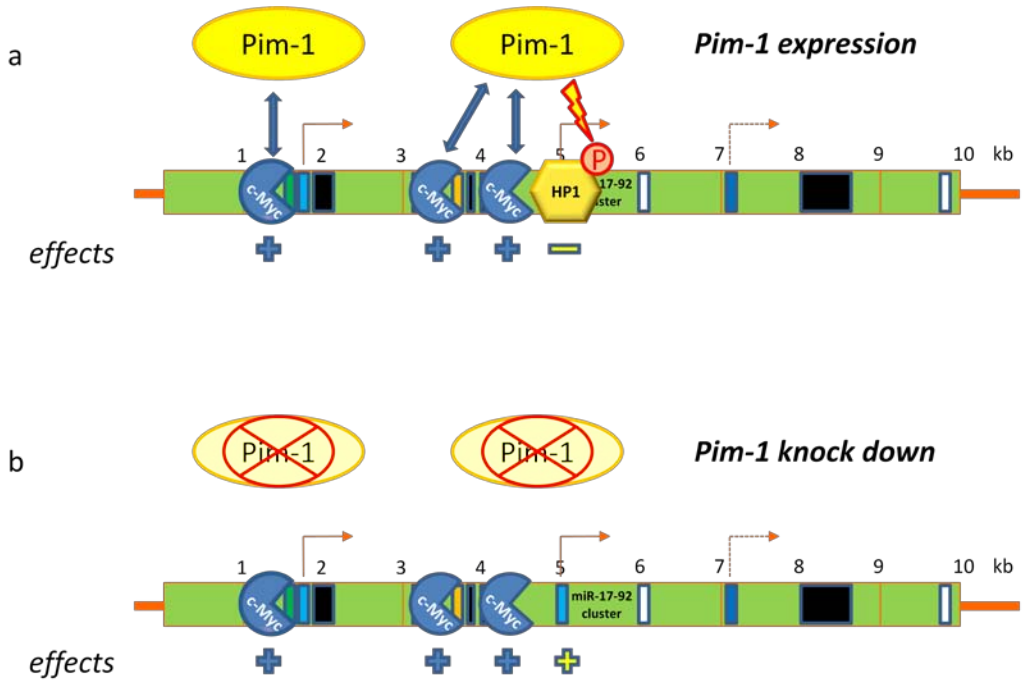

Figure 1.5 Pim-1 kinase interacts with c-Myc at several loci in the genome, which may be relevant also at the miR-17-92 locus (see text). Interactions with HP1γ may cause chromatin rearrangements effecting expression at the locus Chr13Orf25. Pim-1 knockdown (b) could exert effects through altering the phosphorylation state of HP1γ and resulting downstream regulatory events.

1.7 Projects

This work aimed at evaluating the relationship between Pim-1 expression and miR-17-92 cluster expression in K562 cells, as well as putative effects of the cluster. Also, the regulation of Pim-1 itself (by miRNAs) was investigated. For this, several questions had to be answered. First, is there a direct link between cluster expression and Pim-1 protein level? What are the effects of the microRNAs from the cluster? Can a targeting of mature microRNAs of the cluster revert the proliferative phenotype of K562 cells? As Pim-1 plays a prominent role in different cancers and especially in leukemias (see introduction), what microRNAs may be involved in down regulation of Pim-1, and thus are probably not expressed in Pim-1 over-expressing cells?

Different cancer cell lines were profiled for miR-17-92 and Pim-1 expression as well as for a few other miRNAs (e.g. miR-15/16/33/124/144) that seemed to be interesting candidates regarding Pim-1 regulation. To evaluate regulation of Pim-1 by microRNAs, its 3´-UTR was cloned and miR-15/16 and miR-33 binding sites were mutated. A pGL3control vector was used with the 3´-UTR fused to the end of a luciferase gene.

Regulation was evaluated by applying miR-33 mimics and monitoring luciferase expression of the reporter constructs (fig 1.6).

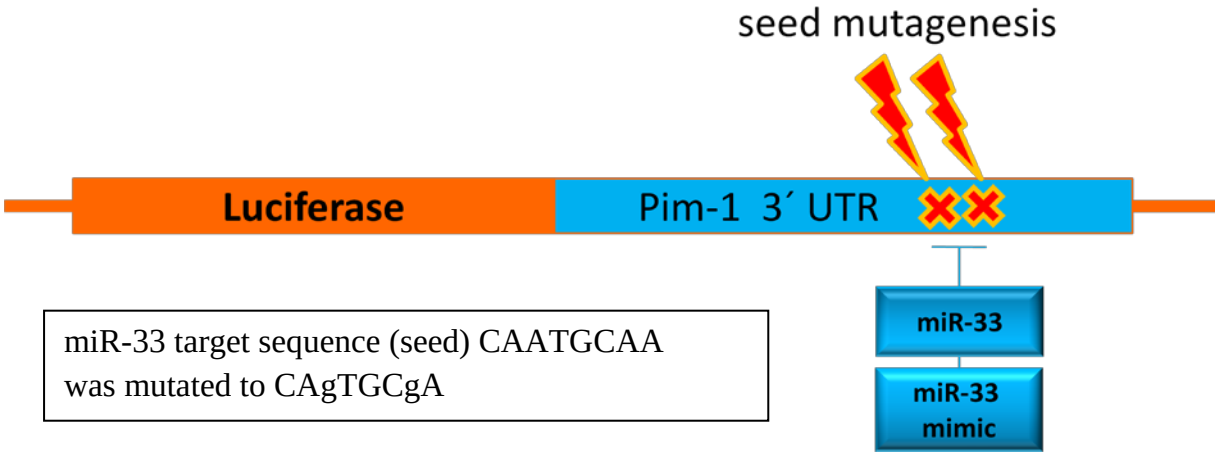

Figure 1.6 Expression vector "pGL3 control" with cloned Pim-1 3´-UTR. Mutation of miRNA target sites is a standard procedure for evaluation of miRNA-binding. Interference of either cellular miR-33 or transfected miR-33 mimics are depicted.

Furthermore, the targeting of mature microRNAs by LNA-antimiRs was evaluated in this work. For this reason, several sizes of LNA antisense oligonucleotides were tested against miR-let-7 using a pGL3control luciferase vector system containing a fully complimentary let-7 target site downstream of the luciferase gene. The p21 3´-UTR was then used as a further test system accompanied by direct detection of cellular p21 protein level after antimiR-17 targeting using Western blot analysis.

It is interesting that the miR-17-92 cluster is flanked by a predicted promoter and a polyadenylation site at its 3´ end. This could mean that the cluster is expressed as an independent transcription unit, compared to transcription from the main locus (chromosome 13, open reading frame 25), so to speak there may be circumstances, e.g. stress, under which such kind of regulation would be important. Expression of the miR-17-92 locus was analyzed after Pim-1 knockdown (via standard siRNAs) using qRT-PCR analysis. To address the question if Pim-1 alters expression differently at regions within the locus, i.e. at the predicted promoter, several sites for quantification were chosen (figure 1.7). To further evaluate the role this internal promoter region immediately in front of the cluster, segments of different size out of this region were cloned into a reporter

vector upstream of a luciferase gene. Putative TATA-boxes were mutated in order to infer effects from altered promoter activity (figure 1.8).

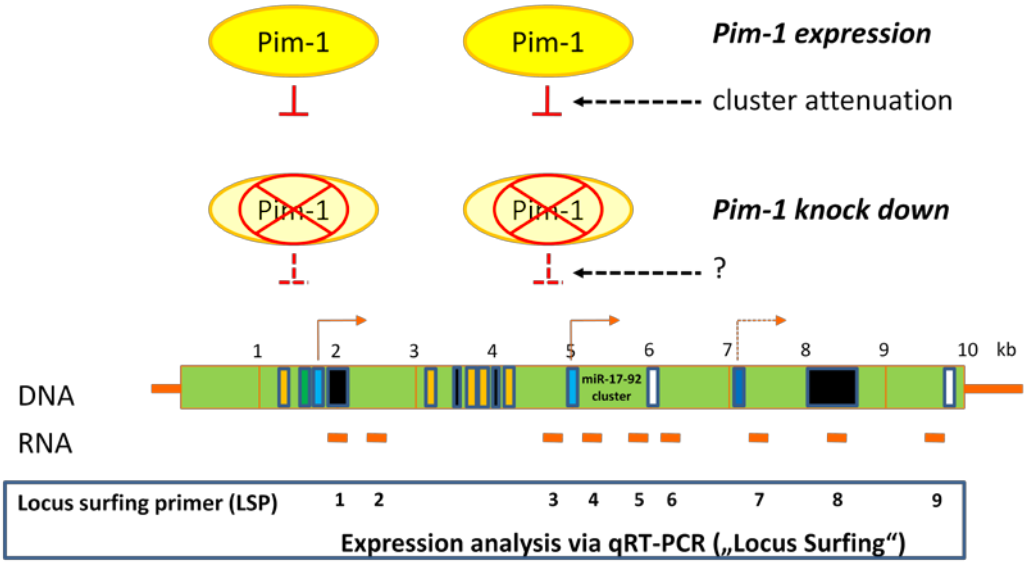

Figure 1.7 Regions within the miR-17-92 cluster locus are shown that should be addressed and quantified with qRT-PCR experiments under Pim-1 knockdown conditions.

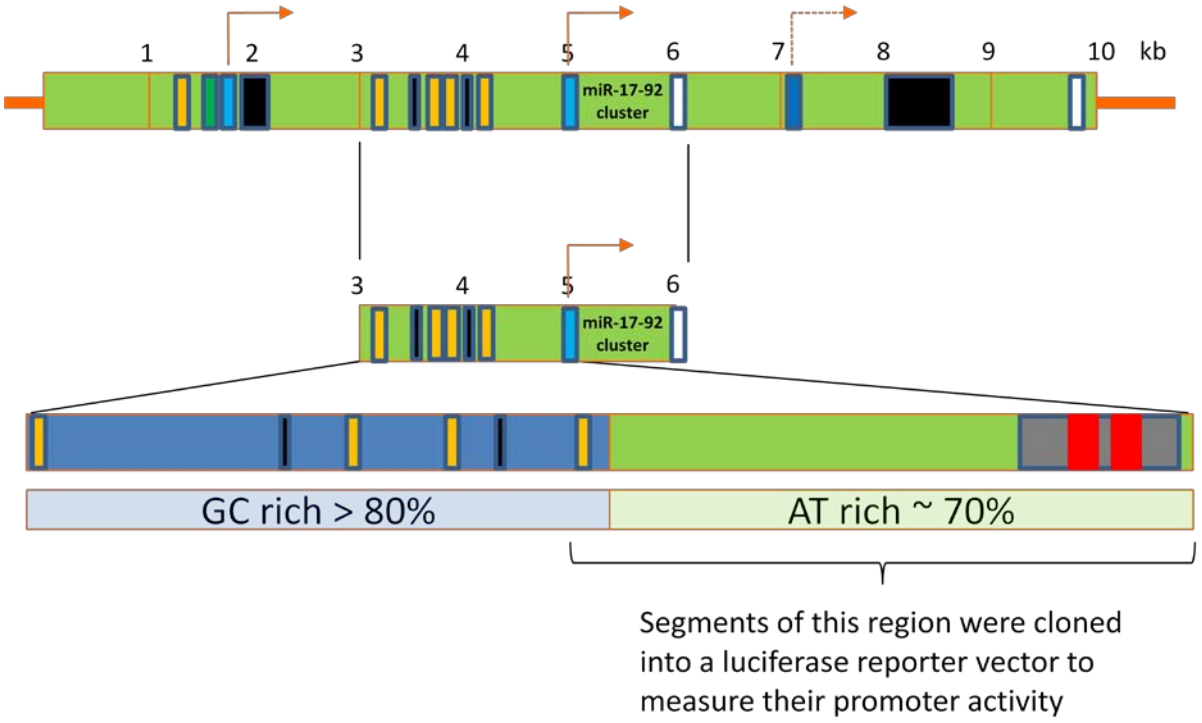

Figure 1.8 Internal promoter region of the miR-17-92 cluster. The magnified region can be divided into two parts. The first part is a GC-rich region (>80%) that ends 1.4 kb 5´ to

the miR-17-92 cluster. Within this region four c-Myc binding sites and exons 2 and 3 of MIRHG1 are located. The GC-rich region is followed by an AT-rich region (~70%) that contains the predicted promoter with two non-consensus TATA-boxes (red boxes). They were mutated and the respective construct was analyzed in luciferase promoter assays.

1.8 References

Aho, T. L., J. Sandholm, et al. (2004). "Pim-1 kinase promotes inactivation of the pro-apoptotic Bad protein by phosphorylating it on the Ser112 gatekeeper site." FEBS Lett **571**(1-3): 43-9.

Akao, Y., Y. Nakagawa, et al. (2007). "Downregulation of microRNAs-143 and -145 in B-cell malignancies." Cancer Sci **98**(12): 1914-20.

Asangani, I. A., S. A. Rasheed, et al. (2008). "MicroRNA-21 (miR-21) post-transcriptionally downregulates tumor suppressor Pdcd4 and stimulates invasion, intravasation and metastasis in colorectal cancer." Oncogene **27**(15): 2128-36.

Aumiller, V. and K. Forstemann (2008). "Roles of microRNAs beyond development--metabolism and neural plasticity." Biochim Biophys Acta **1779**(11): 692-6.

Bachmann, M., C. Kosan, et al. (2006). "The oncogenic serine/threonine kinase Pim-1 directly phosphorylates and activates the G2/M specific phosphatase Cdc25C." Int J Biochem Cell Biol **38**(3): 430-43.

Bachmann, M. and T. Moroy (2005). "The serine/threonine kinase Pim-1." Int J Biochem Cell Biol **37**(4): 726-30.

Bartel, D. P. and C. Z. Chen (2004). "Micromanagers of gene expression: the potentially widespread influence of metazoan microRNAs." Nat Rev Genet **5**(5): 396-400.

Braasch, D. A. and D. R. Corey (2001). "Locked nucleic acid (LNA): fine-tuning the recognition of DNA and RNA." Chem Biol **8**(1): 1-7.

Brennecke, J., A. Stark, et al. (2005). "Principles of microRNA-target recognition." PLoS Biol **3**(3): e85.

Calin, G. A., A. Cimmino, et al. (2008). "MiR-15a and miR-16-1 cluster functions in human leukemia." Proc Natl Acad Sci U S A **105**(13): 5166-71.

Calin, G. A., C. D. Dumitru, et al. (2002). "Frequent deletions and down-regulation of micro- RNA genes miR15 and miR16 at 13q14 in chronic lymphocytic leukemia." Proc Natl Acad Sci U S A **99**(24): 15524-9.

Carleton, M., M. A. Cleary, et al. (2007). "MicroRNAs and cell cycle regulation." Cell Cycle **6**(17): 2127-32.

Carraro, G., A. El-Hashash, et al. (2009). "miR-17 family of microRNAs controls FGF10-mediated embryonic lung epithelial branching morphogenesis through MAPK14 and STAT3 regulation of E-Cadherin distribution." Dev Biol **333**(2): 238-50.

Chaudhuri, K. and R. Chatterjee (2007). "MicroRNA detection and target prediction: integration of computational and experimental approaches." DNA Cell Biol **26**(5): 321-37.

Chen, C., D. A. Ridzon, et al. (2005). "Real-time quantification of microRNAs by stem-loop RT-PCR." Nucleic Acids Res **33**(20): e179.

Chen, J. L., A. Limnander, et al. (2008). "Pim-1 and Pim-2 kinases are required for efficient pre-B-cell transformation by v-Abl oncogene." Blood **111**(3): 1677-85.

Chen, W. W., D. C. Chan, et al. (2005). "Pim family kinases enhance tumor growth of prostate cancer cells." Mol Cancer Res **3**(8): 443-51.

Cheng, A. M., M. W. Byrom, et al. (2005). "Antisense inhibition of human miRNAs and indications for an involvement of miRNA in cell growth and apoptosis." Nucleic Acids Res **33**(4): 1290-7.

Cimmino, A., G. A. Calin, et al. (2005). "miR-15 and miR-16 induce apoptosis by targeting BCL2." Proc Natl Acad Sci U S A **102**(39): 13944-9.

Cloonan, N., M. K. Brown, et al. (2008). "The miR-17-5p microRNA is a key regulator of the G1/S phase cell cycle transition." Genome Biol **9**(8): R127.

Cummins, J. M., Y. He, et al. (2006). "The colorectal microRNAome." Proc Natl Acad Sci U S A **103**(10): 3687-92.

Dai, H., R. Li, et al. (2005). "Pim-2 upregulation: biological implications associated with disease progression and perinueral invasion in prostate cancer." Prostate **65**(3): 276-86.

Dews, M., A. Homayouni, et al. (2006). "Augmentation of tumor angiogenesis by a Myc-activated microRNA cluster." Nat Genet **38**(9): 1060-5.

Diosdado, B., M. A. van de Wiel, et al. (2009). "MiR-17-92 cluster is associated with 13q gain and c-myc expression during colorectal adenoma to adenocarcinoma progression." Br J Cancer **101**(4): 707-14.

Doench, J. G. and P. A. Sharp (2004). "Specificity of microRNA target selection in translational repression." Genes Dev **18**(5): 504-11.

Du, T. and P. D. Zamore (2005). "microPrimer: the biogenesis and function of microRNA." Development **132**(21): 4645-52.

Elmen, J., M. Lindow, et al. (2008). "LNA-mediated microRNA silencing in non-human primates." Nature **452**(7189): 896-9.

Fontana, L., M. E. Fiori, et al. (2008). "Antagomir-17-5p abolishes the growth of therapy-resistant neuroblastoma through p21 and BIM." PLoS One **3**(5): e2236.

Fontana, L., E. Pelosi, et al. (2007). "MicroRNAs 17-5p-20a-106a control monocytopoiesis through AML1 targeting and M-CSF receptor upregulation." Nat Cell Biol **9**(7): 775-87.

Foshay, K. M. and G. I. Gallicano (2007). "Small RNAs, big potential: the role of MicroRNAs in stem cell function." Curr Stem Cell Res Ther **2**(4): 264-71.

Gartel, A. L. (2005). "The conflicting roles of the cdk inhibitor p21(CIP1/WAF1) in apoptosis." Leuk Res **29**(11): 1237-8.

Gartel, A. L. and S. K. Radhakrishnan (2005). "Lost in transcription: p21 repression, mechanisms, and consequences." Cancer Res **65**(10): 3980-5.

Gibcus, J. H., L. P. Tan, et al. (2009). "Hodgkin lymphoma cell lines are characterized by a specific miRNA expression profile." Neoplasia **11**(2): 167-76.

Grimson, A., K. K. Farh, et al. (2007). "MicroRNA targeting specificity in mammals: determinants beyond seed pairing." Mol Cell **27**(1): 91-105.

Grünweller, A. and R. K. Hartmann (2007). "Locked nucleic acid oligonucleotides: the next generation of antisense agents?" BioDrugs **21**(4): 235-43.

Hackenberg, M., M. Sturm, et al. (2009). "miRanalyzer: a microRNA detection and analysis tool for next-generation sequencing experiments." Nucleic Acids Res **37**(Web Server issue): W68-76.

Hafner, M., P. Landgraf, et al. (2008). "Identification of microRNAs and other small regulatory RNAs using cDNA library sequencing." Methods **44**(1): 3-12.

Hammerman, P. S., C. J. Fox, et al. (2005). "Pim and Akt oncogenes are independent regulators of hematopoietic cell growth and survival." Blood **105**(11): 4477-83.

Hayashita, Y., H. Osada, et al. (2005). "A polycistronic microRNA cluster, miR-17-92, is overexpressed in human lung cancers and enhances cell proliferation." Cancer Res **65**(21): 9628-32.

He, L., J. M. Thomson, et al. (2005). "A microRNA polycistron as a potential human oncogene." Nature **435**(7043): 828-33.

Heinrich, P. C., I. Behrmann, et al. (2003). "Principles of interleukin (IL)-6-type cytokine signalling and its regulation." Biochem J **374**(Pt 1): 1-20.

Hossain, A., M. T. Kuo, et al. (2006). "Mir-17-5p regulates breast cancer cell proliferation by inhibiting translation of AIB1 mRNA." Mol Cell Biol **26**(21): 8191-201.

Inomata, M., H. Tagawa, et al. (2009). "MicroRNA-17-92 down-regulates expression of distinct targets in different B-cell lymphoma subtypes." Blood **113**(2): 396-402.

Ivanovska, I., A. S. Ball, et al. (2008). "MicroRNAs in the miR-106b family regulate p21/CDKN1A and promote cell cycle progression." Mol Cell Biol **28**(7): 2167-74.

Jonstrup, S. P., J. Koch, et al. (2006). "A microRNA detection system based on padlock probes and rolling circle amplification." RNA **12**(9): 1747-52.

Kedde, M., M. J. Strasser, et al. (2007). "RNA-binding protein Dnd1 inhibits microRNA access to target mRNA." Cell **131**(7): 1273-86.

Kluiver, J., E. Haralambieva, et al. (2006). "Lack of BIC and microRNA miR-155 expression in primary cases of Burkitt lymphoma." Genes Chromosomes Cancer **45**(2): 147-53.

Koike, N., H. Maita, et al. (2000). "Identification of heterochromatin protein 1 (HP1) as a phosphorylation target by Pim-1 kinase and the effect of phosphorylation on the transcriptional repression function of HP1(1)." FEBS Lett **467**(1): 17-21.

Krutzfeldt, J., N. Rajewsky, et al. (2005). "Silencing of microRNAs in vivo with 'antagomirs'." Nature **438**(7068): 685-9.

Kurreck, J., E. Wyszko, et al. (2002). "Design of antisense oligonucleotides stabilized by locked nucleic acids." Nucleic Acids Res **30**(9): 1911-8.

Kutter, C. and P. Svoboda (2008). "miRNA, siRNA, piRNA: Knowns of the unknown." RNA Biol **5**(4): 181-8.

Lee, C. T., T. Risom, et al. (2006). "MicroRNAs in mammalian development." Birth Defects Res C Embryo Today **78**(2): 129-39.

Lee, E. J., Y. Gusev, et al. (2007). "Expression profiling identifies microRNA signature in pancreatic cancer." Int J Cancer **120**(5): 1046-54.

Leverson, J. D., P. J. Koskinen, et al. (1998). "Pim-1 kinase and p100 cooperate to enhance c-Myb activity." Mol Cell **2**(4): 417-25.

Li, R., S. Waga, et al. (1994). "Differential effects by the p21 CDK inhibitor on PCNA-dependent DNA replication and repair." Nature **371**(6497): 534-7.

Linsley, P. S., J. Schelter, et al. (2007). "Transcripts targeted by the microRNA-16 family cooperatively regulate cell cycle progression." Mol Cell Biol **27**(6): 2240-52.

Losman, J. A., X. P. Chen, et al. (2003). "Protein phosphatase 2A regulates the stability of Pim protein kinases." J Biol Chem **278**(7): 4800-5.

Lu, J., G. Getz, et al. (2005). "MicroRNA expression profiles classify human cancers." Nature **435**(7043): 834-8.

Lu, Y., J. M. Thomson, et al. (2007). "Transgenic over-expression of the microRNA miR-17-92 cluster promotes proliferation and inhibits differentiation of lung epithelial progenitor cells." Dev Biol **310**(2): 442-53.

Ma, J., H. K. Arnold, et al. (2007). "Negative regulation of Pim-1 protein kinase levels by the B56beta subunit of PP2A." Oncogene **26**(35): 5145-53.

Macdonald, A., D. G. Campbell, et al. (2006). "Pim kinases phosphorylate multiple sites on Bad and promote 14-3-3 binding and dissociation from Bcl-XL." BMC Cell Biol **7**: 1.

Maragkakis, M., M. Reczko, et al. (2009). "DIANA-microT web server: elucidating microRNA functions through target prediction." Nucleic Acids Res **37**(Web Server issue): W273-6.

Maroney, P. A., S. Chamnongpol, et al. (2007). "A rapid, quantitative assay for direct detection of microRNAs and other small RNAs using splinted ligation." RNA **13**(6): 930-6.

Mathonnet, G., M. R. Fabian, et al. (2007). "MicroRNA inhibition of translation initiation in vitro by targeting the cap-binding complex eIF4F." Science **317**(5845): 1764-7.

Matsubara, H., T. Takeuchi, et al. (2007). "Apoptosis induction by antisense oligonucleotides against miR-17-5p and miR-20a in lung cancers overexpressing miR-17-92." Oncogene **26**(41): 6099-105.

McLaughlin, J., D. Cheng, et al. (2007). "Sustained suppression of Bcr-Abl-driven lymphoid leukemia by microRNA mimics." Proc Natl Acad Sci U S A **104**(51): 20501-6.

Metzler, M., M. Wilda, et al. (2004). "High expression of precursor microRNA-155/BIC RNA in children with Burkitt lymphoma." Genes Chromosomes Cancer **39**(2): 167-9.

Mikkers, H., M. Nawijn, et al. (2004). "Mice deficient for all PIM kinases display reduced body size and impaired responses to hematopoietic growth factors." Mol Cell Biol **24**(13): 6104-15.

Mochizuki, T., C. Kitanaka, et al. (1999). "Physical and functional interactions between Pim-1 kinase and Cdc25A phosphatase. Implications for the Pim-1-mediated activation of the c-Myc signaling pathway." J Biol Chem **274**(26): 18659-66.

Mraz, M., K. Malinova, et al. (2009). "miR-34a, miR-29c and miR-17-5p are downregulated in CLL patients with TP53 abnormalities." Leukemia **23**(6): 1159-63.

O'Donnell, K. A., E. A. Wentzel, et al. (2005). "c-Myc-regulated microRNAs modulate E2F1 expression." Nature **435**(7043): 839-43.

Ota, A., H. Tagawa, et al. (2004). "Identification and characterization of a novel gene, C13orf25, as a target for 13q31-q32 amplification in malignant lymphoma." Cancer Res **64**(9): 3087-95.

Oulas, A., A. Boutla, et al. (2009). "Prediction of novel microRNA genes in cancer-associated genomic regions--a combined computational and experimental approach." Nucleic Acids Res **37**(10): 3276-87.

Petrocca, F., R. Visone, et al. (2008). "E2F1-regulated microRNAs impair TGFbeta-dependent cell-cycle arrest and apoptosis in gastric cancer." Cancer Cell **13**(3): 272-86.

Pickering, M. T., B. M. Stadler, et al. (2009). "miR-17 and miR-20a temper an E2F1-induced G1 checkpoint to regulate cell cycle progression." Oncogene **28**(1): 140-5.

Place, R. F., L. C. Li, et al. (2008). "MicroRNA-373 induces expression of genes with complementary promoter sequences." Proc Natl Acad Sci U S A **105**(5): 1608-13.

Raymond, C. K., B. S. Roberts, et al. (2005). "Simple, quantitative primer-extension PCR assay for direct monitoring of microRNAs and short-interfering RNAs." RNA **11**(11): 1737-44.

Rodriguez, A., S. Griffiths-Jones, et al. (2004). "Identification of mammalian microRNA host genes and transcription units." Genome Res **14**(10A): 1902-10.

Roh, M., O. E. Franco, et al. (2008). "A role for polyploidy in the tumorigenicity of Pim-1-expressing human prostate and mammary epithelial cells." PLoS One **3**(7): e2572.

Roh, M., B. Gary, et al. (2003). "Overexpression of the oncogenic kinase Pim-1 leads to genomic instability." Cancer Res **63**(23): 8079-84.

Rossig, L., A. S. Jadidi, et al. (2001). "Akt-dependent phosphorylation of p21(Cip1) regulates PCNA binding and proliferation of endothelial cells." Mol Cell Biol **21**(16): 5644-57.

Sampson, V. B., N. H. Rong, et al. (2007). "MicroRNA let-7a down-regulates MYC and reverts MYC-induced growth in Burkitt lymphoma cells." Cancer Res **67**(20): 9762-70.

Schmittgen, T. D., J. Jiang, et al. (2004). "A high-throughput method to monitor the expression of microRNA precursors." Nucleic Acids Res **32**(4): e43.

Schmittgen, T. D., E. J. Lee, et al. (2008). "Real-time PCR quantification of precursor and mature microRNA." Methods **44**(1): 31-8.

Shan, S. W., D. Y. Lee, et al. (2009). "MicroRNA MiR-17 retards tissue growth and represses fibronectin expression." Nat Cell Biol **11**(8): 1031-8.

Shay, K. P., Z. Wang, et al. (2005). "Pim-1 kinase stability is regulated by heat shock proteins and the ubiquitin-proteasome pathway." Mol Cancer Res **3**(3): 170-81.

Swayze, E. E., A. M. Siwkowski, et al. (2007). "Antisense oligonucleotides containing locked nucleic acid improve potency but cause significant hepatotoxicity in animals." Nucleic Acids Res **35**(2): 687-700.

Sylvestre, Y., V. De Guire, et al. (2007). "An E2F/miR-20a autoregulatory feedback loop." J Biol Chem **282**(4): 2135-43.

Tagawa, H., K. Karube, et al. (2007). "Synergistic action of the microRNA-17 polycistron and Myc in aggressive cancer development." Cancer Sci **98**(9): 1482-90.

Tang, F., P. Hajkova, et al. (2006). "MicroRNA expression profiling of single whole embryonic stem cells." Nucleic Acids Res **34**(2): e9.

Valastyan, S., F. Reinhardt, et al. (2009). "A pleiotropically acting microRNA, miR-31, inhibits breast cancer metastasis." Cell **137**(6): 1032-46.

Valoczi, A., C. Hornyik, et al. (2004). "Sensitive and specific detection of microRNAs by northern blot analysis using LNA-modified oligonucleotide probes." Nucleic Acids Res **32**(22): e175.

Varallyay, E., J. Burgyan, et al. (2007). "Detection of microRNAs by Northern blot analyses using LNA probes." Methods **43**(2): 140-5.

Venturini, L., K. Battmer, et al. (2007). "Expression of the miR-17-92 polycistron in chronic myeloid leukemia (CML) CD34+ cells." Blood **109**(10): 4399-405.

Waga, S., G. J. Hannon, et al. (1994). "The p21 inhibitor of cyclin-dependent kinases controls DNA replication by interaction with PCNA." Nature **369**(6481): 574-8.

Wang, Q., Y. C. Li, et al. (2008). "miR-17-92 cluster accelerates adipocyte differentiation by negatively regulating tumor-suppressor Rb2/p130." Proc Natl Acad Sci U S A **105**(8): 2889-94.

Wang, Y. and R. Blelloch (2009). "Cell cycle regulation by MicroRNAs in embryonic stem cells." Cancer Res **69**(10): 4093-6.

Wang, Z., N. Bhattacharya, et al. (2002). "Phosphorylation of the cell cycle inhibitor p21Cip1/WAF1 by Pim-1 kinase." Biochim Biophys Acta **1593**(1): 45-55.

Wark, A. W., H. J. Lee, et al. (2008). "Multiplexed detection methods for profiling microRNA expression in biological samples." Angew Chem Int Ed Engl **47**(4): 644-52.

Xiao, C., L. Srinivasan, et al. (2008). "Lymphoproliferative disease and autoimmunity in mice with increased miR-17-92 expression in lymphocytes." Nat Immunol **9**(4): 405-14.

Xiao, J., B. Yang, et al. (2007). "Novel approaches for gene-specific interference via manipulating actions of microRNAs: examination on the pacemaker channel genes HCN2 and HCN4." J Cell Physiol **212**(2): 285-92.

Xu, Y., T. Zhang, et al. (2005). "Overexpression of PIM-1 is a potential biomarker in prostate carcinoma." J Surg Oncol **92**(4): 326-30.

Yan, B., M. Zemskova, et al. (2003). "The PIM-2 kinase phosphorylates BAD on serine 112 and reverses BAD-induced cell death." J Biol Chem **278**(46): 45358-67.

Yan, H. L., G. Xue, et al. (2009). "Repression of the miR-17-92 cluster by p53 has an important function in hypoxia-induced apoptosis." EMBO J **28**(18): 2719-32.

Yoon, S. and G. De Micheli (2006). "Computational identification of microRNAs and their targets." Birth Defects Res C Embryo Today **78**(2): 118-28.

Yu, Z., C. Wang, et al. (2008). "A cyclin D1/microRNA 17/20 regulatory feedback loop in control of breast cancer cell proliferation." J Cell Biol **182**(3): 509-17.

Zhang, Y., Z. Wang, et al. (2008). "Pim kinase-dependent inhibition of c-Myc degradation." Oncogene **27**(35): 4809-19.

Zhang, Y., Z. Wang, et al. (2007). "Pim-1 kinase-dependent phosphorylation of p21Cip1/WAF1 regulates its stability and cellular localization in H1299 cells." Mol Cancer Res **5**(9): 909-22.

Zhao, Y., M. S. Hamza, et al. (2008). "Kruppel-like factor 5 modulates p53-independent apoptosis through Pim1 survival kinase in cancer cells." Oncogene **27**(1): 1-8.

Zhu, N., L. M. Ramirez, et al. (2002). "CD40 signaling in B cells regulates the expression of the Pim-1 kinase via the NF-kappa B pathway." J Immunol **168**(2): 744-54.

Zippo, A., A. De Robertis, et al. (2007). "PIM1-dependent phosphorylation of histone H3 at serine 10 is required for MYC-dependent transcriptional activation and oncogenic transformation." Nat Cell Biol **9**(8): 932-44.

2 Methods

All methods, constructs and sequences are outlined in the manuscripts of this thesis. Here just some additional information is provided.

2.1 Bacterial cell culture and transformation

E. coli cells were cultured at 37°C in LB medium at 220 rpm in a lab shaker. LB medium was prepared as follows:

LB medium	
Yeast extract	5 g/l
Pepton	10 g/l
NaCl	10 g/l
Agar agar	15 g/l (only for plates)

After preparation, media were autoclaved at 121°C and 1 bar for 20 min in an autoclave and stored at room temperature. Handling of bacteria was performed sterile by working near the flame of a Bunsen Burner. *E. coli* DH5α were used for plasmid maintenance. *E. coli* cells were selected according to the respective resistance gene/plasmid with a concentration of 100µg/ml of the respective antibiotic. Agar plates were poured into 7.5 cm dishes after the Agar was cooked at 100°C and cooled down to ca. 60°C when antibiotics were added. Plates were stored for max. 4 weeks at 4°C. Stocks of bacteria were built from overnight cultures. 500 µl bacteria were mixed with 500 µl autoclaved glycerol and put into liquid nitrogen. After this procedure, stocks were stored at -80°C.

2.2 Preparation of chemically competent *E. coli* DH5α cells

Preparation was done with the help of my co-worker Dan Li and application of her protocol for this, which is taken from her PhD thesis and outlined below.

"To prepare chemically competent *E. coli* DH5α cells, the calcium chloride method was used. This chemical treatment requires no special equipment and gives 10^5-10^6 transformants per microgram DNA. As the strain DH5α is devoid of any antibiotic resistance, cells were handled with particular care during this procedure to avoid contamination.

DH5α cells were first spread from a glycerol stock stored at -80°C onto an LB agar plate and incubated at 37°C for around 16 h. A single freshly developed colony was inoculated into 3ml of LB medium and was grown at 37°C overnight or for at least 6 h in a shaking incubator. Afterwards, 2.5 ml of the culture were transferred into 500 ml of fresh LB medium and further grown until the OD578 reached 0.5-0.6, which took about 4 h. Cells were transferred into two centrifuge bottles and, after cooling on ice for 10 min, harvested at 4,000 rpm (Eppendorf 5810R centrifuge) for 15 min at 4°C. Each cell pellet was suspended in 50 ml of ice-cold 100 mM CaCl2 solution and transferred into two 50 ml tubes kept on ice. Cells were pelleted once more at 7,000 rpm (Eppendorf 5810R) for 10 min at 4°C. Each cell pellet was suspended in 7 ml of ice-cold CaCl2 solution (75 mM, 25% (v/v) glycerol). Finally, aliquots were prepared in vials placed on ice, frozen in liquid nitrogen and stored at -80°C. The frozen competent cells could be stored for up to 1 year without substantial loss of transformation efficiency."

2.3 Transformation of chemically competent *E. coli*

Bacteria were taken from -80°C thawn on ice. 50 µl of bacteria were transferred into 1,5 ml tube and 5 µl of ligation reaction, or plasmid dilution (e.g. 1:1000) were added to the bacteria. The mixture was incubated 30 min on ice followed by 45 seconds at 42 °C. Cells were then incubated for 2 min on ice. After this 300 µl LB-medium (without antibiotics) was added and incubate for 60 min at 37°C at 200 rpm in an Eppendorf thermomixer. Cells were centrifuged and 250 µl of LB medium was discarded. The remaining volume was used for resuspending the cells and plating. After plating incubation was done over night at 37 °C in a standard incubator.

2.4 Cloning

2.4.1 Cloning of 3´UTRs and putative miR-17-92 promoter regions

3´UTRs and miR-17-92 promoter regions were cloned from genomic DNA of K562 cells. Preparation of gDNA was done with Qiagen´s DNeasy Blood & Tissue Kit according to manufacturer´s protocol. Amplification procedure was as follows:

PCR reaction	
gDNA	300 ng
10x Taq buffer with KCl	5 µl
dNTP mix (each 2.5 mM)	1 µl
Primer 1 (100 µM)	0.5 µl
Primer 2 (100 µM)	0.5 µl
25 mM $MgCl_2$	2 µl
Taq Polymerase	2.5 units
water	Adjust to 50 µl

PCR program, 30 cycles (step 2-4)		
step	temperature	time
1	94°C	5 min
2	94°C	45 s
3	56°C	1 min
4	72°C	90 s
5	72°C	7 min
6	10°C	pause

The PCR fragments were purified using Quick Spin columns (Qiagen) and restricted with respective enzymes (see manuscripts). Restriction reactions were performed at 37°C for 2 hours. After this, fragments were purified with a crystal violet gel. The bands were excised and cleaned with Qiagen PCR purification kit or Promega´s "Wizard SV Gel and PCR Clean-Up System" according to manufacturer´s instructions.

Crystal violet gel	
Crystal violet (10 mg/ml in TBE)	1:1000 dilution
TBE buffer	1x
Agarose	1-2.5 %

Running buffer for crystal violet gels is TBE containing 10 µg /ml of the dye

Plasmids were restricted with respective enzymes and dephosphorylated using Fermentas CIAP enzyme.

Dephosphorylation reaction	
10 µg vector	X µl
10x buffer	5 µl
5 u CIAP	5 µl
adjust to	50 µl

The reaction was incubated for 30 min at 37°C. After this another 3 units of enzyme in a volume of 30 µl were added and followed by incubation step of 30 min at 50°C. Finally another 2 units of enzyme were added in a volume 20 µl and incubated for 30 min at 37°C.

Vector was purified with a QIAquick Spin column. For ligation reaction, amount of restricted vector and fragment was calculated according to the formula[1]:

$$Mass_{Fragment}\ [ng] = 5 \times Mass_{Vector}\ [ng] \times Length_{Fragment}\ [bp] / Length_{Vector}\ [bp]$$

Ligation reaction included:

Ligation reaction	
insert	X µl
vector	X µl
10x reaction buffer A	1 µl
T4 DNA Ligase	10 units
Adjust with water	to 10 µl

Ligation program	
37°C	30 min
30°C	30 min
25°C	30 min
20°C	30 min
16°C	3 h
20°C	2 h 30 min
25°C	2 h 30 min
30°C	30 min
16°C	13 h
16°C	pause

2.4.2. Mutation of miRNA binding sites in 3´UTRs and mutation of promoter regions

Mutagenesis PCR was applied for mutation of putative promoter regions as well as annotated miRNA binding sites. Primers were designed according to references (see respective manuscripts). pGL3 control vector containing the respective constructs were used as templates in the mutagenesis PCR reaction. The forward primer contained the

[1] Cornel Mühlhardt, Der Experimentator: Molekularbiologie/Genomics 4. Auflage, Spektrum Akademischer Verlag, Berlin 2003

base exchanges needed to interfere with function of the respective site. A complementary reverse primer was designed and used in the PCR reaction. Primers were physphorylated using T4 PNK (Fermentas). Phosphorylation reaction was performed for 1 h at 37°C with subsequent heat inactivation at 70 °C for 5 min. Subsequent PCR reaction was done with Pfu DNA Polymerase from Fermentas.

Phosphorylation reaction mix	
Primer (100 µM)	5 µl
10x buffer A (for forward reaction)	2.5 µl
10 mM ATP	2.5 µl
T4 PNK	10 units
Adjust with water	To 25 µl

Mutagenesis PCR reaction	
10x Pfu buffer with Mg_2SO_4	10 µl
dNTPs, 2.5 mM	1.6 µl
First primer phosphorylated	2.5 µl
Second primer phosphorylated	2.5 µl
template	100 ng
Mg_2SO_4 25 mM	12 µl
Adjust with water to	100 µl

Mutagenesis PCR program, 15 cycles (step 2-4)		
step		
1	95°C	5 min
2	95°C	1 min
3	50°C	90 s
4	72°C	14 min
5	72°C	10 min
6	8°C	pause

50 µl of a mutagenesis PCR were then restricted with DpnI to get rid of the unmutated template plasmid. For this 1 unit DpnI were added while the total reaction volume was adjusted to 60 µl with water and respective buffer. After incubation for 1 h at 37°C another 10 units of enzyme were added and again incubated for 1 h at 37°C. Volume of the reaction was reduced to ca. 10 µl by using a speed-vac centrifuge at 50°C for 1 h. For transformation of chemically competent bacteria 2 µl of the reaction was added in the respective step.

2.5 Plasmid preparation

Plasmid mini preparation was done using Ferments GeneJET Plasmid Miniprep Kit. Maxi Preps were done with Qiagen´s EndoFree Plasmid Maxi Preparation Kit. All preparations were performed according to the manufacturer´s instructions. All constructs generated were sequenced at Eurofins MWG Operon and manually checked for mutations using EMBL-EBI tool pairwise alignment (http://www.ebi.ac.uk/Tools/emboss/align/).

2.6 Animal cell culture and transfection procedures

2.6.1 Cell culture

Cells were cultured at 37°C and 5 % CO_2 in a humidified incubator. Handling of cells was done in a sterile bench. The K562, Hela, H69 and H209 cells were cultured in RPMI 1640 (PAA) supplemented with 10 % FCS (PAA). All other cell lines were cultured in IMDM containing 10 % FCS. Freeze down of cells was done in the respective medium supplemented with 20 % FCS and 5 % DMSO. For this cells were centrifuged for 5 min at 2050 rpm and supernatant was discarded. After resuspension of the cells in 1 ml freeze down medium, cells were transferred to 2 ml tubes and packed into a styrofoam box filled with paper towel. The box was put to -80°C for at least 24 hours. After this, cells were stored in liquid nitrogen for longer periods.

2.6.2 Electroporation of K562 cells

Cells were harvested from tissue culture flasks (75 cm^2) and transferred to 50 ml tubes. They were centrifuged at 2050 rpm in a Hettich universal 320 centrifuge at room temperature for 5 min. Supernatant was discarded and the cell pellet washed with 10 ml RPMI 1640. Cells were centrifuged again under the same conditions and resuspended in 2.5 ml RPMI 1640 per flask. Cells were counted and adjusted (via another centrifugation step) to a concentration of $1*10^6$ cells / 50 µl with RPMI 1640. 100 µl of cell-suspension was transferred into a 4 mm BioRad GenePulser cuvette and mixed with an appropriate amount of nucleic acid (e.g. 2 µg siRNA per 1 million cells) by gently pipetting up and down two times. Electroporation was then performed with a single pulse in a Biorad GenePulser XCell using a square wave protocol (330V, 10ms). Electroporated cells were

immediately transferred into a well of a 12-well-plate supplemented with 1.5 ml medium if not indicated otherwise.

Cuvettes were used up to 8 times. For this, cuvettes were rinsed with 70 % Ethanol and stored in 70 % ethanol for at least 1 day. After this cuvettes were rinsed with demineralized water and sonicated in demineralized water for 15 min in a Branson Sonifier 250 using the settings "output control" between 2-3 and "Duty" between 20-30. Subsequent to sonification, cuvettes were rinsed with demineralized water again and finally stored in 70 % ethanol for at least 1 day. Cuvettes were then dried for several hours under a sterile bench.

2.7 Luciferase Assay

Luciferase Assays were performed using the Promega Luciferase Assay System. Cells were transfected with 5µg / 1 Mio cells of the pGL3 control vector. For RNAi experiments, nucleic acids were co-transfected. Contructs were cloned either to the XbaI site at the end of the luciferase gene (e.g. 3´UTRs) or in front of the reporter by removing the SV40 promoter by HindIII/BglII restriction (mir-17-92 Promoter assays). If not indicated cells were harvested after 48 hours by centrifugation at 4°C and 2500 rpm in a table centrifuge for 5 min. Cells were then lysed using 100 µl of reporter lyses buffer per 1 Mio cells by pipetting up and down and shaking incubation in a tabletop shaker for 30 min at room temperature. Then 10 µl of lysate were transferred into a well of a white 96-well plate and mixed with 10 µl of substrate solution. This was done in triplicates. Luminescence was measured with a Safire II multiformat platereader (Tecan) using the following settings:

Measurement mode: Luminescence
Integration time (Manual): 10 ms
Plate Definition file: GRE96fw.pdf
Shake duration (Orbital Medium): 3 s

Measurement was performed 2 times immediately after one another, to ensure a more homogenous mixing. Second measurement was taken for data analysis.

2.8 Western blot analysis

Cell transfection was performed as described. For Western blot analysis, cells were centrifuged in a table centrifuge for 5 min at 2500 rpm at 4 °C. Supernatant was removed and cells were lysed in lysis buffer:

Lysis buffer	
Tris HCl	125 mM, pH 6.8
SDS	4 %
2-Mercaptoethanol	1.4 M
Bromphenolblue	0.05 %

1 Mio cells were lysed in 100 µl buffer by vortexing 10 s and heating to 95°C for 5 min in a standard heating block. Lysates were stored at -20°C. 20 µl of each lysate was loaded to a Polyacrylamid Gel (PAGE).

Preparation of Gels (0.75 mm)

If not indicated, 15 % gels were used.

Separation gel	**for 2 gels**
Buffer 1,5 M Tris HCl, pH 8.8 0,6 % SDS	4 ml
30 % PAA	8 ml
Deminarlized water	4 ml
APS 10 %	80 µl
TEMED	20 µl

Collecting gel	**for 2 gels**
0,5 M Tris HCl, pH 6,8 0,6 % SDS	1,8 ml
30 % PAA	1 ml
Deminarlized water	4,7 ml
APS 10 %	24 µl
TEMED	9 µl

Gels were run for 1 h at 180 V using a Mini-Protean system (Bio-Rad) in 1x running buffer (SDS Page Laufpuffer, Roth). Transfer of gels was done in a semi dry blotter (C.B.S. Scientific). For this, Immobilon-P membranes (Millipore) with a pore size of 0.45 µm were prepared as follows:

A single membrane was incubated for 15 s in methanol and washed in water for 2 min. Until assembly gel, membrane and whatman paper was incubated with transfer buffer.

Transfer buffer
25 mM Tris HCl, pH 8.3
192 mM Glycin
10 % Methanol

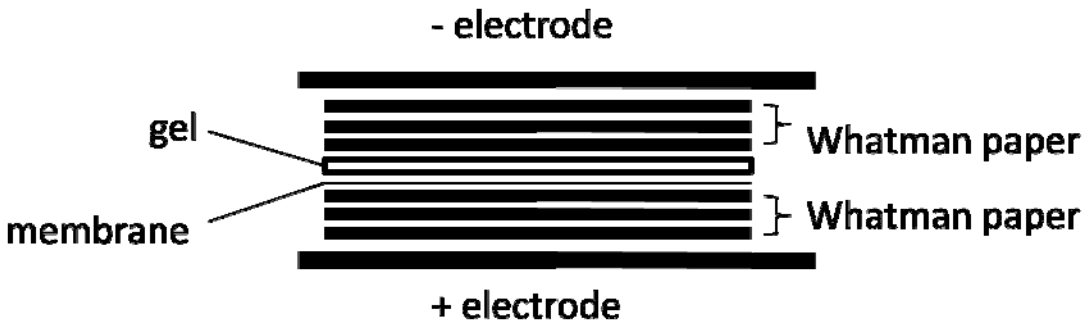

Figure 2.1 Assembly of gel blotting system

Transfer was run for 90 min at 1 mA per cm^2 membrane using an EBU-4000 blotter (C.B.S. Scientific). After transfer, blots were incubated for 2 hours with 5 % milk pouder solution in TBST. Blots were then washed three times with TBST for 10 min. Incubation and dilution of antibodies can be found in the respective manuscripts. Each blot was incubated with Amersham ECL Western blotting reagents according to the manufacturer's protocol. Substrate incubation was performed for 2 minutes. For detection, Kodak BioMax Light Films, Kodak GBX developer/replenisher and GBX fixer/replenisher were used.

TBST	
Tris HCl	10 mM, pH 7.6
NaCl	150 mM
Tween 20	0.1 %

2.9 Nucleic acid methods

2.9.1 Agarose gels

Gels were prepared using TBE buffer. Agarose was used in a range from 0.5 % - 2.5 %. For 100 ml of gel, the respective amount of agarose was added to a glass flask and adjusted to a total volume of 100 ml. After cooking in a conventional microwave, ethidium bromide (Roth) was added according to manufacturer´s instructions. Gels were run at 120 mA for 1 h.

As markers 2-log ladder from NEB and 10 bp ladder from Invitrogen were used according to manufacturer´s instructions. For sample loading, a loading buffer was used at a final concentration of 1x.

5x DNA loading dye	
Glycerin	70%
EDTA	50 mM
Tris HCl	100 mM, pH 7,5
Bromphenolblue	0.05 %
Xylencyanolblue	0.05 %

Gels were visualized in a Bio-Rad gel documentation system (Biostep Transilluminator) under UV-light.

2.9.2 RNA preparation

RNA preparation was done using the RNeasy Mini Prep Kit (Qiagen) or the RNeasy Mini Plus Prep Kit (Qiagen) according to manufacturer´s instructions. The latter kit contains gDNA removal columns. In combination with the former kit an optional on column digestion of gDNA was done according to manufacturer´s protocol using the 20 units TURBO DNase (Ambion) in a total volume of 80 µl. 5 Mio cells K562 were used for preparation with a single column. RNA concentration was determined with a standard photometer (Biomate3, Thermo). Samples were measured three times as 1:100 dilutions in water. For purification of mature miRNAs Ambion´s mirVana miRNA Isolation Kit was used according to manufacturer´s instructions for enrichment of small RNAs. Also 5 Mio K562 cells were used for one column.

A second RNA preparation protocol was used as well. For this, classical phenol/chloroform extraction was performed. Acid phenol was prepared by shaking an appropriate volume of phenol with 1/10 volume 1x TE buffer. The upper liquid phase was discarded and the remaining phenol was 3 times shaken with 1/10 volume sodium acetate (300 mM, pH 5) and liquid phase was discarded each time. Cell pellets were resuspended and lysed using the respective buffer of Qiagen´s RNeasy Kit and the protocol above. One volume of acid phenol was added to the lysed cells and shaken at room temperature for 5 min followed by 5 min centrifugation (13000 rpm, 4°C). The upper liquid phase was transferred to a new tube and an equal volume of chloroform was added and shaken at room temperature for 5 min. A second centrifugation was followed by transferring the upper liquid phase to a new tube. An ethanol precipitation was done as follows: 1/10 volume sodium acetate (300 mM, pH 5) was added as well as 2.5 volumes of ethanol. The mixture was set to -20°C for 30 min to 24 hours. Then a centrifugation step at 13000 rpm (4°C) for 30 min followed. Supernatant was discarded and the pellet dried at room temperature for 5 min. The pellet was resuspended in 30 µl H_2O. To get rid of DNA contamination, a digestion with TURBO DNase from Ambion was done using 20 units and incubation at 37°C for two hours. A second acid phenol/chloroform extraction was done as described above.

2.9.3 Concentration of nucleic acids

For transfection experiments amounts of nucleic acids (siRNAs, LNAs, etc.) were calculated with the formula[2] :

c [µg/ml] ÷ MW of nucleic acid [g/mole] x 10^{-6} g/µg x 10^{3} ml/l = c [M]

Concentrations of nucleic acids in solution were measured in triplicates as 1:100 dilutions in water with a Biomate 3 photometer (Thermo). For DNA absorption 260/280 was used to also determine purity/protein contamination.

[2] Dany Spencer Adams, Lab math: A handbook of Measurements, Calculations, and other Quantitative Skills for use at the bench, Cold Spring Harbour Laboratory Press 2003

2.9.4 RT-PCR

The Fermentas RevertAid H Minus First Strand cDNA Synthesis Kit was used according to manufacturer´s instructions. In short, for one RT-PCR reaction 1 µg of RNA was used with 1 µl of random hexamer primer (provided in the kit). For reverse transcription of mature miRNAs 1 µl of looped primer (100 µM) was used. Looped primers were designed according to references [see manuscripts]. As an example for a looped RT-primer you can see the design for miR-20a below:

5´-GTCGTATCCAGTGCAGGGTCCGAGGTATTCGCACTGGATACGACctacctg-3´
Looped primer for miR-20a

5´-uaaagugcuuauagug**cagguag**-3´
Mature miR-20a

Capital letters indicate the universal part of the primer. Boxes indicate base pairing between those regions so that the primer forms a stem-loop structure with a 3´overhang which is complementary to the targeting strand of the mature miRNA (indicated **bold**). In a standard PCR cycler the following program was used:
RNA and primer are mixed and adjusted to 11 µl with water. They are incubated for 5 min at 80°C and put on ice after this. RiboLock Ribonuclease Inhibitor provided in the kit is not used as it negatively influences the subsequent QT-PCR reaction. The following components are added as one mix:

5x reaction buffer	4 µl
10 mM dNTP mix	2 µl
Water	2 µl

Then reaction is incubated for 5 min at 25°C. After addition of 1 µl RT enzyme (=200 units) 10 min of incubation at 25°C are followed by 60 min at 42°C. Finally the reaction is stopped by heating at 70°C for 10 min and cooling down to 8°C. cDNAs were stored at -20°C.

2.9.5 QT-PCR

Quantitative real time PCR was performed using a Roche LightCycler 2.0 with Software Version 4.05 and the Absolute QPCR SYBR Green Capillary Mix (Thermo Fisher). Each sample was measured in triplicates. For this the following components were mixed:

2x capillary mix	15 µl
Primer pair (5 µM each)	6 µl
Water	3 µl

7.2 µl of cDNA (1:10 dilution for standard RNA, 1:100 dilution for enriched miRNAs) are added to the mix. After mixing by pipetting up and down 10 µl are transferred to a 20 µl glas capillary (Roche). Via a pre-cooled adaptor (Roche) capillaries are centrifuged for 5 s at 2000 rpm in tabletop centrifuge and put into a cycling rotor. Cycling is carried out as follows:
Initial activation of polymerase for 15 min at 95°C followed by

40 cycles of amplification	
temperature	time
95°C	10 s
55°C	20 s
72°C	12 s

Fluorescence acquisition is measured at 72°C in the single measurement mode.

Melting curve	
temperature	time
95°C	0 s
57°C	15 s
98°C	0 s

Fluorescence acquisition was measured at 98°C in the “continues” measurement mode. For a detailed example see appendix. Data were analyzed with the $2^{-\Delta\Delta C}{}_{T}$ method [see manuscripts for reference].

Role of kinase Pim-1, tumor suppressor p21 and the miR-17-92 cluster in human erythroleukemia cells

Kerstin Lange-Grünweller*, Robert Prinz*, Daniela Gutsch†, Achim Aigner†, Roland Karl Hartmann* and Arnold Grünweller*‡

submitted to Neoplasia, Ms.no. 09-1928, Date of submission: 17.11.2009

**Institut für Pharmazeutische Chemie, Philipps-Universität Marburg*
†Institut für Pharmakologie und Toxikologie, Philipps-Universität Marburg

‡to whom correspondence should be addressed

Pharmazeutische Chemie
Philipps-Universität Marburg
Marbacher Weg 6
35037 Marburg, Germany
Tel.: +49-6421-28-25849
Fax: +49-6421-28-25854
E-mail address: gruenwel@staff.uni-marburg.de

Running title: Pim-1 and p21 in erythroleukemia

Key words: Pim-1, p21, microRNA, RNAi, LNA

Abbreviations:
ABTS: 2,2'-Azinobis-3- ethylbenzthiazolin-6-sulfonsäure; Bad, Bcl-2 antagonist of cell death; FCS, fetal calf serum; HP1: heterochromatin protein 1; HRP, horse radish peroxidase; LNA, locked nucleic acids; miRNA, micro RNA; PCNA, proliferating cell nuclear antigen; Pim, proviral integration site for moloney murine leukemia virus; qRT-PCR: quantitative real-time polymerase chain reaction; RNAi, RNA interference; siRNA, small interfering RNA; STAT, signal tranducers and activators of transcription; TBST, Tris-buffered saline Tween-20. UTR: untranslated region; VR1: vanelloid receptor 1

Abstract

The proto-oncogene Pim-1, an anti-apoptotic kinase that acts synergistically with c-Myc to promote tumorigenesis, is overexpressed in the human myeloid leukemia cell line K562. In this study siRNA-mediated knockdown of Pim-1 revealed cell proliferation to be Pim-1-dependent, with a role of Pim-1 in the transition from mitosis to G1-phase of the cell cycle. We further re-analyzed the effects of the phosphatase PP2A inhibitor *okadaic acid* (OA): PP2A is involved in Pim-1 degradation and its inhibition is known to increase Pim-1 levels; also, PP2A can induce apoptosis by dephosphorylation of the pro-apoptotic protein Bad, which is a phosphorylation target of Pim-1. OA-treatment induced a series of so far unnoticed dynamic changes: a short-term increase of Pim-1, followed by its rapid and unexpected complete down-regulation. OA-induced disappearance of Pim-1 was accompanied by a strong but transient induction of the cell cycle inhibitor p21 and a switch from proliferation to apoptosis. RNAi-mediated knockdown of p21 delayed this onset of apoptosis in OA-treated K562 cells. Although untreated growing K562 cells are p21-deficient, substantial amounts of p21 mRNA are detectable. We found that translation of p21 in K562 is completely repressed by microRNAs *miR-17-5p* and *miR-20a* and could be specifically derepressed by transfection of short, seed-directed all-LNA AntimiRs. OA treatment increased the basal p21 mRNA levels approx. 10-fold, and these induced levels persisted despite microRNA-independent disappearance of the p21 protein at later time points. We conclude that tight *miR-17-5p/-20a*-dependent translational repression of p21 and Pim-1 overexpression are key mechanisms to promote proliferation of K562 cells.

Introduction

The activity of kinases and mechanisms that control apoptosis and cell proliferation are often deregulated in cancer cells [1]. Pim-1, a serine/threonine kinase, is up-regulated in several cancer types and can function in a synergistic manner with the transcription factor c-Myc to establish severe forms of B cell lymphomas [2-4].

Pim kinases belong to the small group of constitutively active kinases [5]. Thus, their kinase activity correlates with their cellular expression levels. Expression of Pim-1 is mainly regulated at the transcriptional level by the action of several interleukines and growth factors that activate STAT3 and/or STAT5 via Janus kinases [6, 7]. For the Pim-1 kinase, several phosphorylation targets have been identified, such as Cdc25A [8] and Cdc25C [9], HP1gamma [10], Tudor-SN [11], p21 [12] and others (for review see 7]).

The stability of Pim-1 is controlled by the heat shock proteins Hsp90 and Hsp70 as well as the protein phosphatase PP2A [13-15]. Hsp90 increases the half-life of Pim-1 by protecting it from proteasomal degradation, whereas Hsp70 has the opposite effect [15]. The prolyl-isomerase Pin1 is thought to mediate binding of phosphorylated Pim-1 to the regulatory subunit B56-beta of PP2A, leading to dephosphorylation by the catalytic subunit of PP2A followed by ubiquitinylation and degradation of Pim-1 via the proteasome [14]. Additionally, PP2A can induce apoptosis by dephosphorylation of the pro-apoptotic protein Bad [16], which is also a phosphorylation target of Pim-1 and Pim-2 [17, 18]. Pim-dependent Bad phosphorylation at serine 112 results in its cytoplasmic sequestration by binding to the 14-3-3 protein. This interaction suppresses apoptosis because it prevents Bad from triggering mitochondrial cytochrome c release [19]. Based on these findings, the specific inhibition of PP2A by *okadaic acid* (OA) would be expected to induce an anti-apoptotic effect by stabilising Pim-1 and abrogating the dephosphorylation of Bad. However, this seems to contradict previous findings that have demonstrated an apoptotic response to OA treatment in the human myeloid leukemia cell line K562 [20, 21]. To shed light on these apparent discrepancies, we reinvestigated the relation between Pim-1 expression levels and induction of apoptosis in K562 cells. This revealed so far unnoticed time-dependent changes: a short term increase followed by a rapid degradation of Pim-1. By using RNAi we found Pim-1 to be essential for cell proliferation and cell cycle progression but without any effect on apoptosis.

Furthermore, we found the cell cycle inhibitor p21, a phosphorylation target of Pim-1[22], to be transiently induced after OA addition to K562 cells. Of note, the phosphorylated form of p21 localises to the nucleus, where it is thought to sterically interrupt the interaction of unphosphorylated p21 with PCNA, which then relieves the p21-mediated blockage of the DNA synthesis machinery [22, 23]. We show that p21 can function as an inducer of apoptosis because siRNA-mediated knockdown of p21 delays the OA-dependent induction of apoptosis in K562 cells. Finally, the observed differences in p21 expression upon OA-treatment prompted us to analyse the role of miRNAs on the repression of p21 translation. We found basal p21 mRNA levels in K562 cells to be completely repressed on the translational level by the *miR-106b* family members *miR-17-5p* and *miR-20a* encoded in the *miR-17-92* cluster. Therefore, our findings suggest a complex and time-dependent network of Pim-1 and p21 effects especially on cell proliferation and highlights the cooperative role of miRNAs in translational repression of p21.

Material and Methods

Oligonucleotides, siRNAs and antibodies

Locked nucleic acids (LNA) antisense oligonucleotides (AntimiRs) were purchased from RiboTask (Odense, Denmark). anti-*miR-17-5p*: 5'-CTGTAAGCACT[mU]T; anti-*miR-20a*: 5'-CTATAAGCA[mC]T[mU]TA; all residues were LNA, except for isolated 2'-O-methyl pyrimidines marked as mU and mC. LNA-14mers directed against *let-7a* (5´-AACCTACTACCTCA-3´) and *Escherichia coli* RNase P RNA [24] were used as negative controls. Small interfering (si)RNAs (sense and antisense strands) were purchased from Dharmacon (Boulder, USA): Pim-1 siRNA, 5'-GAUAUGGUGUGUGGAGAUAUU and 5'-UAUCUCCACACACCAUAUCUU. Vanilloid receptor 1 (VR1) siRNA (5'-GCGAUCUUCUAUUCAAdTdT and 5'-GUUGAAGUAGAAGAUGCGCdTdT) was used as an unrelated negative control; VR1 is expressed in neuronal cells, but not in leukemia cells [25]; Pim-1 knockdown effects on cell proliferation and apoptosis were confirmed with a second Pim-1 specific siRNA (5'-GGAACAACAUUUACAACUCdTdT and 5´-GAGUUGUAAAUGUUGUUCCdTdT). The p21 siRNA was from Santa Cruz Biotechnology (sc-29427; Santa Cruz, CA, USA). Antibodies against p21 (sc-6246), Pim-1 (sc-13513), Hsp70 (sc-1060), beta-Actin (sc-47778), PP2A-B56-beta (sc-6117), c-Myc (sc-40), Tudor-SN (sc-34753), as well as the secondary antibody (sc-2005) were from Santa Cruz Biotechnology. The anti-HP1gamma antibody (05-690) was obtained from Upstate (Millipore, MA, USA) and the phospho-Bad antibody (7E11) was obtained from Cell Signaling Technology (Danvers, MA, USA).

Cell culture and transfection

Cell lines were cultured under standard conditions (37°C, 5% CO_2 in a humidified atmosphere) in RPMI 1640 containing 10 % FCS (PAA, Cölbe, Germany). For knockdown experiments, K562 cells were electroporated in 4 mm cuvettes with a single pulse at 330 V for 10 ms using a BioRad GenePulser XCell (Biorad, München, Germany). For 1 x 10^6 cells 2 µg Pim-1 siRNA, 0.5 µg LNA-AntimiRs or 0.7 µg p21 siRNA were used. Transfection of HeLa cells (8 x 10^4 cells) was performed in 24-well plates with Lipofectamine 2000. Briefly, 24 h after seeding in 500 µl RPMI 1640 with 10% FCS, 0.5 µg of vector DNA (plasmid "pGL3 control" with a *let-7a* or an inverted *let-7a* target sequence) were co-transfected with 0, 10, 50, or 100 nM of each LNA-AntimiR according to the manufacturer's protocol. Complexation was performed in Optimem medium (Invitrogen, Karlsruhe, Germany) without serum. The transfection volume was 100 µl for each well. For inhibition of cellular PP2A *Okadaic acid* (OA) (Biomol, Hamburg, Germany) was added to the cells at a final concentration of 100 nM as recommended by the manufacturer for cell culture experiments (see also reference [14]).

Cell Cycle Analysis

K562 cells were transfected with siRNAs against Pim-1 or VR1 as a negative control [25]. After 24 h nocodazol was added to the cells (final concentration 100 ng / ml). Cells were incubated for additional 24 h with nocodazol to synchronise cells in the M-phase of the cell cycle. Then cells were washed with PBS and fresh medium was added to release the cells from the mitotic block. Cells were cultivated for additional 48 h before fixation in 70% ethanol. After RNase A treatment, propidium iodide was added to a final concentration of 50 µg /ml. DNA content of the cells was analysed by FACS using an FACSCalibur (Becton-Dickinson, Heidelberg, Germany).

RNA preparation and quantitative real-time (qRT)-PCR

Total RNA was isolated with the RNeasy Mini Kit (Qiagen, Hilden, Germany). RT-PCR was conducted using the Fermentas RevertAid H Minus First Strand cDNA Synthesis Kit (Fermentas, St. Leon-Roth, Germany) with 1 µg total RNA. Quantitative PCR was performed in duplicate in a LightCycler from Roche (Penzberg, Germany) with the Absolute QPCR SYBR Green Capillary Mix (Thermo Scientific, Hamburg, Germany). All procedures and reactions were carried out according to the protocols provided by the manufacturers. The mRNA levels were calculated from the crossing points by the $2^{-\Delta\Delta C_T}$ method [26] to the obtained crossing points values. The *β-actin* gene was used as an internal control.

Primers were obtained from Metabion (Metabion, Martinsried, Germany) and designed with Universal ProbeLibrary (Roche Applied Biosciences, Mannheim, Germany). *p21*: forward 5′-TCACTGTCTTGTACCCTTGTGC-3′, reverse 5′-GGCGTTTGGAGTGGTAGAAA-3′); *β-actin*: forward 5′-CCAGAGGCGTACAGGGATAG-3′, reverse 5′-CCAACCGCGAGAAGATGA-3′; *miR-17-92* cluster: forward 5′-CAGTAAAGGTAAGGAGAGCTCAATCTG-3′, reverse 5′-TCAGATTATTCTTTAGCTTAGTGGTTGTATG-3′.

Western blotting

Cells were resuspended in lysis buffer (125 mM Tris-HCl pH 6.8, 4 % SDS, 1.4 M 2-mercaptoethanol, 0.05 % bromophenol blue) and heated at 95°C for 5 min. Samples were loaded onto 10% or 15% SDS-polyacrylamide gels and run for 1 h at 180 V. Proteins were transferred to an Immobilon-P PVDF membrane (Millipore, MA, USA) for 90 min at 1 mA per cm^2 membrane using an EBU-4000 blotter (C.B.S. Scientific, CA, USA). Primary and secondary antibodies were diluted in TBST 1:200 (p21, Tudor-SN), 1:500 (Pim-1, B56-beta), 1:1000 (Hsp70, c-Myc), 1:2000 (p-Bad), 1:4000 (HP1gamma), 1:10000 (β-Actin) and 1:10000 (goat anti-mouse IgG-HRP). After a final washing step, blots were incubated with Amersham ECL or ECLplus Western blotting reagents according to the manufacturer's protocol. For detection, Kodak BioMax Light Films, Kodak GBX developer/replenisher and GBX fixer/replenisher were used.

Luciferase reporter assays, plasmid construction and seed mutagenesis

To determine the effects of AntimiR-LNAs against mature *miR-17-5p* and *miR-20a* on the expression of the p21 protein, the 3′-untranslated region (UTR) of p21 was cloned into the pGL3 control luciferase reporter vector (Promega, Mannheim, Germany) via its *Xba*I site. The 3`-UTR was initially amplified from K562 genomic DNA with the forward primer 5′-TCTAGACCTCAAAGGCCCGCTCTA-3′ and reverse primer 5′-TCTAGAGGAGGAGCTGTGAAAGACACA-3′; the amplicon was subcloned into a pCR2.1-TOPO vector as part of the TOPO TA Cloning kit (Invitrogen, Karlsruhe, Germany) before final insertion into the pGL3 vector. PCR mutagenesis of the miRNA target sites was done according to Brennecke et al. [27] using the following primers (sites of mutation underlined):

5′-target site forward: 5′-GAAGTAAACAGATGG<u>G</u>ACT<u>G</u>TGAAGGGGCCTCACC-3′,
5′- target site reverse: 5′-GGTGAGGCCCCTTCA<u>C</u>AGT<u>C</u>CCATCTGTTTACTTC-3′,
3′-target site forward: 5′-CTCCCCAGTTCATTG<u>G</u>ACT<u>G</u>TGATTAGCAGCGGAA-3′,
3′-target site reverse: 5′-TTCCGCTGCTAATCA<u>C</u>AGT<u>C</u>CAATGAACTGGGGAG-3′.

1 µg of pGL3 derivatives were co-transfected with 0.5 µg of AntimiR-LNAs per 1 x 10^6 cells. After 48 h, luciferase assays were performed using the Promega Luciferase Assay System. Briefly, cells were resolved in 100 µl lysis buffer, and 10 µl of lysate were mixed

with 25 µl substrate and immediately measured with a Safire^2 microplate reader (Tecan, Crailsheim, Germany) in 96-well plates.

Analysis of phosphorylated Bad levels

To detect phosphorylation of Bad at serine 112, the CASE^{TM} kit from Superarray (Frederick, MD, USA) and poly-D-lysine coated plates (Corning Costar, NY, USA) were used. The amounts of phospho-Bad and total Bad were determined with two different antibodies in colour reactions; in both cases, absorbance was measured at 450 nm with a Safire^2 microplate reader (Tecan, Germany), and the ratio of phospho-Bad to Bad was calculated. Note that the total Bad levels remained essentially unchanged in all measurements shown in Figures 1 *F* and 2 *A* (variation ≤ 20%). For the determination of relative cell number, cells were stained with Coomassie blue. Absorbance was measured at 595 nm and the ratio of phospho-Bad to Bad was normalised to the estimated cell number.

Apoptosis and proliferation assays

Using the "Cell Death Detection ELISA" (Roche, Germany), microtiter plates were pre-coated with an anti-histone antibody (clone H 11-4), incubated with lysed cells, followed by the addition of an anti-DNA antibody (clone MCA–33) and incubation for 90 minutes. For detection of mono- and oligonucleosomes an 2,2'-Azinobis-3- ethylbenzthiazolin-6-sulfonsäure (ABTS) substrate solution was applied. Absorbance was measured with a Safire^2 microplate reader at 405 nm.

To determine cell proliferation, 1 x 10^4 cells were seeded and cultivated under standard conditions. At the time points indicated, cells were pelleted and resuspended in 100 µl PBS, and 10 µl of the tetrazolium salt WST-1 were added to determine the activity of mitochondrial dehydrogenases. Absorbance was measured after incubation at 37°C for 2 h at 450 nm with 600 nm as reference wavelength using a Safire^2 microplate reader.

Results

PP2A inhibition causes dynamic changes in Pim-1 and p21 levels

Among 17 different human cancer cell lines we tested, K562 cells were found to have the highest Pim-1 protein levels (data not shown), consistent with earlier reports [28]. High levels of Pim-1 depend on the presence of growth factors and correlate with low levels of apoptosis; depriving K562 cells of growth factors increased apoptosis and caused a large decrease in Pim-1 protein levels (Supplementary Figure S1), which is in line with previous findings (for review see [7]). The levels of the anti-apoptotic Pim-1 protein were previously shown to increase after 1 h of treatment with the PP2A-specific inhibitor *okadaic acid* (OA) in the murine hematopoietic cell line BaF3 [14], although OA treatment was reported to induce apoptosis [21]. Thus, to scrutinise the correlation between Pim-1 expression and apoptosis, we analysed the Pim-1 levels in K562 cells at different time points of OA treatment. This revealed time-dependent opposite effects on Pim-1 (Figure 1*A*). In the first 3 h, Pim-1 levels increased, which was paralleled by a slight decrease in the basal apoptotic levels as measured by DNA fragmentation (Figures 1*A* and 1*C*). However, after 3 h of OA treatment Pim-1 levels declined rapidly, which was paralleled by a strong but transient induction of the p21 protein (Figure 1*A*); highest p21 levels were observed between 4 and 12 h after OA treatment followed by subsequent down-regulation of p21 (see 24 h of OA treatment). Monitoring Pim-1 and p21 for longer time points (up to 4 days) revealed a decrease of both proteins to undetectable levels at ≥ 36 h of PP2A inhibition (Figure 1*B*).

Moreover, prolonged incubation with OA changed the morphology of K562 cells to megakaryocytes [29], which could be observed from time point 36 h on (data not shown). After 48 h beta-Actin and Hsp70 levels started to drop indicating degradation of the cytoskeleton and progressive cell death (Figure 1*B*). The incubation with OA had no effect on the steady-state levels of PP2A during the first 24 h, as inferred from unchanged levels of B56-beta, the PP2A subunit that interacts with Pim-1 (data not shown). Also, we did not observe any OA-dependent increase in the levels of Hsp70 (Figure 1*A*) which mediates Pim-1 degradation. We thus conclude that K562 cells can activate an alternative yet unknown degradation pathway to eliminate Pim-1, which is independent from the known Pim-1 regulators PP2A and Hsp70.

A further consequence of OA treatment was the induction of apoptosis in K562 cells (Figure 1*C*). An increased apoptotic rate could be measured ~6 h after OA addition (Figure 1*C*) and reached a maximum level after 48 h.

Based on the fact that p21 protein levels largely increased ~4 h after OA addition (Figure 1*A*), we asked if p21 mRNA may be present in K562 cells which normally do not express the p21 protein. We were indeed able to detect substantial amounts of p21 mRNA by qRT-PCR (Figure 1*D*). These levels were up-regulated approx. 10-fold at 6 h after drug addition, consistent with the strong increase of p21 protein at this time point. Elevated p21 mRNA levels persisted up to 24 h (Figure 1*D*), whereas p21 protein levels dropped again at this or later time points (Figures 1*A*, *B*).

OA-dependent increase in Bad phosphorylation

The coincidence of OA-induced apoptosis and down-regulation of Pim-1 at later time points (> 5 h) raised the question if Pim-1 degradation might be responsible for the increase in apoptosis. One target of Pim-1 is the apoptotic regulator Bad. Pim-dependent phosphorylation of Bad leads to its cytoplasmic retention, which establishes the anti-apoptotic state of Bad. Upon dephosphorylation, which can be catalysed by PP2A, Bad regains the capacity to interact with Bcl-xL to induce apoptosis. To examine if the down-regulation of Pim-1 may increase the levels of dephosphorylated Bad, we analysed the ratio of Bad phosphorylated at serine 112 to unphosphorylated Bad. We were unable to detect basal levels of phosphorylated Bad in untreated K562 cells, but phosphorylated Bad became visible after cells had been exposed to OA (Figures 1*E*, *F*). Quantitation of Bad phosphorylation by a phospho-Bad-specific ELISA revealed a fast increase in phospho-Bad levels (~1.7-fold) due to PP2A inhibition. This correlated with the observed stabilisation of Pim-1 and the slight short-term anti-apoptotic effect during the first 3 h of OA treatment (Figures 1*A*, *C*). Yet at later time points, phospho-Bad levels further increased to approx. 3-fold compared to untreated cells (Figure 1*F*) despite the fact that Pim-1 was degraded. This indicates that the observed increase in apoptosis at > 5 h of OA treatment is mediated by a separate, Bad-independent pathway. Therefore, we examined if the pro-apoptotic factor Bim [30-32] may play a role in this process. Western blot analysis revealed that the extended long version of Bim, Bim_{EL}, is present in K562 cells. However, similar to Pim-1, Bim_{EL} disappeared 4 h after OA addition (Supplementary Figure S2). This excluded Bim as a candidate to trigger apoptosis in K562 cells.

Pim-1 knockdown inhibits cell proliferation

An efficient knockdown of Pim-1 by RNAi (Supplementary Figure S3*A*) was generated to reveal effects specific to Pim-1. Silencing of Pim-1 had no effects on the expression levels of its phosphorylation targets HP1gamma, p21 and Tudor-SN. In addition, neither c-Myc nor B56-beta levels were affected (Supplementary Figure S3*A*). We further tested phosphorylation levels of the Bad protein after Pim-1 knockdown. We expected a

decrease in cellular phospho-Bad levels due to abrogating the Pim-1-catalysed phosphorylation of Bad, and, as a consequence, an increase in apoptosis. However, phospho-Bad levels remained unchanged after Pim-1 knockdown (Figure 2*A*), as was the disposition of cells to undergo apoptosis (Figure 2*B*). This indicates that other cellular kinases like Akt [1] take over the function of Pim-1 with respect to phosphorylation of Bad and that a direct effect of Pim-1 on apoptosis is not evident in K562 cells.

In contrast, proliferation assays revealed that the Pim-1 knockdown caused inhibition of cell proliferation (Figure 2*C*). This was accompanied by a weak but measurable effect on cell cycle, leading to decreased cell numbers in the G1 phase and increased cell numbers in G2/M (Supplementary Figure S3*B*). Treatment of cells with nocodazol followed by release of the cells from the mitotic block enhanced the effect of the Pim-1 knockdown on cell cycle (Figure 2*D*). Under these conditions the number of cells in G1-phase were substantially decreased compared to nocodazol-treated control cells. Likewise, the number of cells in G2/M-phase was elevated, demonstrating that Pim-1 is involved in regulating the progression of cells through G2/M-phase. We further observed that two days after releasing the cells from the nocodazol block in G2/M-phase, control cells (treated with control siRNA) but not Pim-1 knockdown resumed proliferation. However, three days after nocodazol treatment (six days after siRNA transfection) the Pim-1 knockdown cells also regained their capacity to proliferate (data not shown), suggesting that siRNA inhibition attenuates after this period.

Induction of p21 favours apoptosis

Since K562 cells are p53-deficient [33] and Bad was excluded (see above) as the trigger of apoptosis in OA-treated K562 cells, we focussed our attention on p21. As mentioned, p21 is essentially not detectable in K562 cells (Figure 1*A*). However, its OA-dependent induced expression suggested the need for a checkpoint control of the cell cycle under these conditions. To address the functional link between OA-dependent p21 expression and induction of apoptosis (Figures 1*A*, *C*), we combined RNAi against p21 with subsequent OA treatment. Under these conditions, p21 induction was repressed to a large extent (12 h) or even below (other time points) the level of detection (Figure 3*A*). The p21 knockdown prevented OA-dependent activation of apoptosis at time point 6 h, but apoptosis increased again at time point 12 h (Figure 3*B*). These findings demonstrate an essential role for p21 at the early onset (after 6 h) of apoptosis under conditions of PP2A inhibition. Furthermore, this suggests a compensation mechanism that becomes operational when p21 is down-regulated, thus substituting p21 in apoptosis induction.

Basal p21 levels are repressed by miR-17-5p and miR-20a

The fact that K562 cells harbour substantial basal levels of p21 mRNA, but do not express detectable amounts of p21 protein, suggest that p21 expression is controlled on the post-transcriptional level. Interestingly, the 3´-UTR of p21 mRNA harbours two target sites for members of the *miR-106b* microRNA family [34]. Two members of this family, *miR-17-5p* and *miR-20a*, are encoded in the *miR-17-92* cluster that is overexpressed in K562 cells and in human lung cancer cells (Figure 4*A*; [35, 36]).

To address whether p21 mRNAs are under the control of *miR-17-5p/-20a*, we pursued an AntagomiR approach. However, instead of applying the commonly used 2´-O-methylated antisense oligonucleotides directed against the full-length mature miRNA [37], we explored shorter all-LNA AntimiRs (8- to 14-mers) complementary to the seed region in order to develop efficient and highly specific AntimiRs for further *in vivo* studies. A *let-7a* target side in the 3'-UTR of a luciferase reporter gene was used to determine the minimum AntimiR length for efficient miRNA inactivation [27]. Derepression leading to about 80% of maximum luciferasse expression was obtained with a 10-mer all-LNA AntimiR at 50 nM (Figure 4*B*),

and all-LNA 12- or 14-mer AntimiRs essentially fully derepressed the luciferase reporter at a concentration of 10 nM (Figure 4*B*). Based on these findings, we transfected K562 cells with 14-mer all-LNA-AntimiRs against *miR-17-5/-20a* to analyse translational repression of p21 mRNA. Indeed, these LNA-AntimiRs specifically released p21 mRNA from miRNA-dependent translational repression as shown by the appearance of p21 protein (Figure 4*C*). We then transfected the all-LNA-AntimiRs into K562 cells followed by addition of OA to test if miRNAs *miR-17-5p* and *miR-20a* are responsible for the down-regulation of p21 levels after 24 h following its transient burst of expression (see Figure 1*A*). However, the presence of these LNA-AntimiRs did not affect the dynamic changes in p21 expression (Figure 4*D*), demonstrating that *miR-17-5p/-20a* neither affected the increase in p21 expression nor its down-regulation at the protein level at later time points of OA treatment. We further investigated the effects of AntimiRs against *miR-17-5p/-20a* on apoptosis because it was reported that an AntagomiR approach against these two miRNAs induces apoptosis in lung cancer cells [36]. Yet, no such effect was seen in K562 cells (Figure 4*E*) demonstrating that the OA-induced large increase in p21, but not basal low expression levels, can induce apoptosis. This suggests that the role of suppression of basal p21 protein levels in K562 cells is to favour rapid cell cycle progression rather than affecting apoptosis (see Discussion).

Mutagenesis of miR-17-5p/-20a seeds in the 3´-UTR of p21

To analyse the regulation of p21 by miRNAs of the *miR-106b* family in more detail, we fused the 3'-UTR of the p21 mRNA to a luciferase reporter gene. Luciferase activity was increased 1.7-fold when the p21 3'-UTR reporter construct was co-transfected with LNA-AntimiRs specific for *miR-17-5p* and *miR-20a*, (Figure 5). Surprisingly, mutagenesis of the 5'-proximal seed (seed 1) failed to cause a significant derepression of luciferase reporter expression. However, mutagenesis of the second seed (seed 2) resulted in luciferase derepression, comparable in strength to the observed AntimiR effect on the wildtype reporter (Figure 5), indicating selective miRNA binding to the seed 2 target region. Surprisingly, combining the seed 2 mutant construct with AntimiR treatment enhanced luciferase derepression to a level (~ 2.5-fold) comparable to that when both seeds are mutated. As expected, AntimiR treatment of the construct with both seeds mutated showed no further effect. Our findings indicate a cooperative effect of the two seeds in translational repression of p21 mRNA.

Discussion

Our primary interest was a better understanding of the role of Pim-1 with regard to cell proliferation and apoptosis. The human myeloid leukemia cell line K562 was selected as a model cell line since it expresses particularly high levels of Pim-1. It had already been established that Pim-1 is able to interact with c-Myc on the chromatin level, which mediates Pim-1-catalysed histone H3 phosphorylation, thus activating transcription of various genes and increasing the transformation capacity of the cell [4]. It was further known that Pim-1 is able to phosphorylate Bad and thus counteract apoptosis [17, 19].

We applied two strategies to analyse the function of Pim-1 in K562 cells in more detail: (i) siRNA-mediated knockdown to deplete cells specifically of Pim-1 and (ii) treatment of cells with the PP2A inhibitor OA. The latter more indirect strategy was pursued because there are intimate functional links between PP2A and Pim-1: PP2A is involved in Pim-1 degradation and its inhibition is known to increase Pim-1 levels; also, PP2A can induce apoptosis by dephosphorylation of the pro-apoptotic protein Bad, which is a phosphorylation

target of Pim-1. Also, OA treatment had been shown to increase the cellular levels of Pim-1 after 1 h of drug addition in the murine hematopoietic cell line BaF3 [14], which is expected owing to reduced PP2A-mediated Pim-1 degradation. However, this observed increase in cellular Pim-1 levels apparently contradicted the reported observation that OA treatment causes mitotic arrest and apoptosis in K562 cells [21].

Time-resolved effects of OA treatment

To clarify the apparent discrepancy between the expected Pim-1 stabilisation and the induction of apoptosis upon PP2A inhibition by OA (see above), we analysed K562 cells at different time points after OA addition. This unveiled dynamic time-dependent changes of Pim-1 levels. Furthermore, a Bad-independent pathway is able to induce apoptosis in K562 cells. Also, considering that phospo-Bad levels did not change after Pim-1 knockdown (Figure 2*A*), we infer that another kinase than Pim-1 is able to phosphorylate Bad and, combined with the missing dephosphorylation activity of PP2A after OA treatment, results in increased phospho-Bad levels.

OA induces transient p21 expression

Another novel finding of our study is the transient induction of p21 upon OA treatment, resulting from an increase in p21 mRNA levels. In contrast, the basal levels of p21 mRNA in K562 cells under standard growth conditions were found to be translationally repressed by *miR-17-5p* and *miR-20a* (Figures 4*C-E*). These miRNAs, which belong to the *miR-106b* family, are encoded in the *miR-17-92* cluster that is highly expressed in K562 cells (Figure 4*A*) and other chronic myeloid leukemia cell lines [35]. It has been reported that miRNAs from the *miR-106b* family are able to regulate the cell cycle by reducing p21 levels in immortalised human mammary epithelial cells (HMECs) [34]. In HMECs, constitutive p21 protein levels were detectable, which were reduced approximately 2-fold when *miR-106b* was overexpressed or increased 1.5-fold when cells were transfected with AntimiRs against the *miR-106b* family [34]. This is in line with the commonly observed fine tuning of gene expression by miRNAs [38, 39]. In comparison, the situation in K562 cells fundamentally differs in that the two *miR-106b* family members entirely suppress translation of basal p21 mRNA levels. Based on our findings, we think it likely that the blockage of translation of basal p21 mRNA levels by *miR-17-5p/-20a* contributes to a diminished checkpoint control in K562 cells, thus favouring proliferation.

To understand the miRNA-dependent repression of p21 in more detail, we performed seed mutagenesis experiments. To our surprise, the mutagenesis of seed 1 had essentially no effect on the expression of a luciferase reporter, whereas mutagenesis of seed 2 caused a 1.7-fold derepression, equal in strength to the AntimiR effect (Figure 5). Secondary structure predictions (Mfold) [40] of the p21 3´-UTR suggest that seed 2 is embedded in a structurally less rigid and A/U-richer region than seed 1 (data not shown). In line with our seed mutagenesis experiments, this would explain why *miR-17-5p/-20a* primarily target seed 2. Nevertheless, mutagenesis of both seeds resulted in a cooperative effect (2.5-fold derepression), suggesting that miRNA-mediated translational repression in the p21 3'-UTR is mechanistically more complex.

P21 protein levels were only transiently elevated after OA addition in K562 cells and became again non-detectable at 24 h, although p21 mRNA levels remained high and apoptosis continued. We could exclude *miR-17-5p/-20a* as being responsible for the down-regulation of p21 protein at later time points because blocking these miRNAs by LNA-AntimiRs did not alter the OA-dependent p21 expression profile. Therefore, other mechanisms of translational repression and/or induction of p21 decay pathways must be responsible for the observed p21 disappearance at later time points.

A pre-incubation of cells with siRNAs against p21 delayed the induction of OA-dependent apoptosis (Figure 3*B*). This may be related to the protein's capacity to interact with PCNA during S-phase to stall the replication fork to ensure repair of damaged DNA [41]. Furthermore, p21 stabilises cyclin B1 and therefore the Cdk1/Cyclin B1 complex, which should result in a delay of mitosis [42].

Previously, ectopic p53 expression in K562 cells, which lack the tumor suppressors p53 and ARF, induced growth arrest, apoptosis and the transactivation of p21; simultaneous overexpression of c-Myc counteracted p53-induced apoptosis and down-regulated transcriptional activation of several p53 target genes including p21 [43, 44]. At first sight, these observations would be consistent with a key role for p21 in promoting apoptosis in K562 cells in general. Yet, in the same cell line, antisense inhibition of p21 did not reduce p53-mediated apoptosis [43], nor did up-regulation of p21 by p53 mutant proteins promote apoptosis [45]. Thus, a role for p21 in apoptosis seems to be context-dependent, and the delay in apoptosis induction upon silencing of p21 in K562 cells may be a specific consequence of PP2A inhibition. Assuming that Pim-1 phosphorylates p21 [12] also in K562 cells, the complete absence of Pim-1 in K562 cells after > 3 h of OA-treatment and the concomitant transient induction of p21 may result in a prevalence of unphosphorylated p21. This, in turn, may favour a more persistent block of the replication fork by interaction of p21 with PCNA, thus triggering the observed p21-dependent onset of apoptosis.

Pim-1 is essential for cell proliferation, but not apoptosis, in K562 cells

The reduction of endogenous Pim-1 levels by RNAi was previously shown to affect the proliferation capacity in the human lung carcinoma cell line H1299 and in K562 cells [22, 46]. Our efficient knockdown of Pim-1 protein levels in K562 cells (Figure 2*A*), resulting in inhibition of cell proliferation (Figure 2*D*), substantiates these findings. In contrast to Zhang et al., [46], however, we did not observe significant reductions in c-Myc levels upon Pim-1 knockdown (Supplementary Figure S3*A*). Instead, we demonstrate that a Pim-1 knockdown in K562 cells affects the cell cycle by decreasing the number of cells in G1 while increasing the number of those in G2/M-phase (Figure 2*D*), indicating a role of Pim-1 in promoting the transition from G2/M to G1.

RNAi against Pim-1 had no effect on apoptosis, which is in line with the absence of a Pim-1 effect on the phosphorylation status of Bad (Figure 2*A*). Thus, at least in the absence of expression of the Pim-1 target p21, an effect of Pim-1 on apoptosis is not evident. Finally, our and previous findings suggest that the functional relationships of Pim-1 in the cellular context are expected to be complex and the list of known Pim-1 targets is likely incomplete. Thus, towards understanding the regulatory network of Pim-1 and the molecular basis underlying the cell proliferation block after Pim-1 knockdown, comparative global analyses of cells expressing Pim-1 at largely different levels will be required.

Conclusions

Figure 6 summarises our findings. We have shown that inhibition of PP2A in K562 cells results in time-dependent dynamic and converse changes in the levels of Pim-1 and p21. OA-dependent induction of apoptosis is Bad-independent and an early onset of OA-induced apoptosis depends on transient expression of p21, as shown by siRNA-mediated knockdown of p21. K562 cells are able to entirely repress translation of basal levels of p21 mRNA by miRNAs *miR-17-5p* and *miR-20a*; yet, these miRNAs have no effect on the disappearance of p21 at later time points of OA treatment. Pim-1 has no detectable effect on apoptosis but is essential for proliferation of K562 cells. The complete cell proliferation block upon Pim-1 depletion and the mild phenotype of Pim kinase knockout mice [47] emphasise the potential of Pim-1 as an anti-cancer drug target.

Acknowledgements

We thank Sandra Dall, Moana Klein and Dennis Streng for technical support. This study was supported by the Fritz Thyssen Stiftung (Az. 10.06.1.186) and the Deutsche Forschungsgemeinschaft (HA 1672/7-3/4/5), and funded in part by a grant from the Deutsche Krebshilfe to D.G. and A.A.

References

[1] Amaravadi R, and Thompson CB (2005). The survival kinases Akt and Pim as potential pharmacological targets. J. Clin. Invest. **115**, 2618-2624.

[2] van Lohuizen M, Verbeek S, Krimpenfort P, Domen J, Saris C, Radaszkiewicz T, and Berns A. (1989). Predisposition to lymphomagenesis in pim-1 transgenic mice: cooperation with c-myc and N-myc in murine leukemia virus-induced tumors. Cell **56**, 673-682.

[3] Verbeek S, van Lohuizen M, van der Valk M, Domen J, Kraal G, and Berns, A (1991). Mice bearing the E mu-myc and E mu-pim-1 transgenes develop pre-B-cell leukemia prenatally. Mol. Cell. Biol. **11**, 1176-1179.

[4] Zippo A, De Robertis A, Serafini R, and Oliviero, S (2007). PIM1-dependent phosphorylation of histone H3 at serine 10 is required for MYC-dependent transcriptional activation and oncogenic transformation. Nat. Cell. Biol. **9**, 932-944.

[5] Qian KC, Wang L, Hickey ER, Studts J, Barringer K, Peng C. Kronkaitis A, Li J, White A, Mische S, and Farmer B (2005). Structural basis of constitutive activity and a unique nucleotide binding mode of human Pim-1 kinase. J. Biol. Chem. **280**, 6130-6137.

[6] Heinrich PC, Behrmann I, Haan S, Hermanns HM, Müller-Newen G, and Schaper F (2003). Principles of interleukin (IL)-6-type cytokine signalling and its regulation. Biochem. J. **374**, 1-20.

[7] Bachmann M, and Möröy T (2005). The serine/threonine kinase Pim-1. Int. J. Biochem. Cell. Biol. **37**, 726-730.

[8] Mochizuki T, Kitanaka C, Noguchi K, Muramatsu T, Asai A, and Kuchino Y (1999). Physical and functional interactions between Pim-1 kinase and Cdc25A phosphatase. Implications for the Pim-1-mediated activation of the c-Myc signaling pathway. J. Biol. Chem. **274**, 18659-18666.

[9] Bachmann M, Kosan C, Xing PX, Montenarh M, Hoffmann I, and Möröy T (2006). The oncogenic serine/threonine kinase Pim-1 directly phosphorylates and activates the G2/M specific phosphatase Cdc25C. Int. J. Biochem. Cell. Biol. **38**, 430-443.

[10] Koike N, Maita H, Taira T, Ariga H, and Iguchi-Ariga SM (2000). Identification of heterochromatin protein 1 (HP1) as a phosphorylation target by Pim-1 kinase and the effect of phosphorylation on the transcriptional repression function of HP1. FEBS Lett. **467**, 17-21.

[11] Leverson JD, Koskinen PJ, Orrico FC, Rainio EM, Jalkanen KJ, Dash AB, Eisenman RN, and Ness SA (1998). Pim-1 kinase and p100 cooperate to enhance c-Myb activity. Mol. Cell **2**, 417-425.

[12] Wang Z, Bhattacharya N, Mixter PF, Wei W, Sedivy J, and Magnuson NS (2002). Phosphorylation of the cell cycle inhibitor p21Cip1/WAF1 by Pim-1 kinase. Biochim. Biophys. Acta. **1593**, 45-55.

[13] Losman JA, Chen XP, Vuong BQ, Fay S, and Rothman PB, (2003). Protein phosphatase 2A regulates the stability of Pim protein kinases. J. Biol. Chem. **278**, 4800-4805.

[14] Ma J, Arnold HK, Lilly MB, Sears RC, and Kraft AS (2007). Negative regulation of Pim-1 protein kinase levels by the B56beta subunit of PP2A. Oncogene **26**, 5145-5153.

[15] Shay KP, Wang Z, Xing PX, McKenzie IF, and Magnuson NS (2005). Pim-1 kinase stability is regulated by heat shock proteins and the ubiquitin-proteasome pathway. Mol. Cancer Res. **3**, 170-181.

[16] Chiang CW, Kanies C, Kim KW, Fang WB, Parkhurst C, Xie M, Henry T, and Yang E (2003). Protein phosphatase 2A dephosphorylation of phosphoserine 112 plays the gatekeeper role for BAD-mediated apoptosis. Mol. Cell. Biol. **23**, 6350-6362.

[17] Aho TL, Sandholm J, Peltola KJ, Mankonen HP, Lilly M, and Koskinen PJ (2004). Pim-1 kinase promotes inactivation of the pro-apoptotic Bad protein by phosphorylating it on the Ser112 gatekeeper site. FEBS Lett. **571**, 43-49.

[18] Yan B, Zemskova M, Holder S, Chin V, Kraft A, Koskinen PJ, and Lilly M (2003). The PIM-2 kinase phosphorylates BAD on serine 112 and reverses BAD-induced cell death. J. Biol. Chem. **278**, 45358-45367.

[19] Macdonald A, Campbell DG, Toth R, McLauchlan H, Hastie CJ, and Arthur JS (2006). Pim kinases phosphorylate multiple sites on Bad and promote 14-3-3 binding and dissociation from Bcl-XL. BMC Cell Biol. **10**, 7:1.

[20] Benito A, Lerga A, Silva M, Leon J, and Fernandez-Luna JL (1997). Apoptosis of human myeloid leukemia cells induced by an inhibitor of protein phosphatases (okadaic acid) is prevented by Bcl-2 and Bcl-X(L). Leukemia **11**, 940-944.

[21] Lerga A, Richard C, Delgado MD, Cañelles M, Frade P, Cuadrado MA, and León J (1999). Apoptosis and mitotic arrest are two independent effects of the protein phosphatases inhibitor okadaic acid in K562 leukemia cells. Biochem. Biophys. Res. Commun. **260**, 256-64.

[22] Zhang Y, Wang Z, and Magnuson NS (2007). Pim-1 kinase-dependent phosphorylation of p21Cip1/WAF1 regulates its stability and cellular localization in H1299 cells. Mol. Cancer Res. **5**, 909-922.

[23] Rössig L, Jadidi AS, Urbich C, Badorff C, Zeiher AM, and Dimmeler S (2001). Akt-dependent phosphorylation of p21(Cip1) regulates PCNA binding and proliferation of endothelial cells. Mol. Cell. Biol. **21**, 5644-5657.

[24] Gruegelsiepe H, Brandt O, and Hartmann RK (2006). Antisense inhibition of RNase P: mechanistic aspects and application to live bacteria. J Biol Chem. **281**, 30613-30620.

[25] Grünweller A, Wyszko E, Bieber B, Jahnel R, Erdmann VA, and Kurreck J (2003). Comparison of different antisense strategies in mammalian cells using locked nucleic acids, 2'-O-methyl RNA, phosphorothioates and small interfering RNA. Nucleic Acids Res. **31**, 3185-3193.

[26] Schmittgen TD (2001). Real-time quantitative PCR. Methods **25**, 383-385.

[27] Brennecke J, Stark A, Russell RB, and Cohen SM (2005). Principles of microRNA-target recognition. PLoS Biol. **3**, e85.

[28] Amson R, Sigaux F, Przedborski S, Flandrin G, Givol D, and Telerman A (1989). The human protooncogene product p33pim is expressed during fetal hematopoiesis and in diverse leukemias. Proc. Natl. Acad. Sci. U S A **86**, 8857-8861.

[29] Muñoz-Alonso MJ, Acosta JC, Richard C, Delgado MD, Sedivy J, and León J (2005). p21Cip1 and p27Kip1 induce distinct cell cycle effects and differentiation programs in myeloid leukemia cells. J. Biol. Chem. **280**, 18120-18129.

[30] Luciano F, Jacquel A, Colosetti P, Herrant M, Cagnol S, Pages G, and Auberger P (2003). Phosphorylation of Bim-EL by Erk1/2 on serine 69 promotes its degradation via the proteasome pathway and regulates its proapoptotic function. Oncogene. **22**, 6785-6793.

[31] Ventura A, Young AG, Winslow MM, Lintault L, Meissner A, Erkeland SJ, Newman J, Bronson RT, Crowley D, Stone JR, Jaenisch R, Sharp PA, and Jacks T (2008). Targeted deletion reveals essential and overlapping functions of the miR-17 through 92 family of miRNA clusters. Cell **132**, 875-886.

[32] Fontana L, Fiori ME, Albini S, Cifaldi L, Giovinazzi S, Forloni M, Boldrini R, Donfrancesco A, Federici V, Giacomini P, Peschle C, and Fruci D (2008). Antagomir-17-5p abolishes the growth of therapy-resistant neuroblastoma through p21 and BIM. PLoS ONE **3**, e2236.

[33] Ehinger M, Nilsson E, Persson AM, Olsson I, and Gullberg U (1995). Involvement of the tumor suppressor gene p53 in tumor necrosis factor-induced differentiation of the leukemic cell line K562. Cell Growth Differ. **6**, 9-17.

[34] Ivanovska I, Ball AS, Diaz RL, Magnus JF, Kibukawa M, Schelter JM, Kobayashi SV, Lim L, Burchard J, Jackson AL, Linsley PS, and Cleary MA (2008). MicroRNAs in the miR-106b family regulate p21/CDKN1A and promote cell cycle progression. Mol. Cell. Biol. **28**, 2167-2174.

[35] Venturini L, Battmer K, Castoldi M, Schultheis B, Hochhaus A, Muckenthaler MU, Ganser A, Eder M, and Scherr M (2007). Expression of the miR-17-92 polycistron in chronic myeloid leukemia (CML) CD34+ cells. Blood **109**, 4399-4405.

[36] Hayashita Y, Osada H, Tatematsu Y, Yamada H, Yanagisawa K, Tomida S, Yatabe Y, Kawahara K, Sekido Y, and Takahashi T (2005). A polycistronic microRNA cluster, miR-17-92, is overexpressed in human lung cancers and enhances cell proliferation. Cancer Res. **65**, 9628-9632.

[37] Krützfeldt J, Rajewsky N, Braich R, Rajeev KG, Tuschl T, Manoharan M, and Stoffel M (2005). Silencing of microRNAs in vivo with 'antagomirs'. Nature **438**, 685-689.

[38] Baek D, Villén J, Shin C, Camargo FD, Gygi SP, and Bartel DP (2008). The impact of microRNAs on protein output. Nature **455**, 64-71.

[39] Selbach M, Schwanhäusser B, Thierfelder N, Fang Z, Khanin R, and Rajewsky N (2008). Widespread changes in protein synthesis induced by microRNAs. Nature **455**, 58-63.

[40] Zuker M (2003). Mfold web server for nucleic acid folding and hybridization prediction. Nucleic Acids Res. **31**, 3406-3415.

[41] Waga S, Hannon GJ, Beach D, and Stillman B (1994). The p21 inhibitor of cyclin-dependent kinases controls DNA replication by interaction with PCNA Nature **369**, 574-578.

[42] Charrier-Savournin FB, Château MT, Gire V, Sedivy J, Piette J, and Dulic V (2004). p21-Mediated nuclear retention of cyclin B1-Cdk1 in response to genotoxic stress. Mol. Biol. Cell. **15**, 3965-3976.

[43] Ceballos E, Delgado MD, Gutierrez P, Richard C, Müller D, Eilers M, Ehinger M, Gullberg U, and León J (2000). c-Myc antagonizes the effect of p53 on apoptosis and p21WAF1 transactivation in K562 leukemia cells. Oncogene **19**, 2194-2204.

[44] Ceballos E, Muñoz-Alonso MJ, Berwanger B, Acosta JC, Hernández R, Krause M, Hartmann O, Eilers M, and León J (2005). Inhibitory effect of c-Myc on p53-induced

apoptosis in leukemia cells. Microarray analysis reveals defective induction of p53 target genes and upregulation of chaperone genes. Oncogene **24**, 4559-4571.

[45] Kobayashi T, Consoli U, Andreeff M, Shiku H, Deisseroth AB, and Zhang W (1995). Activation of p21WAF1/Cip1 expression by a temperature-sensitive mutant of human p53 does not lead to apoptosis. Oncogene **11**, 2311-2316.

[46] Zhang Y, Wang Z, Li X, and Magnuson NS (2008). Pim kinase-dependent inhibition of c-Myc degradation. Oncogene **27**, 4809-4819.

[47] Mikkers H, Nawijn, M, Allen J, Brouwers C, Verhoeven E, Jonkers J, and Berns A (2004). Mice deficient for all PIM kinases display reduced body size and impaired responses to hematopoietic growth factors. Mol Cell Biol. **24**, 6104-6115.

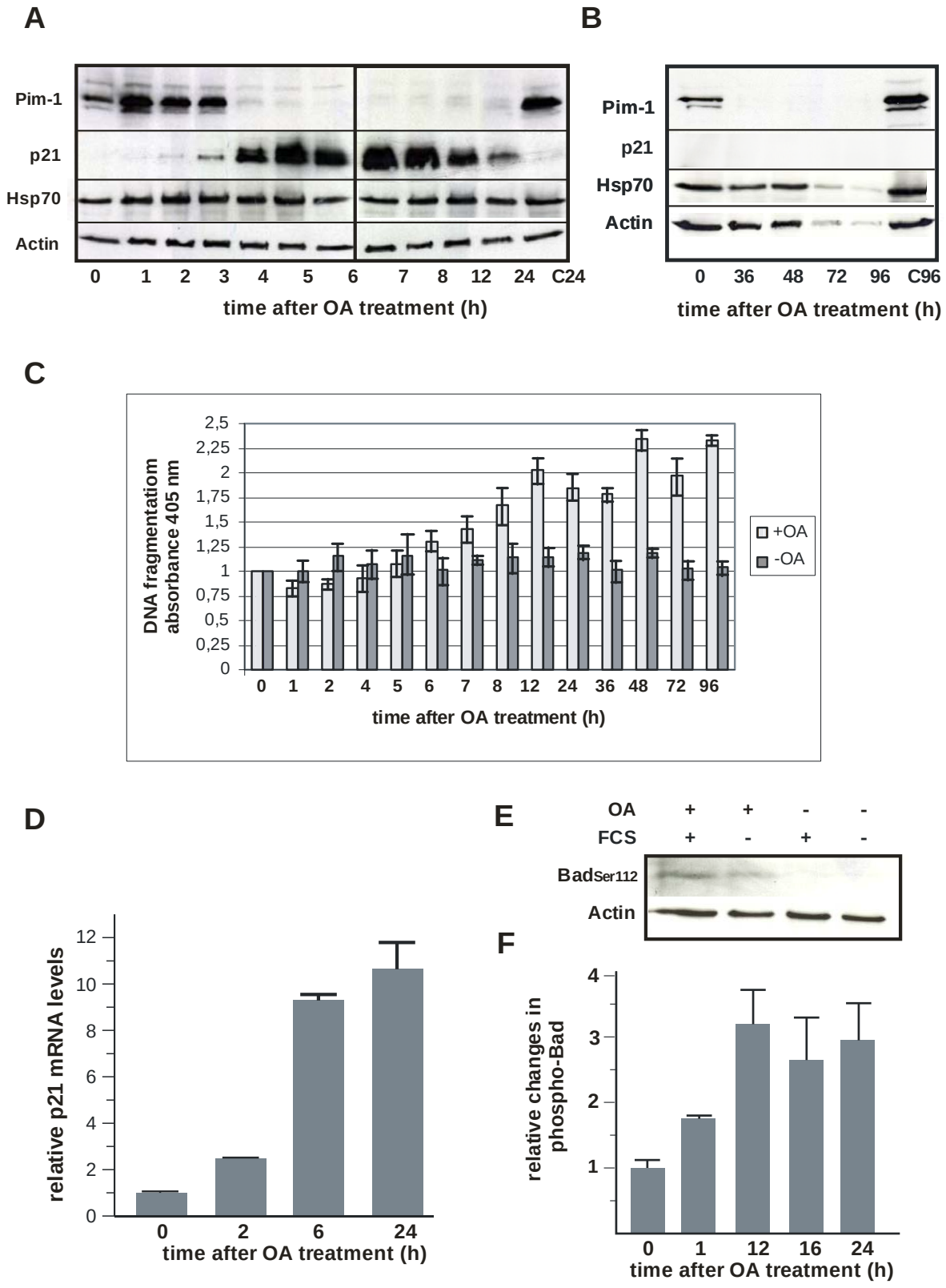

Fig.1

Figure 1. Effects of PP2A inhibition on Pim-1, p21 and phospho-Bad levels as well as apoptosis. (A) K562 cells were treated for the indicated times (up to 24 h) with 100 nM OA. After cell lysis proteins were separated on 15% SDS-PAA gels and expression levels of Pim-1, p21 and Hsp70 were analysed by Western blotting with beta-Actin as a loading control.

C24, mock-treated cells (no OA addition) after 24 h. (B) Protein levels (as in panel *A*) at later time points of OA treatment (36 to 96 h). Time point 0, cells lysed immediately after OA addition; C96, mock-treated cells (no OA addition) after 96 h. (C) DNA fragmentation at different time points after OA addition as a measure of apoptosis; cells were grown as in panels (A) and (B). Untreated cells (-OA) were used as controls for each time point. (D) p21 mRNA levels analysed by qRT-PCR. Cells were treated with 100 nM OA for the indicated times, followed by isolation of total RNA and reverse transcription. Quantitation of p21 mRNA was conducted with a light cycler and *actin* as an internal standard. OA treatment induced an approx. 10-fold increase in p21 mRNA levels compared to the basal level. (E) Western blot analysis with an antibody specific for Bad phosphorylated at serine 112. Cells were treated for 24 h with 100 nM OA in the presence of 10% (+) or 0.1% (-) FCS. Before OA addition, -FCS cells were deprived of serum for 72 h. Phosphorylation of Bad at serine 112 could only be detected in the presence of OA. (F) Cells were treated with 100 nM OA for the indicated time periods. The amount of phosphorylated Bad was estimated by a quantitative ELISA. The ratio of serine 112-phosphorylated Bad protein to total Bad protein was determined and normalised to the cell number. Note that the total Bad levels remained essentially unchanged at different time points (variation $\leq$ 20%). The results shown in (C), (D) and (F) represent mean values from at least three independent experiments; errors bars are standard deviations (SD).

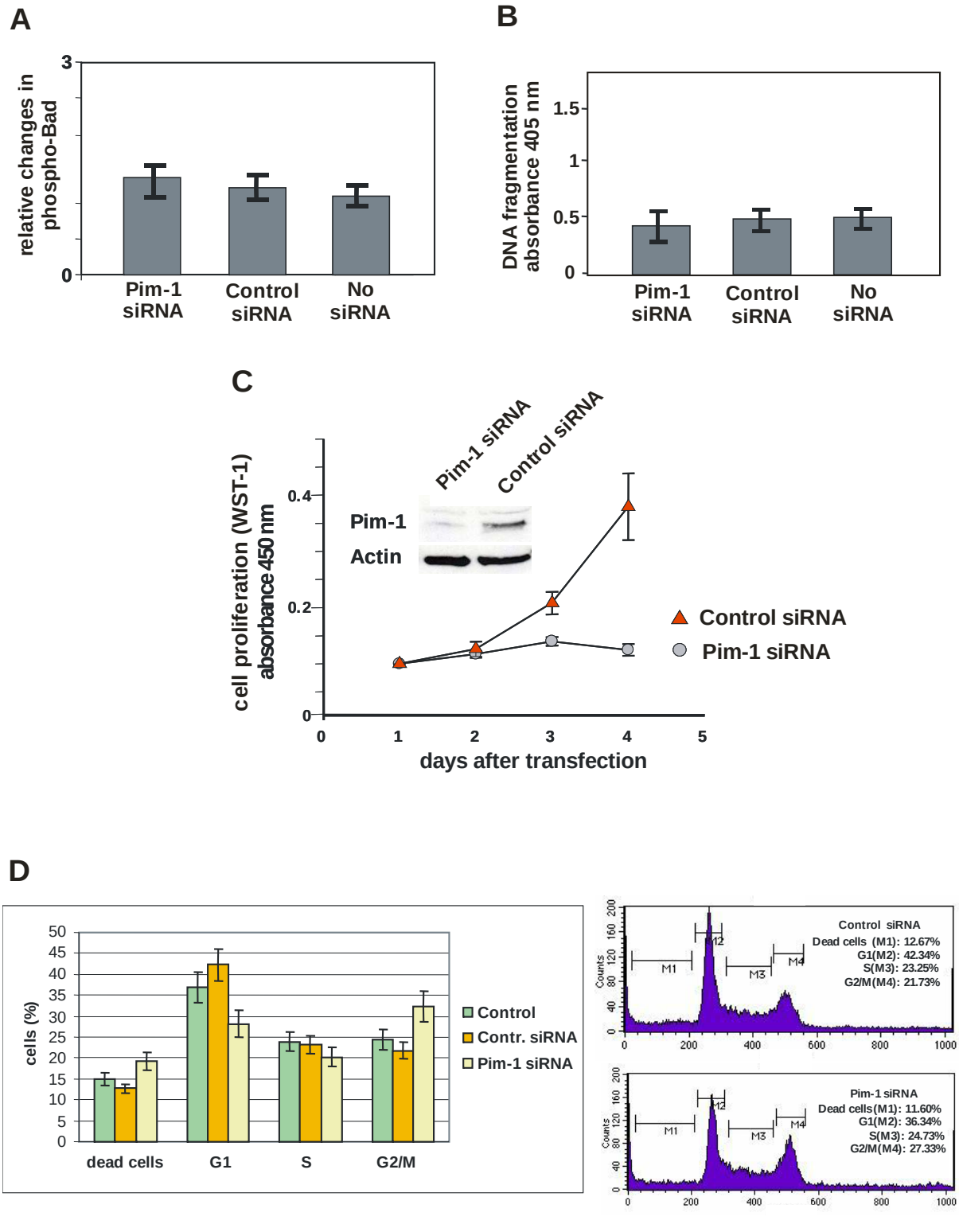

Fig. 2

Figure 2. Effects of Pim-1 knockdown on Bad phosphorylation at serine 112, apoptosis and cell proliferation. (A) Fraction of serine 112-phosphorylated Bad for cells transfected with the Pim-1-specific siRNA, a sequence-unrelated control siRNA (VR1 siRNA) or without any siRNA; for further details, see legend to Fig. 1 F. (B) As in (A), but quantitation of DNA

fragmentation as a measure of apoptosis. (C) Knockdown of Pim-1 inhibited the proliferation of K562 cells. K562 cells were transfected with the Pim-1-specific siRNA or the control VR1 siRNA and cell proliferation, inferred from the cleavage of the tetrazolium salt WST-1 to formazan by the overall activity of mitochondrial dehydrogenases, was measured at the indicated time points post-transfection. (D) Knockdown of Pim-1 in combination with nocodazol treatment reveals interference with transition from G2/M to G1 phase of the cell cycle. K562 cells were transfected with the Pim-1-specific siRNA or the control VR1 siRNA. After 24 h, nocodazol was added; the drug was washed out after another 24 h; cells were analysed by FACS 48 h after release from the nocodazol-dependent M-phase block. Values were derived from three independent experiments. Representative FACS profiles of propidiume iodide stained cells after siRNA treatment are shown at the right. Data shown in (A) - (D) represent mean values from at least three independent experiments; errors bars, SD.

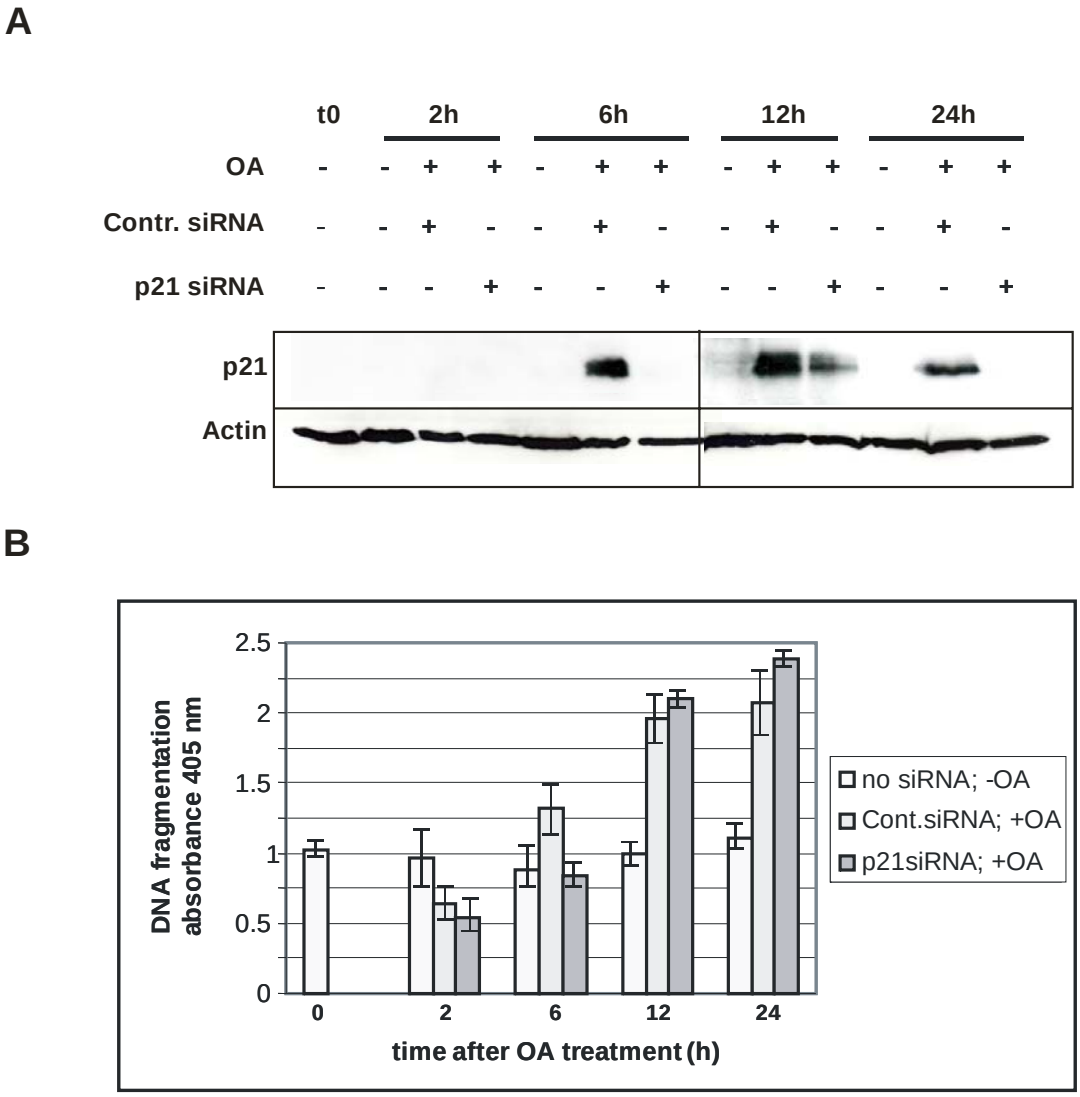

Figure 3. p21 silencing retards the onset of apoptosis in OA-treated K562 cells. (A) Cells were transfected with the p21-specific or a control (VR1) siRNA; after 24 h, 100 nM OA was added to the cells, which were harvested after further 2, 6, 12 and 24 h of incubation; p21 and beta-Actin levels were analysed by Western blotting; mock-treated cells (no siRNA, no OA) were analysed in parallel; t0, K562 cells before siRNA transfection and OA addition. (B) Apoptosis was measured at the same time points as in panel (A) by the DNA fragmentation ELISA (see Experimental section). Shown are mean values from at least three independent experiments; errors bars, SD.

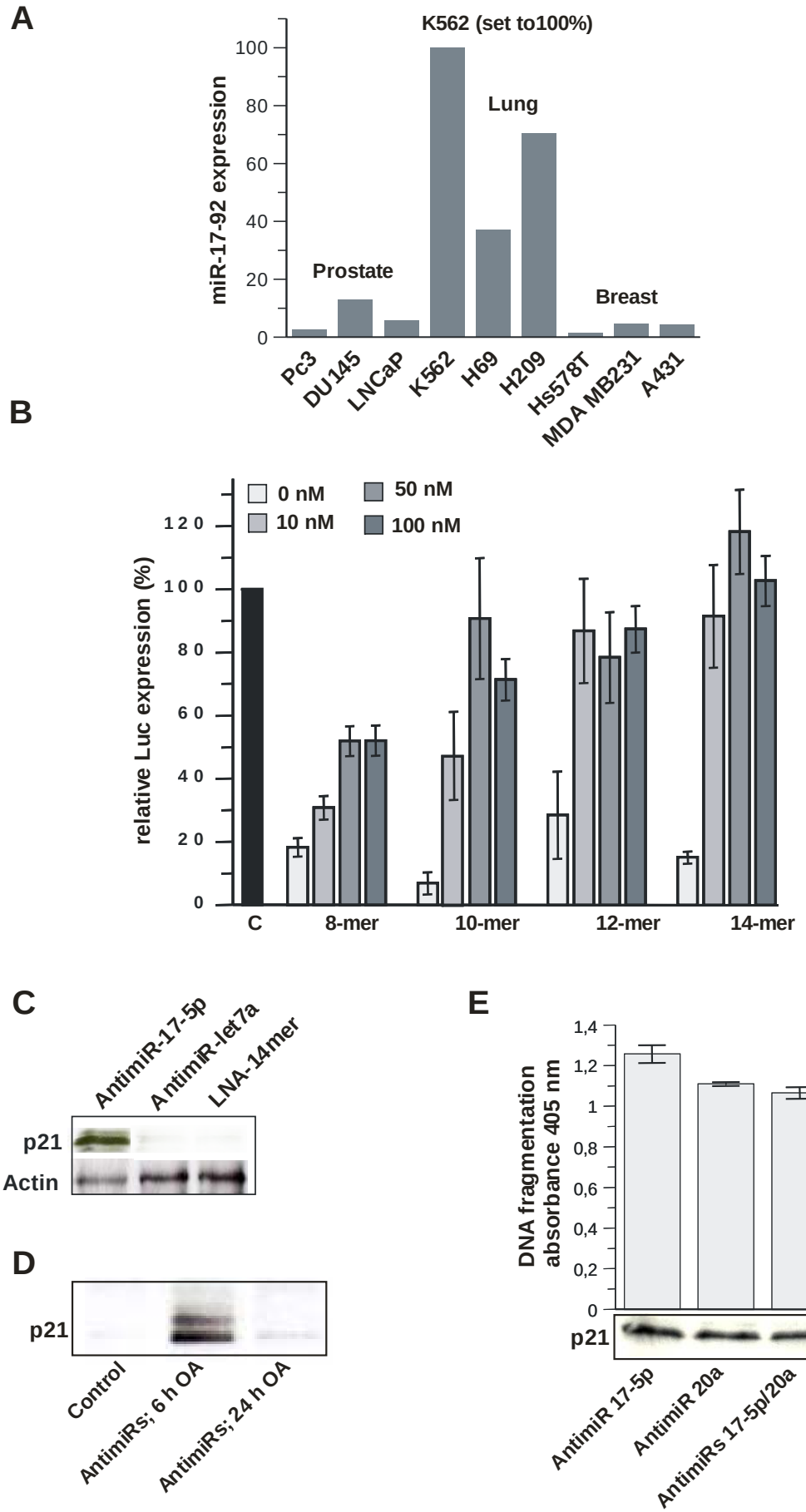
A
K562 (set to100%)
Lung
Prostate
Breast
miR-17-92 expression
100
80
60
40
20
0
Pc3
DU145
LNCaP
K562
H69
H209
Hs578T
MDA MB231
A431
B
0 nM
10 nM
50 nM
100 nM
relative Luc expression (%)
120
100
80
60
40
20
0
C
8-mer
10-mer
12-mer
14-mer
C
AntimiR-17-5p
AntimiR-let7a
LNA-14mer
p21
Actin
D
p21
Control
AntimiRs; 6 h OA
AntimiRs; 24 h OA
E
DNA fragmentation absorbance 405 nm
1,4
1,2
1
0,8
0,6
0,4
0,2
0
p21
AntimiR 17-5p
AntimiR 20a
AntimiRs 17-5p/20a
Control

Fig. 4

Figure 4. Translation of basal p21 mRNA levels is entirely repressed by *miR-17-5p* and *miR-20a.* (A) Expression levels of the *miR-17-92* cluster in different cell lines demonstrating overexpression in K562 cells. (B) Inhibition of the miRNA *let-7a* by short all-LNA AntimiRs, 8, 10, 12 or 14 nt in length, directed against the seed region of *let-7a*; AntimiRs were co-transfected with a luciferase reporter construct harbouring a single *let-7a* binding site. Concentrations of the LNA-AntimiRs are indicated. C, expression of a luciferase reporter harbouring an inverted *let-7a* sequence (set to 100%); the extent of derepression of reporter translation by the LNA-AntimiRs was normalised to this control. (C) p21 protein levels increase after transfection of K562 cells with 14-mer all-LNA-AntimiRs complementary to miRNAs *miR-17-5p* and *miR-20a* encoded in the *miR-17-92* cluster. 14-mer all-LNA AntimiRs against *let-7a* and *Escherichia coli* RNase P RNA served as negative controls. Beta-Actin served as a loading control. (D) Transfection of K562 cells with LNA-AntimiRs against *miR-17-5p* and *miR-20a* neither affected the transient burst of p21 protein expression after 6 h nor the disappearance of p21 after 24 h of OA treatment. 24 h after transfection of cells with LNA-AntimiRs, OA was added. Control: no OA added. (E) Transfection of K562 cells with AntimiRs against *miR-17-5p* and *miR-20a* did not result in the induction of apoptosis, as measured by DNA fragmentation 24 h post-transfection. AntimiR-dependent derepression of p21 is shown by the Western blot at the bottom of the graph. Quantitative comparison of OA-induced p21 expression and AntimiR-dependent p21 derepression revealed 4-fold higher p21 levels after OA-treatment (data not shown). Data shown in panels B and E represent mean values derived from at least three independent experiments; errors bars, SD.

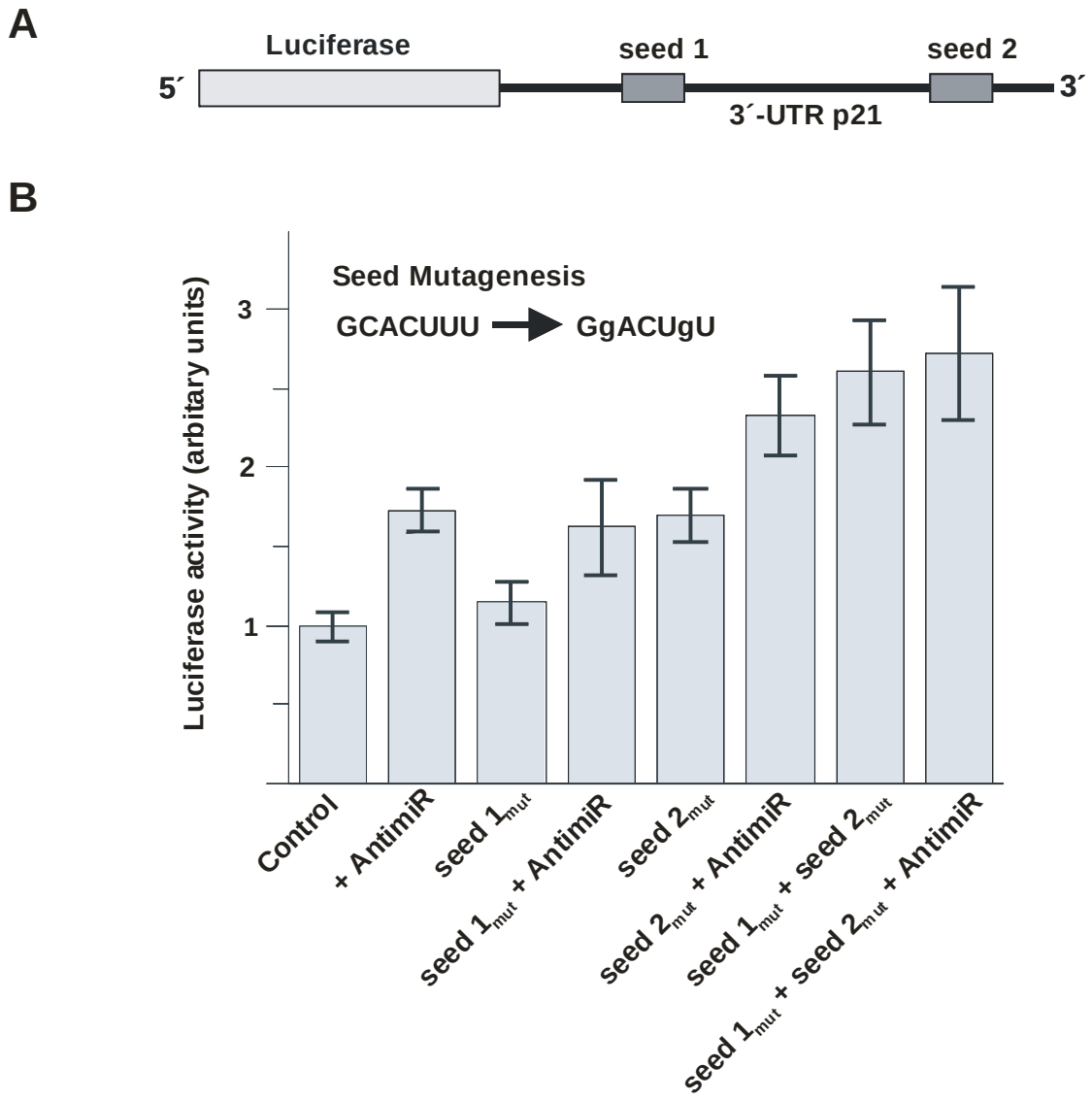

Figure 5. Mutagenesis of *miR-17-5p*/*-20a* seeds in the 3'-UTR of p21 mRNA. (A) Schematic presentation of the luciferase reporter consisting of the firefly luciferase structural gene fused to the p21 3'-UTR (control). (B) Luciferase expression was increased ~1.7-fold by transfection of cells with a mixture of LNA-AntimiRs against *miR-17-5p* and *miR-20a*. Mutagenesis of the 5'-proximal seed (seed 1) did not alter luciferase repression, whereas mutagenesis of seed 2 derepressed luciferase expression to a similar extent as transfection with LNA-AntimiRs. Mutagenesis of both seeds revealed a cooperative effect, as inferred from a 2.5-fold increase in luciferase activity. Seeds 1 and 2 were mutated from 5'-GCACUUU to 5'-GgACUgU. The shown data represent mean values derived from at least three independent experiments; errors bars, SD.

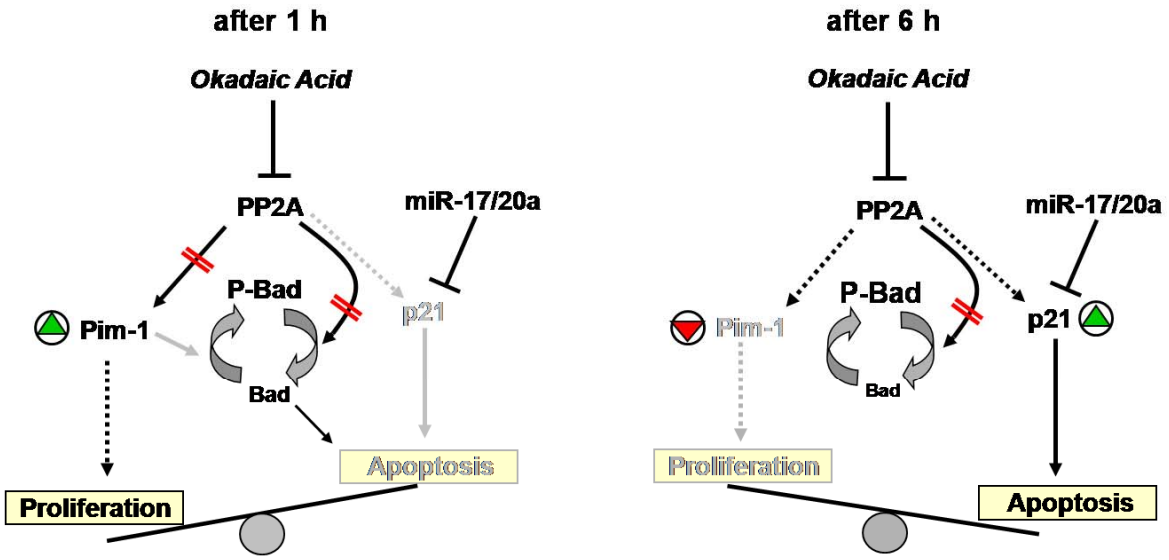

Fig. 6

Figure 6. Summary scheme to illustrate how the investigated cellular components affect the proliferative and/or apoptotic status of K562 cells. The OA-induced switch from proliferation to apoptosis affects the expression levels of Pim-1 and p21 in a time-dependent dynamic manner. Illustrated is the situation after 1 h (left) and 6 h (right) of OA treatment. In untreated K562 cells, the translation of basal p21 mRNA is completely blocked by miRNAs *miR-17-5p* and *miR-20a*. This block is overrun at late stages of OA-treatment (right panel) owing to 10-fold higher p21 mRNA levels. The strong transcriptional and translational upregulation of p21 following OA-caused PP2A inhibition leads to the onset of Bad-independent apoptosis. Pim-1 expression promotes proliferation, inferred from the fact that a specific siRNA-mediated knockdown of Pim-1 blocks proliferation. Note that Pim-1 dependent phosphorylation of Bad could be compensated by other kinases. Dotted lines, indirect effects; green and red circled triangles: increased and decreased levels, respectively; black arrow with two red lines indicates blocked PP2A activity; grey symbols indicate not activated or expressed; lines capped with a short perpendicular line illustrate inhibition.

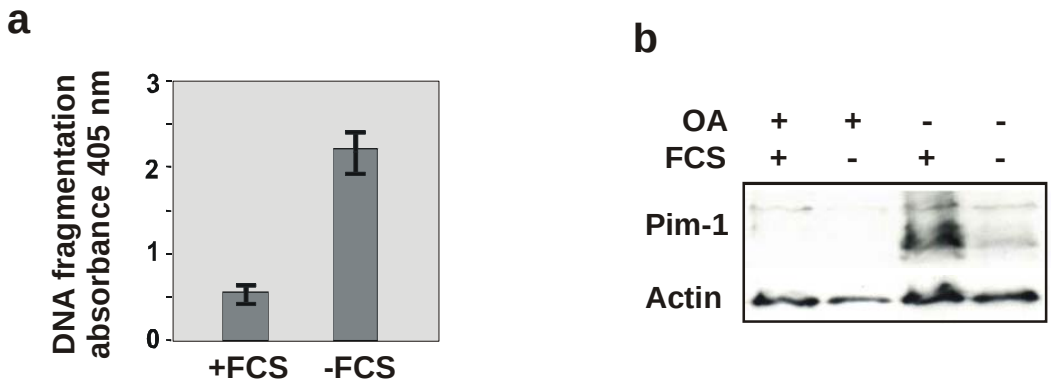

Supplementary Figure S1

(A) K562 cells were incubated for 72 h in the presence of 10% (+) or 0.1% (-) FCS. Apoptosis was quantified with a DNA fragmentation ELISA (see Materials and Methods). Results are based on three independent experiments. **(B)** K562 cells were treated for 24 h with 100 nM OA in the presence of 10% (+) or 0.1% (-) FCS. After cell lysis proteins were separated on a 10% SDS-PAA gel and the expression of Pim-1 was analyzed by western blotting with actin as a loading control.

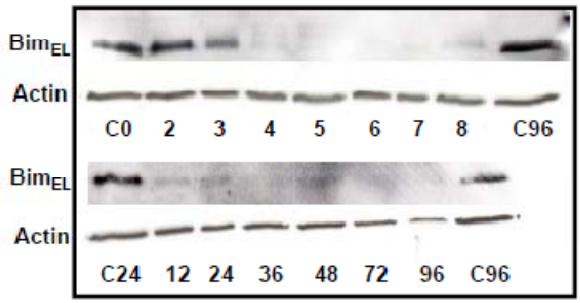

K562 cells were treated for the indicated times (up to 96 h) with 100 nM OA. After cell lysis proteins were separated on 10% SDS-PAA gels and expression level of BimEL was analyzed by Western blotting with beta-Actin as a loading control. C0, C24 and C96 mock-treated cells (no OA-addition) after 0, 24 and 96 h. After 4 h of OA treatment the pro-apoptotic-factor BimEL is completely down-regulated.

Supplementary Figure S2

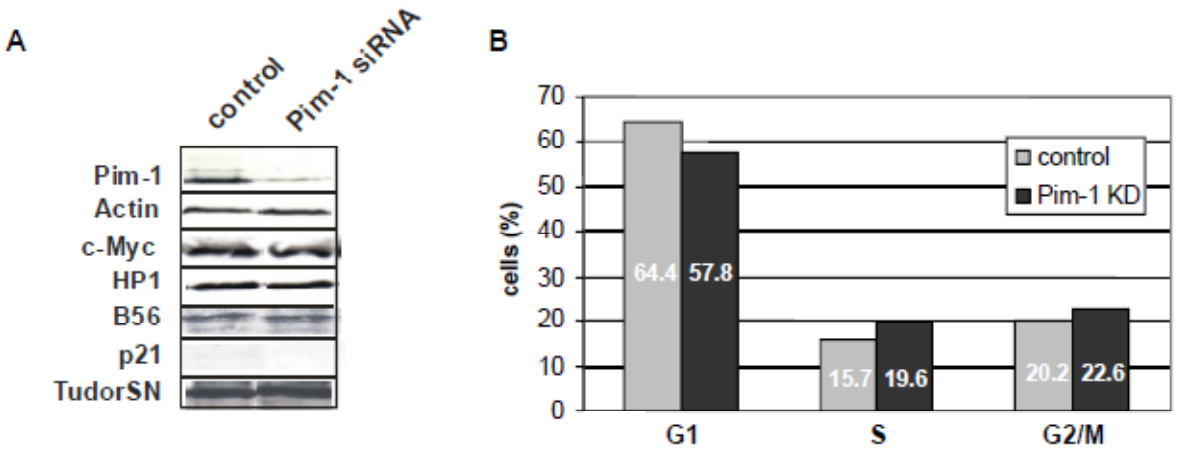

(A) K562 cells were transfected by electroporation with a Pim-1-specific siRNA. After 24 h cells were lysed and proteins were separated by 15 % SDS-PAGE. Expression of the indicated proteins was compared for untransfected cells versus Pim-1 knockdown cells by Western blotting. (B) Cell cycle analysis by treating fixed K562 cells with propidium jodid. Comparison of K562 cells with K562/Pim-1 knockdown cells demonstrated a reduced percentage of cells in G1 phase after RNAi. Cell analysis was performed by FACS.

Supplementary Figure S3

Contributions to this manuscript by the author of this thesis:

Experiments for figure 1D, figure 4A, 4B, 4C, figure 5, figure S3 (Pim-1, Actin, c-Myc, HP1, p21, TudorSN). Materials and methods for respective experiments; establishing transfection/electroporation protocols for K562 cells.
Proofreading of the first version of the manuscript and its second revision.

Regulation of the proto-oncogene Pim-1 by miR-33a

Arnold Grünweller*
Roland K. Hartmann*
Kerstin Lange-Grünweller*
Robert Prinz*
Maren Thomas*
(in alphabetical order)

*Institut für Pharmazeutische Chemie, Philipps-Universität Marburg

In collaboration with Achim Aigner and Ulrike Weirauch, Institut für Pharmakologie und Toxikologie, Philipps-Universität Marburg

Pharmazeutische Chemie
Philipps-Universität Marburg
Marbacher Weg 6
35037 Marburg, Germany

Running title: miR-33a and cancer

Keywords: Pim-1, microRNA, miR-33a, proliferation, cell cycle

ABSTRACT

Nothing is known about the function of the miRNA miR-33a. Here we present first evidence that the proto-oncogenic serine/threonine kinase Pim-1 is a target for regulation by miR-33a: Pim-1, which harbours a highly conserved binding site for miR-33a, is downregulated by a miR-33a mimic in the erythroleukemia cell line K562 (high Pim-1 expression levels) and in the colon carcinoma cell line LS174T (moderate Pim-1 levels). A screen for miRNA expression revealed that K562 and LS174T cells have only low endogenous miR-33a levels, whereas other oncogenic miRNAs, namely miR-17-5p, miR-20a and miR-214, are overexpressed. Seed mutagenesis of the miR-33a target sequence in a luciferase reporter fused to the 3′-UTR of Pim-1 demonstrated the specificity of miR-33a dependent downregulation. A seed-directed LNA-antimiR (14-mer) slightly increased luciferase expression, suggesting that basal endogenous miR-33a levels in K562 cells exert a weak regulatory effect on the Pim-1 3'-UTR. Transfection of K562 and LS174T cells with a miR-33a mimic decelerated proliferation. The miR-33a dependent cell cycle defect could be assigned to an increased number of cells in G1-phase after.

INTRODUCTION

MiRNAs are important regulators of gene expression, controlling developmental processes like embryonic stem cell differentiation, several metabolic pathways, cell proliferation, apoptosis and stress responses (Bartel, 2004). Like siRNAs, miRNAs are loaded into Argonaute (Ago)-containing "RNA-induced silencing complexes (RISC)" called miRNPs (Wang et al., 2009). In general, miRNAs have partial complementarity to their target mRNAs leading to translational inhibition or degradation of the respective mRNA in P-bodies (Liu et al., 2005; Rehwinkel et al., 2005). A prerequisite for miRNA interaction with mRNA targets is the so-called seed region covering nucleotides 2-8 of the mature miRNA strand. This region forms a continuous duplex with the target followed by a short unpaired region and a second less stringent base-pairing interaction (Lewis et al., 2005; Grimson et al., 2007).

A growing number of miRNAs are involved in the development of cancer or metastasis, e.g. miR-21, members of the miR-17-92 cluster or miR-155, and are therefore called oncogenic miRNAs (Esquela-Kerscher and Slack, 2006). For example, the miR-17-92 cluster is localized to a chromosomal region which is often amplified in B-cell lymphomas, leading to miRNA overexpression (Ota et al., 2004). Additionally, other oncogenes like the transcription factor c-Myc are involved in the transcriptional regulation of miRNAs (O´Donnell et al., 2005). Oncogenic miRNAs can downregulate targets that are involved in the regulation of apoptosis or cell cycle progression, such as the phosphatase PTEN, the transcription factor E2F1 or the apoptotic regulator Bim (for review see Croce , 2009).

Other miRNAs, e.g. miR-15a, miR-16-1, let-7a and miR-145, have tumor suppressor activity by controlling targets that can inhibit apoptosis or promote cell cycle progression, such as Bcl-2, Ras, Myc or cyclins (Cimmino et al., 2006; Johnson et al., 2005; Iorio et al., 2005). In several tumors, these miRNAs are downregulated or not expressed at all (Garzon et al., 2009). For example, miR-15a and miR-16-1 are encoded in the chromosomal region 13q14.3 and loss of this region is the most common genomic aberration in chronic lymphocytic leukemia (CLL) (Calin et al., 2002). Likewise, these two miRNAs are also often downregulated or not expressed in prostata carcinomas (Bonci et al., 2008).

The tumor suppressor function of miRNAs is mainly directed against classical oncogenes, including the small G-protein Ras, the transcription factor c-Myc or cell cycle-dependent kinases like CDK4 and CDK6 (Croce, 2009). To our knowledge, there are no further examples of oncogenic kinases regulated by miRNAs. However, the activities of oncogenic

kinases are often deregulated in cancer cells (Amarvadi and Thompson, 2005). Therapeutic efforts have focused on the treatment of such kinases to eliminate their anti-apoptotic properties (Crowell et al., 2007; Martelli et al., 2007). Pim-1, a serine/threonine kinase, is up-regulated in several cancer types and can function in a synergistic manner with the transcription factor c-Myc to establish severe forms of B cell lymphomas (van Lohuizen et al., 1989; Verbeek et al., 1991; Zippo et al., 2007). Pim kinases belong to the small group of constitutively active kinases (Qian et al., 2005) and their kinase activity correlates with their cellular expression levels. For Pim-1, several phosphorylation targets have been identified, such as Cdc25A (Mochizuki et al., 1999), p21 (Wang et al., 2002) and others (for review see Bachmann and Möröy, 2005). Expression of Pim-1 is mainly regulated at the transcriptional level by the action of several interleukines and growth factors that activate STAT3 and/or STAT5 via Janus kinases (Heinrich et al., 2003; Bachmann and Möröy, 2005). Neither a regulation of Pim-1 by miRNAs nor a target for miR-33a have been described so far. Our data demonstrate that Pim-1 is a target for miRNA-dependent regulation by miR-33a, and overexpression of this miRNA inhibited proliferation of the two cancer cell lines under study.

MATERIALS AND METHODS

Oligonucleotides and antibodies

The miR-33a Mimic (GUGCAUUGUAGUUGCAUUGCA), control Mimic (UCACAACCUCCUAGAAAGAGUAGA), miR-15a Mimic (UAGCAGCACAUAAUGGUUUGUG) and miR-16-1 Mimic (UAGCAGCACGUAAAUAUUGGCG) were purchased from Thermo Scientific. Pim-1 siRNA (5'-GAUAUGGUGUGUGGAGAUAUU and 5'-UAUCUCCACACACCAUAUCUU) were purchased from Dharmacon (Boulder, USA). An all-LNA-AntimiR against miR-33a (5´-GTGCATTGTAGTTTG-3´) was purchased from RiboTask (Odense, Denmark). Antibodies against Pim-1 (sc-13513), beta-Actin (sc-47778) as well as the secondary antibodies (sc-2004, sc-2005) were from Santa Cruz Biotechnology.

Cell culture and transfection

Cell lines (K562, LS174T, PC-3, DU145, LNCaP, K562, LS180, Skov-3, H69 and H209) were cultivated under standard conditions (37°C, 5% CO_2 in a humidified atmosphere) in RPMI 1640 medium containing 10 % FCS (PAA, Cölbe, Germany). For transfection of K562

cells with miRNA mimics or siRNA, cells were electroporated in 4 mm cuvettes with a single pulse at 330 V for 10 ms using a BioRad GenePulser XCell (Biorad, München, Germany). For 1 x 10^6 cells, 2 µg of the respective Mimic or Pim-1 siRNA was used. LS174T cells were transfected with miRNA Mimics using the INTERFERin siRNA transfection reagent (Peqlab, Erlangen, Germany) according to the manufacturer's protocol. Briefly, 1 x 10^3, 1.5 x 10^5 or 2.5 x 10^5 cells were seeded in 96 well, 24 well or 12 well plates, respectively, and cultivated under standard conditions. For complexation, 0.25 to 1 µl Interferin per pmol miRNA Mimic was incubated with the RNA in serum-free medium for 10 min at room temperature. Complexes were added to the wells (5 µl Inteferin complexed with 5 pmol miRNA for 24-well plates, 0.625 µl Interferin complexed with 2.5 pmol miRNA for 96-well plates), followed by incubation at 37°C in the presence of 5% CO_2 for 72 h (time point of knockdown efficacy determination) or for the time period indicated in Fig. 6 (proliferation and apoptosis assays).

RNA preparation and looped-primer qRT-PCR; qRT-PCR

Total RNA was isolated with the RNeasy Mini Kit (Qiagen, Hilden, Germany). RT-PCR was conducted using the Fermentas RevertAid H Minus First Strand cDNA Synthesis Kit (Fermentas, St. Leon-Roth, Germany) with 1 µg total RNA. Quantitative PCR was performed in duplicate in a LightCycler from Roche (Penzberg, Germany) with the Absolute QPCR SYBR Green Capillary Mix (Thermo Scientific, Hamburg, Germany). All procedures and reactions were carried out according to the protocols provided by the manufacturers. The mRNA levels were calculated from the crossing points by the $2^{-\Delta\Delta C_T}$ method (Schmittgen, 2001) to the obtained crossing points values. Primers were obtained from Metabion (Metabion, Martinsried, Germany) and designed with Universal ProbeLibrary (Roche Applied Biosciences, Mannheim, Germany). All primers that were used for quantitative looped-primer PCR are listed in the supplementary file.

Western blotting

Cells were resuspended in lysis buffer (125 mM Tris-HCl pH 6.8, 4 % SDS, 1.4 M 2-mercaptoethanol, 0.05 % bromophenol blue) and heated at 95°C for 5 min. Samples were loaded onto 15% SDS-polyacrylamide gels and run for 1 h at 180 V. Proteins were transferred to an Immobilon-P PVDF membrane (Millipore, MA, USA) for 90 min at 1 mA per cm^2 membrane using an EBU-4000 blotter (C.B.S. Scientific, CA, USA). Primary and secondary antibodies were diluted in TBST (Tris-buffered saline Tween-20) 1:500 (Pim-1), 1:2000

(CDK6), 1 1:10000 (β-Actin) and 1:4000 (secondary antibodies). After a final washing step, blots were incubated with Amersham ECL or ECLplus Western blotting reagents according to the manufacturer's protocol. For detection, Kodak BioMax Light Films, Kodak GBX developer/replenisher and GBX fixer/replenisher were used.

Plasmid construction, seed mutagenesis and luciferase reporter assay

The 3'-untranslated region (UTR) of human Pim-1 was cloned into the pGL3 control luciferase reporter vector (Promega, Mannheim, Germany) via its *Xba*I site. The 3'-UTR was initially amplified from K562 genomic DNA with the forward primer 5'-GCTCTAGAGCTGTCAGATGCCCGAGGG-3′ and reverse primer 5'-GCTCTAGAGCAATAAGATCTCTTTTATTCCCCTGT-3′. GC pairs were introduced at the 5′end for more efficient restriction according to instructions from NEB. PCR mutagenesis of the miRNA-33a target site was done according to Brennecke et al. (2005) using the following primers (sites of mutation underlined):

5′-AAAAAATGCACAAACAGTGCGATCAACAGAAAAGCT-3′

5′-AGCTTTTCTGTTGATCGCACTGTTTGTGCATTTTTT-3′

10 µg of pGL3 derivatives were co-transfected with 2 µg of miRNA mimics per 1 x 10^6 K562 cells. After 48 h, luciferase assays were performed using the Promega Luciferase Assay System. Briefly, cells were resolved in 100 µl lysis buffer, and 10 µl of lysate were mixed with 25 µl substrate and immediately measured with a Safire^2 microplate reader (Tecan, Crailsheim, Germany) in 96-well plates.

Proliferation assays and cell cycle analysis

To determine K562 metabolic activity as a measure of cell proliferation, 1 x 10^4 cells were seeded and cultivated under standard conditions. At the time points indicated, cells were pelleted and resuspended in 100 µl PBS, and 10 µl of the tetrazolium salt WST-1 were added to determine the activity of mitochondrial dehydrogenases. Absorbance was measured after incubation at 37°C for 2 h at 450 nm with 600 nm as reference wavelength using a Safire^2 microplate reader.

For the assessment of LS174T cell proliferation, 1 x 10^3 cells / well were seeded in 96-well plates and transfected as described above. At the time points indicated, WST-1 was diluted 1:10 in serum-free medium and 50 µl were added to the cells. After incubation for 1 h at 37°C, absorbance at 450 nm was measured using a MRX microplate reader.

For cell cycle analysis, 2,5 x 10^5 cells were seeded in 12-well plates and transfected as described above. 72 h after transfection, cell growth was synchronized by adding 100 ng/ml nocodazole to arrest the cell cycle in the G0-G1 phase. After incubation overnight, the medium was replaced with nocodazole-free medium and cells were incubated for another 24 h. Alternatively, to monitor cells during cell cycle arrest, cells were treated with 100 ng/ml nocodazole 96 h after transfection (Sigma, Munich, Germany), followed by incubation overnight. Cells were then harvested and fixed in 70% ethanol in PBS for 1 h on ice. After incubation with 50 µg/ml RNase A at 37°C for 30 min, cells were stained with 50 µg/ml propidium iodide and subjected to flow cytometric analysis using a FACSCalibur flow cytometer.

Assays to determine apoptosis

Using the "Cell Death Detection ELISA" (Roche, Germany), microtiter plates were pre-coated with an anti-histone antibody (clone H 11-4), incubated with lysed cells, followed by the addition of an anti-DNA antibody (clone MCA–33) and incubation for 90 minutes. For detection of mono- and oligonucleosomes, an 2,2'-Azinobis-3-ethylbenzthiazolin-6-sulfonsäure (ABTS) substrate solution was applied. Absorbance was measured with a Safire^2 microplate reader at 405 nm.

To determine the apoptosis in LS174T cells, the Caspase-Glo 3/7 Assay (Promega, Mannheim, Germany) was used acccording to the manufacturer's protocol. Briefly, 1 x 10^3 cell were seeded in 96-well plates and transfected as described above. After 120 h, the caspase Glo 3/7 substrate was diluted 1+1 in serum-free medium and 100 µl were added to the cells

prior to incubating for 1 h at room temperature. For the detection of caspase activity, luminescence was measured using a FLUOstar OPTIMA microplate reader. In parallel, total cell numbers were determined by the WST-1 assay as described above, and readings from caspase 3/7 measurements were normalized for cell densities.

RESULTS

Screening for Pim-1 expression levels in various tumor cell lines

Pim-1 is up-regulated in several cancer types, acts synergistically with c-Myc in B cell lymphoma development, and plays a key role for proliferation of cancer cells (van Lohuizen et al., 1989; Verbeek et al., 1991; Zippo et al., 2007; Zhang et al., 2008; Lange-Grünweller et al., 2010). Since Pim-1 expression levels are particularly high in our major model cell line K562, we were interested in relating this to Pim-1 expression in a broad spectrum of other tumor cell lines. For this purpose, 23 different cell lines from six different tumor types (breast, colon, prostata, melanoma, leukemia and ovarian) were analysed for Pim-1 expression by qRT-PCR (Fig. 1 A). This analysis confirmed that K562 cells stand out in terms of Pim-1 (mRNA) expression levels which are tenfold higher than those of the leukemia cell line BM87 showing the second highest Pim-1 mRNA levels. Apart from K562 cells, substantial amounts of Pim-1 mRNA were also detected in a group of other cell lines, including BM87, LS174T, LOVO, LS-180 (colon cancer), DU145, PC3 (prostate cancer), A2780 (ovarian cancer) and A431 (breast cancer). Analysis of Pim-1 levels by Western blotting for selected cell lines (Fig. 1 B) revealed a good correlation with the qRT-PCR data: K562 cells also had the highest protein levels, followed by members of the aforementioned group of cell lines (LS-180, LS174T, DU145 and PC3). In contrast, Pim-1 protein levels were below the detection limit of our Western blot setup for cell lines with lower mRNA levels, such as Skov-3 and LNCap (Fig. 1 B).

The 3'-UTR of Pim-1 harbours a conserved binding site for miR-33a

The particularly high expression of Pim-1 in K562 cells posed the question if Pim-1 expression in these cells is not only transcriptionally but also posttranscriptionally deregulated. We thus analysed the mRNA of Pim-1 for putative miRNA binding sites by TargetScan 4.1 (www.**targetscan**.org). Five conserved sites were identified for binding of miR-124/506, miR-26, miR-15a/-16-1, miR-24 and miR-33a. For miR-33a, the seed region

from position 2-8 nt and the anchor A (Grimson et al., 2007) were found to be completely conserved between human, mouse, rabbit, dog and even chicken. Moreover, an unpaired nucleotide stretch (positions 10-12) and a second pairing region between nt 13-17, perfectly matching the Grimson rules (Grimson et al., 2007), was found to be conserved in all five eukaryotes (Fig. 2). We excluded miR-124 as a serious candidate for regulation of Pim-1 mRNA translation in K562 cells, because miR-124 is mainly expressed in the brain and involved in neurogenesis and neuronal differentiation (Cheng et al., Nat. Neuroscience, 2009; Makeyev et al., Mol. Cell, 2007). Likewise, we disregarded miR-26 since it is evolutionary poorly conserved and has a lower context score compared to miR-33a (context score percentile for miR-26a is 77 and for miR-33a is 98 from 100). We further considered miR-15a /-16-1 as candidate regulators of Pim-1 expression due to their well-characterized tumor suppressor activities (Cimmino et al, PNAS, 2005; Aqeilan et al., Cell Death Differ. 2009), although their context score percentile was lower than that for miR-33a (50 for miR-15a and 67 for miR-16-1). This is reflected in a lower adherence to the Grimson rules and a lower evolutionary conservation of the putative miR-15a /-16-1 target site in the Pim-1 3'-UTR (Fig. 2). Suppression of the tumor suppressor p16 has been attributed to miR-24 (Lal et al., 2008). MiR-24 was not considered further here due to a lower context score percentile (77) for its target site in the Pim-1 3'-UTR. In conclusion, the predicted target site for miR-33a appeared as the most promising candidate site for miRNA regulation. Of note, no target or cellular function of miR-33a has been described so far.

Profiling of selected miRNAs in Pim-1 expressing tumor cell lines

Prediction of miR-15a /-16-1 and miR-33a target sites in the Pim-1 3'-UTR prompted us to analyse their expression levels. For this analysis, we chose the cell lines K562 and LS174T as model systems for very high and moderate Pim-1 expression, respectively. MiRNA profiles obtained for a selected set of miRNAs (including miR-423-5p and miR-374 as references that show minimal variability in cell lines, as recommended by Applied Biosystems for TaqMan microRNA assays) were determined by the looped-primer qRT-PCR technique, as shown in Fig. 3. Surprisingly, the miRNA miR-16-1, to which tumor suppressor functions have been assigned (Cimmino et al, PNAS, 2005; Aqeilan et al., Cell Death Differ. 2009), showed the highest expression levels in both cell lines; levels of the related miRNA-15a were much lower than those for miR-16-1, but still elevated relative to those of the reference miRNA-423. Within the set of analysed miRNAs, also miR-214, a miRNA involved in cell survival and in

antagonizing apoptosis (Cheng et al., 2005), as well as the oncogenic miRNAs miR-17-5p and miR-20a encoded in the miR-17-92 cluster were found to be expressed at high levels. The miRNAs with seeds in the Pim-1 3'-UTR (miR-24, miR-26a, miR-33a and miR-124) have only low expression levels in both cell lines.

Pim-1 is a target of miR-33a

Relatively low expression of miR-33a in K562 and LS174T cells suggested the possibility to down-regulate Pim-1 protein expression by transfection of cells with a miR-33a mimic. Western blotting, using an optimised unspecific mimic (Thermo Scientific) as control, demonstrated substantial downregulation of Pim-1 by the miR-33a mimic, but not by corresponding miR-15a and miR-16-1 mimics in K562 cells (Fig. 4 A). A related analysis in LS174T cells further revealed an approx. twofold reduction in Pim-1 mRNA levels upon transfection with the miR-33a mimic (Fig. 4 B). We further compared the miR-33a dependent downregulation of Pim-1 with the knockdown efficiency of a Pim-1 specific siRNA (Lange-Grünweller et al., 2010). The knockdown effect caused by the miR-33a mimic was as persistent as for the siRNA within 96 h posttransfection of K562 cells, but weaker than for the siRNA (Fig. 4 C). A weaker knockdown by the miR-33a mimic is consistent with the general trend of miRNAs to repress expression of individual targets more mildly than siRNAs (Selbach et al., 2008).

Specificity of miR-33a binding to the Pim-1 3'-UTR

To independently confirm repression of Pim-1 expression by the miR-33a mimic (Fig. 4 A, C), we cloned the 3'-UTR of Pim-1 into a luciferase reporter vector (pGL3 control). K562 cells were cotransfected with this construct, either alone or together with the miR-33a or control mimic. A significant reduction of luciferase activity of around 50% was measured for the miR-33a mimic compared to the controls (Fig. 5 A). We further scruitinized the specificity of the observed miR-33a effect on Pim-1 expression by mutation of the miR-33a seed binding site in the 3'-UTR of Pim-1 (from 5'-CAATGCAA to 5'-CAGTGCGA). Luciferase reporter assays were performed with lysates derived from K562 cells transfected with the wildtype or mutated Luc-Pim-1 constructs, either in combination with the control Mimic, the miR-33a mimic, or an LNA-antimiR complementary to miR-33a. Combining the wildtype Luc-Pim-1 construct with the miR-33a mimic reduced luciferase activity 3 to 4-fold relative to the control mimic in this set of experiments (Fig. 5 B). The antimiR had, if at all, a

very minor effect on reporter expression, in line with the very low miR-33a levels in K562 cells (Fig. 3). In contrast to the reporter gene carrying the wildtype 3'-UTR of Pim-1, miR-33a dependent luciferase repression was almost fully abrogated (Fig. 5 B) when the seed target region was mutagenized. The mutagenized construct also tended to give rise to slightly increased luciferase activity (with control mimic or antimiR) compared to the wildtype construct, supporting the notion that low levels of endogenous miR-33a may mildly repress the reporter with the native Pim-1 3'-UTR.

A miR-33a mimic decelerates proliferation

Previous studies (Zhang et al., 2008; Lange-Grünweller et al., 2010) have documented a direct role of Pim-1 in regulating proliferation of K562 cells. We thus hypothesised that miR-33a may also negatively affect cell proliferation by reducing the levels of Pim-1. In a first experimental setup, where we transfected K562 cells with the miR-33a mimic under normal growth conditions (10% FCS), no effect of miR-33a on proliferation could be observed. However, when we reduced the level of FCS to 2% in the medium, proliferation of K562 cells was affected by miR-33a. This can be explained with the observation that Pim-1 levels decrease in K562 cells with decreasing concentrations of growth factors (Lange-Grünweller et al., 2010). For LS174T cells, a deceleration of cell growth owing to the miR-33a mimic was already seen in the presence of 10% FCS, which is attributable to the lower expression levels of Pim-1 in LS174T relative to K562 cells (Fig. 1 B).

Discussion

In our study we have used the webtool TargetScan 5.1 to analyse Pim-1 mRNA for putative miRNA target sites. This serine/threonine kinase is an important proto-oncogene which is up-regulated in several cancer types (van Lohuizen et al. 1989; Dhanasekaran et al. 2001; Bachmann and Moroy 2005) and which can function in a synergistic manner with the transcription factor c-Myc to establish severe forms of B cell lymphomas (van Lohuizenet al., 1989, Verbeek et al., 1991, Zippo et al., 2007). Regulation of Pim-1 expression can be mainly observed at the transcriptional level, however the protein has a short half-life of less than 1 hour in tumor cells and only minutes in normal cells (Liang et al., 1996; Shay et al., 2005). Regulation of Pim-1 expression at the post-transcriptional level e.g. by miRNAs has not been investigated so far. By using TargetScan 5.1 we picked up a highly conserved target site for binding of miR-33a in the 3´-UTR of Pim-1. This sequence contains an 8-mer seed region

which defines the interaction with the miRNA and additionally an anchor A, a position at the 3´-end of the target sequence which is often found and conserved in functional miRNA target sites. Moreover, an unpaired region followed by a second pairing region, is also conserved from human to chicken in the miR-33a target site of the Pim-1 3´UTR. Therefore, this sequence has a very high context score (a value defined by TargetScan, which predicts the possibility of functional miRNA binding) making miR-33a a perfect miRNA to regulate Pim-1 mRNA post-transcriptionally. To test this assumption we transfected a miR-33a Mimic into K562 cells, an erythroleukemia cell line which overexpresses Pim-1, and found substantial downregulation of Pim-1 at the protein level. This demonstrates that a well defined target prediction programme can be successfully used to identify new miRNA targets. Another predicted target of miR-33a is CDK6. Current findings indicate that not all CDKs are essential for cell cycle regulation (among them CDK6), but rather appear important only in distinct tissues and cancer identities (Malumbres and Barbacid, 2009). It has a much higher context score (-0.80) compared to that predicted for Pim-1 (-0.40), but the predicted pairing of miR-33a/b to those target sites in CDK6 differs substantially (see results, and suppl. figure S1) and we see no regulation after miR-33 targeting (data not shown). Thus global predictions and high ranking targets may give hints to miR-regulation of respective genes, but a detailed analysis of local pairing characteristics may in some cases be more informative, i.e. global context is less important than local context. This means that not all rules that are applied by TargetScan (Grimson et al. 2007) may contribute with their currently assigned emphasis to miR-target interaction in vivo. Another possibility is that CDK6 is regulated by other miRs in K562 and Hela cells, as it has an extensive 3´-UTR (~10 kb) where at least 50 conserved miR-binding sites are predicted by the current version of TargetScan (v5.1). So, if several miRs are already bound to their target sites, this may influence binding of further miRs. For those with lower cellular abundance we may observe competitive and stoichiometric effects in terms of target site access. We can find binding sites for miR-16 and miR-214, both of which are expressed in high amounts in the cell lines we analysed (figure 3). They have comparable binding characteristics as are predicted for miR-33 (suppl. figure S1).

In tumors miRNAs can be lost or overexpressed thus making them new candidates for cancer therapies. MiRNAs with tumor suppressor activity can be substituted or overexpressed in tumor cells by using miRNA Mimics whereas oncogenic miRNAs can be blocked with AntimiRs. Interestingly, most of the miRNAs with tumor suppressor activity like miR-15a / 16-1 or let-7 have more than one genomic location. This is also the case for miR-33 as two

singular members are located in the genome at different positions (miR-33a at chromosome 22 q13.2 and miR-33b at chromosome 17 p11.2). It was speculated that the presence of more than one genomic copy of the miRNA could be an evolutionary conserved mechanism to preserve function of an important miRNA if one allele is deleted or silenced (Garzon et al., 2009). Although derived from different chromosomal loci, miR-33a and miR-33b differ only in one additional nucleotide (A) at the 3´ end which is present in miR-33a but abesent in miR-33b. We cannot exclude the possibility that in our profiling using the looped primer RT-PCR method from Chen et al. (2005) miR-33b contributed to some extent to the measured fraction of miR-33a. A looped primer designed for miR-33b may better discriminate against mir-33a due to steric interference caused by the extra A residue at the 3'-end of miR-33a.

The observation that one miRNA can have several targets (up to 200 targets per miRNA) and that miRNAs have more fine-tuning than knockdown properties has brought them into the focus for therapeutic intervention to induce apoptosis or cell cycle arrest in tumor cells. A recent report from the Mendell group (Kota et al., 2009) demonstrated that the concept of miRNA replacement therapies could be successfully applied in a mouse model of hepatocellular carcinoma. Since miR-26a, a miRNA with tumor suppressor activity, is strongly downregulated in mouse and human liver tumors, the authors pursued an AAV-derived delivery strategy for systemic administration of miR-26a *in vivo*. Overexpression of miR-26a in HepG2 cells induces a G1 arrest by targeting the cyclins D2 and E2. Importantly, AAV-dependent overexpression of miR-26a led to the induction of tumor-specific apoptosis and, as a consequence, to a dramatic protection from disease without any toxicity (Kota et al., 2009). This was the first proof-of-concept study demonstrating that miRNAs can be used as general anti-cancer compounds. Very recently, the Slack group demonstrated the therapeutic potential of let-7 (Trang et al., 2009), a miRNA family whose members map to chromosomal regions frequently deleted in lung cancer (Calin et al., 2004). Exogenous delivery of let-7 to established tumors in mouse models of non-small-cell lung cancer significantly reduced the tumor burden. This is a further example of miRNA replacement therapy as a promising approach in cancer treatment. However, the route of miRNA delivery for therapeutic applications in the clinic is still an important issue. Liver and lung tissues are known for efficient uptake of miRNAs and siRNAs delivered by different ways. Other tissues such as the brain could not be reached by standard application systems, illustrating the many questions that have to be answered before miRNAs can be used in clinical applications.

The observation that miRNAs have moderate effects on their targets (~ 2-fold inhibition) raises the question why an oncogenic kinase like Pim-1 which is strongly regulated at the transcriptional level and additionally by PP2A-dependent degradation via the proteasome (Shay et al., 2005) is a target for further fine-tuning regulation by a miRNA? One explanation could be the fact that Pim-1 has a redundant function in cells by phosphorylating similar targets as Akt kinase (Amaravadi and Thompson, 2005). Pim-1 seems to lack unique functions thus making this kinase dispensable in knockout mice, which show only moderate phenotypes when all three subtypes of Pim-kinases are deleted (Mikkers et al., 2004). Only if Pim-1 is overexpressed like in the p53-deficient K562 cells tumorigenesis is promoted. In the normal cellular context Pim-1 is weakly or not expressed. However the function of Akt in regulating the balance between proliferation and apoptosis is central and essential for cells (Amaravadi and Thompson, 2005). Therefore, a backup system for this important kinase might be helpful for cells to counteract deregulated Akt kinase activity (Muraski et al., 2007). Such a backup system has to be fine-tuned and somehow coupled to the regulation of Akt kinase, because it only has to replace its function in conditions of Akt failure, otherwise high levels of Pim-1 expression would reconstitute the phenotypic effects of Akt overexpression. We speculate that miRNA-dependent (down)regulation of Pim-1 supports the function of Akt and enables cells to adjust the balance between proliferation and apoptosis. In cells like K562, Pim-1 overexpression would thus be indicative of a deregulated Akt kinase backup system. Fine-tuning of such cellular backup systems could be a function of miRNAs which is not addressed so far. For those reasons, Pim-1 and the Pim-1-regulating miRs appear as interesting targets for interference in therapeutic settings.

Here we have added miR-33a to the list of miRNAs with tumor suppressor activity. We have shown that the oncogenic kinase Pim-1 is a target of miR-33a and that overexpression of miR-33a by transfecting a miR-33a Mimic decelerates proliferation in colon cancer and leukemia cell lines. Other targets of miR-33a are waiting to be identified. In our study we have also analysed CDK6 as a putative target for miR-33a regulation because CDK6 contains two putative binding sites for miR-33a in its 3´-UTR but, in this case no miR-33a dependent downregulation could be seen in HeLa and K562 cells. Regarding the plethora of putative binding sites for miRs located in the CDK6 3´-UTR, it becomes clear that we need information on real miR-binding to those sites. Thus, our future goal is to identify further targets of miR-33a by using high throughput methods such as RIP-Chip (Tan et al., 2009) to pinpoint those predicted targets that are bound *in vivo*. This should lead to more information

about the cellular context of miR-33a/b. Until now we have not identified a cell line or primary cells with high expression levels of miR-33a, a prerequisite to analyse the normal cellular function of this miRNA. However, the fact that Pim-1 is a target of miR-33a and its overexpression has anti-proliferative effects might bring this miRNA into the focus for therapeutic applications. Currently we are on the way to examine the effects of miR-33a in several mouse tumor models.

References

1. Bartel DP. MicroRNAs: genomics, biogenesis, mechanism, and function. Cell. 2004 Jan 23;116(2):281-97. Review.

2. Wang HW, Noland C, Siridechadilok B, Taylor DW, Ma E, Felderer K, Doudna JA, Nogales E. Structural insights into RNA processing by the human RISC-loading complex. Nat Struct Mol Biol. 2009 Nov;16(11):1148-53. Epub 2009 Oct 11.

3. Liu J, Valencia-Sanchez MA, Hannon GJ, Parker R. MicroRNA-dependent localization of targeted mRNAs to mammalian P-bodies. Nat Cell Biol. 2005 Jul;7(7):719-23. Epub 2005 Jun 5.

4. Rehwinkel J, Behm-Ansmant I, Gatfield D, Izaurralde E. A crucial role for GW182 and the DCP1:DCP2 decapping complex in miRNA-mediated gene silencing. RNA. 2005 Nov;11(11):1640-7. Epub 2005 Sep 21.

5. Lewis BP, Burge CB, Bartel DP. Conserved seed pairing, often flanked by adenosines, indicates that thousands of human genes are microRNA targets. Cell. 2005 Jan 14;120(1):15-20.

6. Grimson A, Farh KK, Johnston WK, Garrett-Engele P, Lim LP, Bartel DP. MicroRNA targeting specificity in mammals: determinants beyond seed pairing. Mol Cell. 2007 Jul 6;27(1):91-105.

7. Esquela-Kerscher A, Slack FJ. Oncomirs - microRNAs with a role in cancer. Nat Rev Cancer. 2006 Apr;6(4):259-69. Review.

8. Ota A, Tagawa H, Karnan S, Tsuzuki S, Karpas A, Kira S, Yoshida Y, Seto M. Identification and characterization of a novel gene, C13orf25, as a target for 13q31-q32 amplification in malignant lymphoma. Cancer Res. 2004 May 1;64(9):3087-95.

9. Croce CM. Causes and consequences of microRNA dysregulation in cancer. Nat Rev Genet. 2009 Oct;10(10):704-14. Review.

10. Cimmino A, Calin GA, Fabbri M, Iorio MV, Ferracin M, Shimizu M, Wojcik SE, Aqeilan RI, Zupo S, Dono M, Rassenti L, Alder H, Volinia S, Liu CG, Kipps TJ, Negrini M, Croce CM. miR-15 and miR-16 induce apoptosis by targeting BCL2. Proc Natl Acad Sci U S A. 2005 Sep 27;102(39):13944-9. Epub 2005 Sep 15.

11. Johnson SM, Grosshans H, Shingara J, Byrom M, Jarvis R, Cheng A, Labourier E, Reinert KL, Brown D, Slack FJ. RAS is regulated by the let-7 microRNA family. Cell. 2005 Mar 11;120(5):635-47.

12. Iorio MV, Ferracin M, Liu CG, Veronese A, Spizzo R, Sabbioni S, Magri E, Pedriali M, Fabbri M, Campiglio M, Ménard S, Palazzo JP, Rosenberg A, Musiani P, Volinia S, Nenci I, Calin GA, Querzoli P, Negrini M, Croce CM. MicroRNA gene expression deregulation in human breast cancer. Cancer Res. 2005 Aug 15;65(16):7065-70

13. Garzon R, Calin GA, Croce CM. MicroRNAs in Cancer. Annu Rev Med. 2009;60:167-79.

14. Calin GA, Dumitru CD, Shimizu M, Bichi R, Zupo S, Noch E, Aldler H, Rattan S, Keating M, Rai K, Rassenti L, Kipps T, Negrini M, Bullrich F, Croce CM. Frequent deletions and down-regulation of micro- RNA genes miR15 and miR16 at 13q14 in chronic lymphocytic leukemia. Proc Natl Acad Sci U S A. 2002 Nov 26;99(24):15524-9. Epub 2002 Nov 14.

15. Bonci D, Coppola V, Musumeci M, Addario A, Giuffrida R, Memeo L, D'Urso L, Pagliuca A, Biffoni M, Labbaye C, Bartucci M, Muto G, Peschle C, De Maria R. The miR-15a-miR-16-1 cluster controls prostate cancer by targeting multiple oncogenic activities. Nat Med. 2008 Nov;14(11):1271-7. Epub 2008 Oct 19.

16. O'Donnell KA, Wentzel EA, Zeller KI, Dang CV, Mendell JT. c-Myc-regulated microRNAs modulate E2F1 expression. Nature. 2005 Jun 9;435(7043):839-43

17. Amaravadi, R. and Thompson, C. B. (2005) The survival kinases Akt and Pim as potential pharmacological targets. J. Clin. Invest. 115, 2618-2624.

18. Crowell JA, Steele VE, Fay JR. (2007). Targeting the AKT protein kinase for cancer chemoprevention. *Mol Cancer Ther*. 6: 2139-2148.

19. Martelli AM, Tazzari PL, Evangelisti C, Chiarini F, Blalock WL, Billi AM, et al. (2007). Targeting the phosphatidylinositol 3-kinase/Akt/mammalian target of rapamycin module for acute myelogenous leukemia therapy: from bench to bedside. *Curr Med Chem*. 14: 2009-2023.

20. van Lohuizen M, Verbeek S, Krimpenfort P, Domen J, Saris C, Radaszkiewicz T, Berns A. (1989). Predisposition to lymphomagenesis in pim-1 transgenic mice: cooperation with c-myc and N-myc in murine leukemia virus-induced tumors. *Cell* 56: 673-682.

21. Verbeek S, van Lohuizen M, van der Valk M, Domen J, Kraal G, Berns A. (1991). Mice bearing the E mu-myc and E mu-pim-1 transgenes develop pre-B-cell leukemia prenatally. *Mol Cell Biol*. 11: 1176-9.

22. Zippo A, De Robertis A, Serafini R, Oliviero S. (2007). PIM1-dependent phosphorylation of histone H3 at serine 10 is required for MYC-dependent transcriptional activation and oncogenic transformation. *Nat Cell Biol*. 9: 932-944.

23. Qian KC, Wang L, Hickey ER, Studts J, Barringer K, Peng C, Kronkaitis A, et al. (2005). Structural basis of constitutive activity and a unique nucleotide binding mode of human Pim-1 kinase. *J Biol Chem*. 280: 6130-6137.

24. Mochizuki T, Kitanaka C, Noguchi K, Muramatsu T, Asai A, Kuchino Y. (1999). Physical and functional interactions between Pim-1 kinase and Cdc25A phosphatase. Implications for the Pim-1-mediated activation of the c-Myc signaling pathway. *J Biol Chem*. 274: 18659-18666.

25. Wang Z, Bhattacharya N, Mixter PF, Wei W, Sedivy J, Magnuson NS. (2002). Phosphorylation of the cell cycle inhibitor p21Cip1/WAF1 by Pim-1 kinase. *Biochim Biophys Acta*. 1593: 45-55.

26. Bachmann M, Möröy T. (2005). The serine/threonine kinase Pim-1. *Int J Biochem Cell Biol*. 37: 726-730.

27. Heinrich, P. C., Behrmann, I., Haan, S., Hermanns, H. M., Müller-Newen, G. and Schaper, F. (2003) Principles of interleukin (IL)-6-type cytokine signalling and its regulation. Biochem. J. 374, 1-20.

28. Schmittgen, T. D. (2001) Real-time quantitative PCR. Methods 25, 383-385.

29. Brennecke, J., Stark, A., Russell, R. B. and Cohen, S. M. (2005) Principles of microRNA-target recognition. PLoS Biol. 3, e85.

30. Cheng LC, Pastrana E, Tavazoie M, Doetsch F. miR-124 regulates adult neurogenesis in the subventricular zone stem cell niche. Nat Neurosci. 2009 Apr;12(4):399-408. Epub 2009 Mar 15.

31. Makeyev EV, Zhang J, Carrasco MA, Maniatis T. The MicroRNA miR-124 promotes neuronal differentiation by triggering brain-specific alternative pre-mRNA splicing. Mol Cell. 2007 Aug 3;27(3):435-48.

32. Aqeilan RI, Calin GA, Croce CM. miR-15a and miR-16-1 in cancer: discovery, function and future perspectives. Cell Death Differ. 2009 Jun 5.

33. Lange Grünweller et al., 2009 Neoplasia (submitted)

34. Selbach, M., Schwanhäusser, B., Thierfelder, N., Fang, Z., Khanin, R. and Rajewsky, N. (2008) Widespread changes in protein synthesis induced by microRNAs. Nature **455**, 58-63.

35. Zhang Y, Wang Z, Li X, and Magnuson NS (2008). Pim kinase-dependent inhibition of c-Myc degradation. Oncogene **27**, 4809-4819.

36. Cheng AM, Byrom MW, Shelton J, Ford LP. Antisense inhibition of human miRNAs and indications for an involvement of miRNA in cell growth and apoptosis. Nucleic Acids Res. 2005 Mar 1;33(4):1290-7.

44. Liang H, Hittelman W, Nagarajan L. Ubiquitous expression and cell cycle regulation of the protein kinase PIM-1. Arch Biochem Biophys. 1996 Jun 15;330(2):259-65.

45. Shay KP, Wang Z, Xing PX, McKenzie IF, and Magnuson NS (2005). Pim-1 kinase stability is regulated by heat shock proteins and the ubiquitin-proteasome pathway. Mol. Cancer Res. 3, 170-181.

46. Kota J, Chivukula RR, O'Donnell KA, Wentzel EA, Montgomery CL, Hwang HW, Chang TC, Vivekanandan P, Torbenson M, Clark KR, Mendell JR, Mendell JT. Therapeutic microRNA delivery suppresses tumorigenesis in a murine liver cancer model. Cell. 2009 Jun 12;137(6):1005-17.

47. Trang P, Medina PP, Wiggins JF, Ruffino L, Kelnar K, Omotola M, Homer R, Brown D, Bader AG, Weidhaas JB, Slack FJ. Regression of murine lung tumors by the let-7 microRNA. Oncogene. 2009 Dec 7.

48. Calin GA, Sevignani C, Dumitru CD, Hyslop T, Noch E, Yendamuri S, Shimizu M, Rattan S, Bullrich F, Negrini M, Croce CM. Human microRNA genes are frequently located at fragile sites and genomic regions involved in cancers. Proc Natl Acad Sci U S A. 2004 Mar 2;101(9):2999-3004. Epub 2004 Feb 18.

49. Mikkers H, Nawijn, M, Allen J, Brouwers C, Verhoeven E, Jonkers J, and Berns A (2004). Mice deficient for all PIM kinases display reduced body size and impaired responses to hematopoietic growth factors. Mol Cell Biol. 24, 6104-6115.

50. Muraski JA, Rota M, Misao Y, Fransioli J, Cottage C, Gude N, Esposito G, Delucchi F, Arcarese M, Alvarez R, Siddiqi S, Emmanuel GN, Wu W, Fischer K, Martindale JJ, Glembotski CC, Leri A, Kajstura J, Magnuson N, Berns A, Beretta RM, Houser SR, Schaefer EM, Anversa P, Sussman MA. Pim-1 regulates cardiomyocyte survival downstream of Akt. Nat Med. 2007 Dec;13(12):1467-75. Epub 2007 Nov 25. Erratum in: Nat Med. 2008 Mar;14(3):350.

51. Lal A, Kim HH, Abdelmohsen K, Kuwano Y, Pullmann R Jr, Srikantan S, Subrahmanyam R, Martindale JL, Yang X, Ahmed F, Navarro F, Dykxhoorn D, Lieberman J, Gorospe M. (2008). p16(INK4a) translation suppressed by miR-24. *PLoS ONE* **3** (3): e1864.

52. Chen C, Ridzon DA, Broomer AJ, Zhou Z, Lee DH, Nguyen JT, Barbisin M, Xu NL, Mahuvakar VR, Andersen MR, Lao KQ, Livak KJ, Guegler KJ (2005). Real-time quantification of microRNAs by stem-loop RT-PCR. Nucleic Acids Res **33**(20): e179.

Supplementary File:

hsa-miR-15a, RT-PCR looped primer:
5′-GTCGTATCCAGTGCAGGGTCCGAGGTATTCGCACTGGATACGACcacaaac-3′
QT PCR forward primer: 5′-TAGCAGCACATAATGGTTTGTG-3′

hsa-miR-16-1, RT-PCR looped primer:
5′-GTCGTATCCAGTGCAGGGTCCGAGGTATTCGCACTGGATACGACcgccaat-3′
QT PCR forward primer: 5′- TAGCAGCACGTAAATATTGGCG-3′

hsa-miR-17, RT-PCR looped primer:
5′-GTCGTATCCAGTGCAGGGTCCGAGGTATTCGCACTGGATACGACctacctg-3′
QT-PCR forward primer: 5′-CAAAGTGCTTACAGTGCAGGTAG-3′

hsa-miR-20a, RT-PCR looped primer:
5′-GTCGTATCCAGTGCAGGGTCCGAGGTATTCGCACTGGATACGACctacctg-3′
QT-PCR forward primer: 5′-TAAAGTGCTTATAGTGCAGGTAG-3′

hsa-miR-24-1, RT-PCR looped primer:
5′-GTCGTATCCAGTGCAGGGTCCGAGGTATTCGCACTGGATACGACctgttc-3′
QT-PCR forward primer: 5′-TGGCTCAGTTCAGCAGGAACAG-3′

hsa-miR-33a, RT-PCR looped primer:
5′-GTCGTATCCAGTGCAGGGTCCGAGGTATTCGCACTGGATACGACtgcaatg-3′
QT-PCR forward primer: 5′-GTGCATTGTAGTTGCATTGCA-3′

hsa-miR-124-1, RT-PCR looped primer:
5′-GTCGTATCCAGTGCAGGGTCCGAGGTATTCGCACTGGATACGACggcattc-3′
QT-PCR forward primer: 5′-TAAGGCACGCGGTGAATGCC-3′

hsa-miR-195, RT-PCR looped primer:
5′-GTCGTATCCAGTGCAGGGTCCGAGGTATTCGCACTGGATACGACgccaata-3′
QT-PCR forward primer: 5′-TAGCAGCACAGAAATATTGGC-3′

hsa-miR-214, RT-PCR looped primer:
5′-GTCGTATCCAGTGCAGGGTCCGAGGTATTCGCACTGGATACGACactgcct-3′
QT-PCR forward primer: 5′-ACAGCAGGCACAGACAGGCAGT-3′

hsa-miR-374a, RT-PCR looped primer:
5′-GTCGTATCCAGTGCAGGGTCCGAGGTATTCGCACTGGATACGACcacttat-3′
QT-PCR forward primer: 5′-TTATAATACAACCTGATAAGTG-3′

hsa-miR-423, RT-PCR looped primer:
5′-GTCGTATCCAGTGCAGGGTCCGAGGTATTCGCACTGGATACGACaaagtct-3′
QT-PCR forward primer: 5′-TGAGGGGCAGAGAGCGAGACTTT-3′

hsa-miR-486, RT-PCR looped primer:
5′-GTCGTATCCAGTGCAGGGTCCGAGGTATTCGCACTGGATACGACggggctc-3′
QT-PCR forward primer: 5′-TCCTGTACTGAGCTGCCCCGAG-3′
Universal reverse primer: 5′-GGACCCTGCACTGGATACGAC-3′

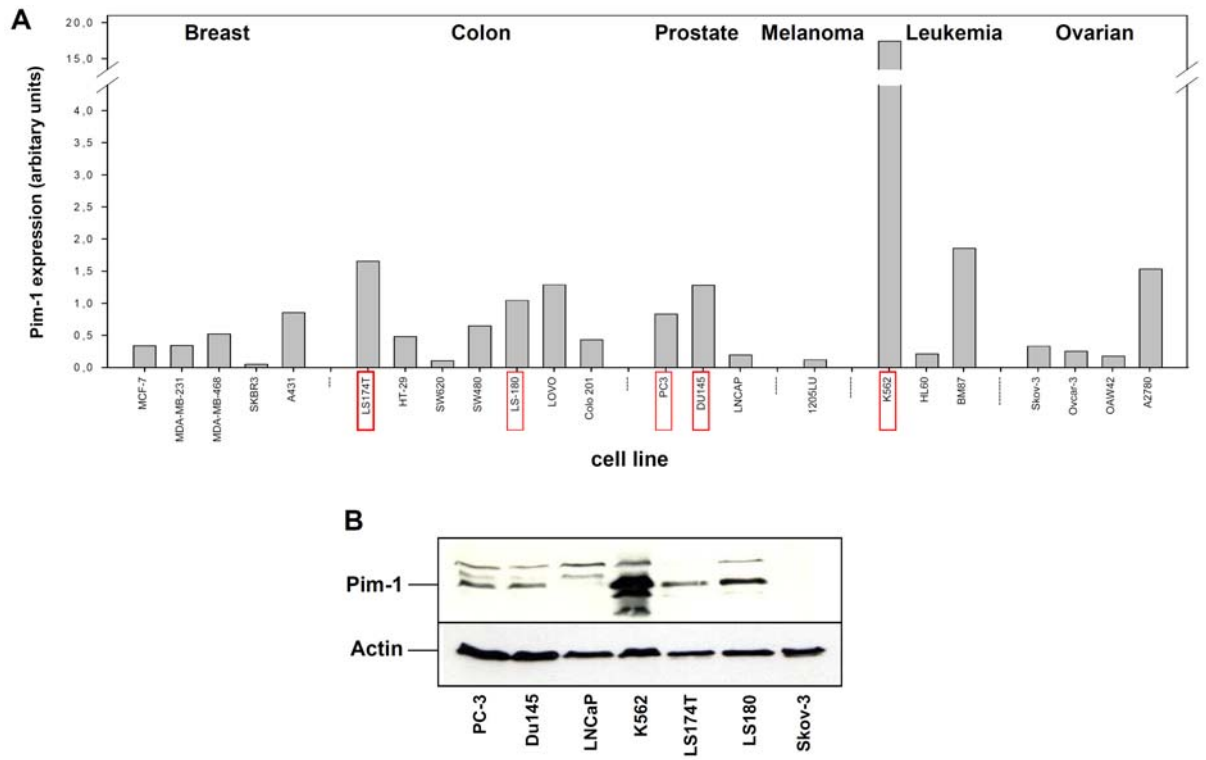

Figure 1

Figure 1: The 3´UTR of Pim-1 harbours a highly conserved miR-33a binding site.

Schematic presentation of the human Pim-1 mRNA. Five conserved target sites for miRNA binding are located in the 3´UTR. The target site for miR-33a is the most conserved site and is in a sequence context predicted to be optimal for miRNA binding (context score percentile of 98 from 100). The seed region (nt 2-8) is fully conserved from human to chicken as well as the central loop region (nt 10-12) and the second pairing region demonstrating that this site is a perfect candidate for the predicted miR-33a binding. For comparison the predicted target site for miR-15a is also shown. Here the target sequence in the Pim-1 3´UTR is less conserved between human and chicken. Moreover, the central loop region and the second pairing region are less evolved thus leading to a lower context score for miRNA binding to this target region.

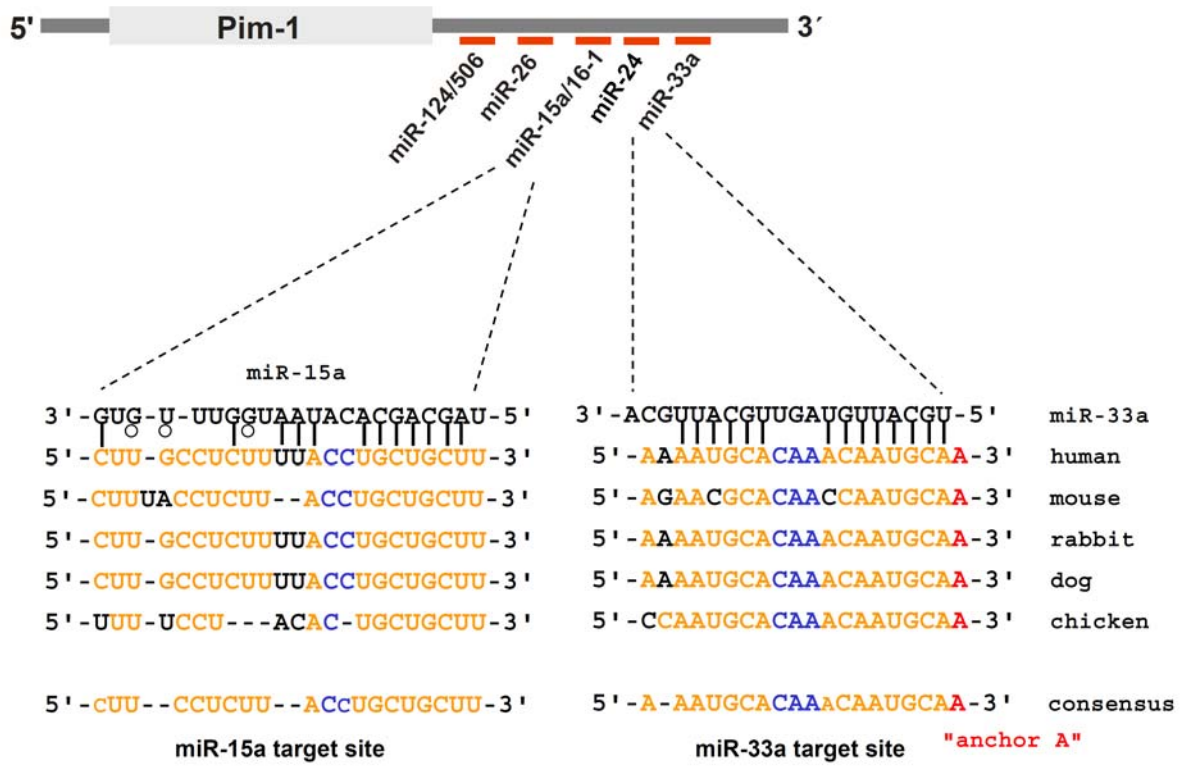

Figure 2

Figure 2: Expression of Pim-1 in selected cancer cell lines.

(A) Screening of 23 different tumor cell lines for Pim-1 expression by quantitative real-time PCR. Highest Pim-1 values were measured in colon and leukaemia cell lines. The red boxed cell lines were further analysed for Pim-1 expression by western blotting. **(B)** Western blot analysis revealed expression of Pim-1 in the indicated cell lines. The erythroleukemia cell line K562 shows highest expression levels of Pim-1. As a loading control beta-Actin was used.

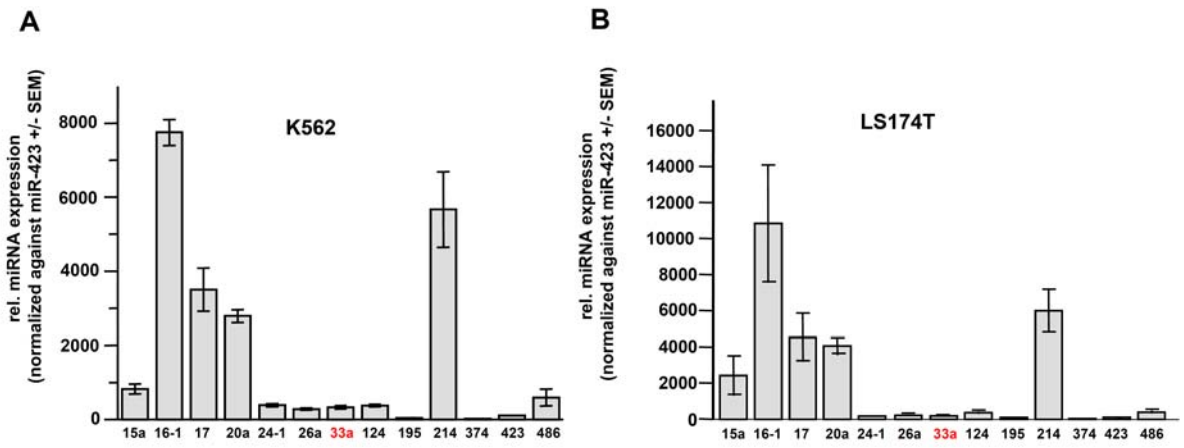

Figure 3

Figure 3: miRNA profiling in K562 and LS174T cells

(A) Expression profiling of selected miRNAs in K562 cells using the looped-primer technique. The miRNA miR-33a is expressed at very low levels whereas other miRNAs (miR-16-1, miR-17-5p, miR-20a and miR-214) are overexpressed. QRT-PCR were normalized against miR-423. Values were obtained from at least three separate experiments. **(B)** Expression profiling of miRNAs in LS174T cells. A similar expression pattern of miRNAs like in K562 cells is found in LS174T cells. Again, miR-33a is only weakly expressed.

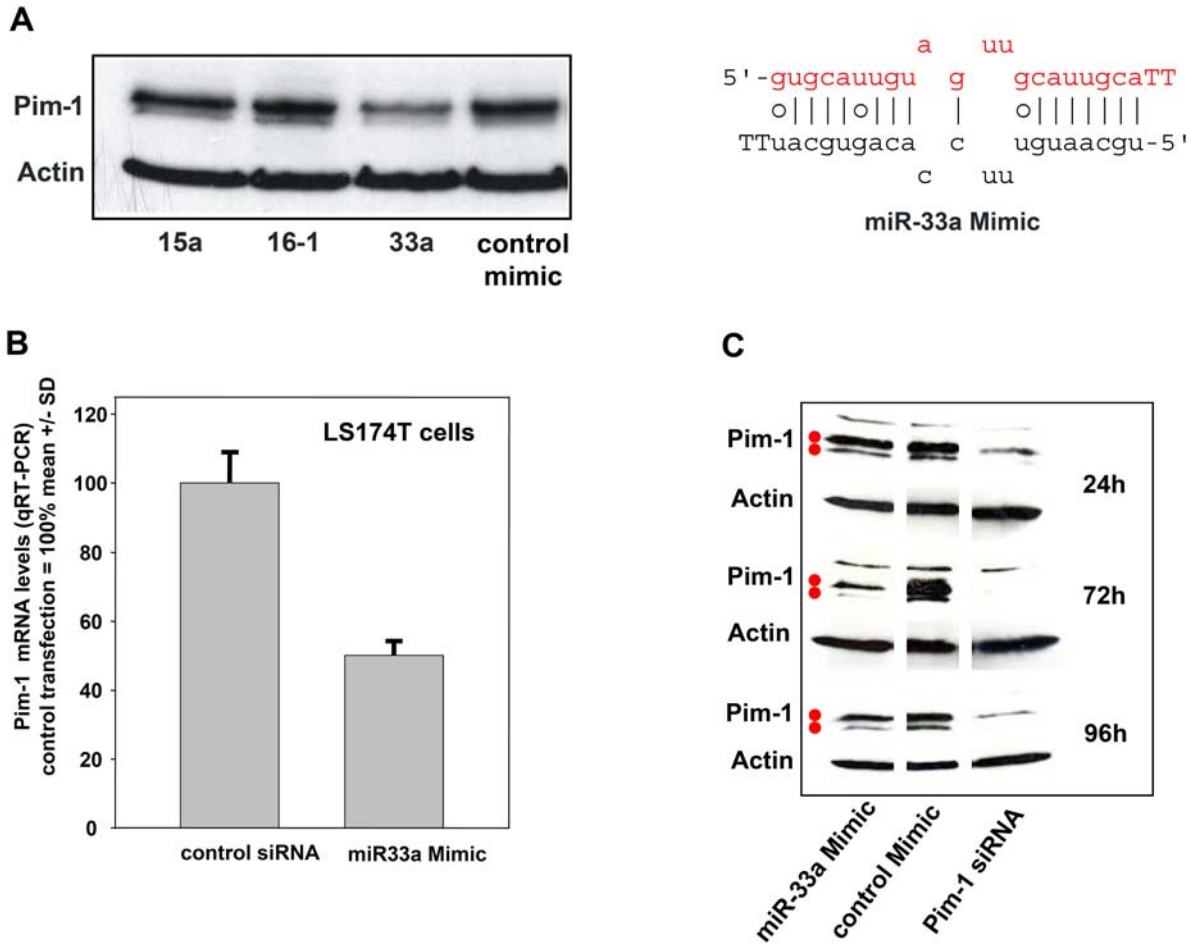

Figure 4

Figure 4: Human Pim-1 is a target for miR-33a.

(A) Pim-1 is downregulated by a transfected miR-33a Mimic in K562 cells whereas transfection of a control Mimic as well as miR-15a and miR-16-1 Mimics have no effect on Pim-1 levels. Probes were separated on 15% SDS-PAA gels and analysed by Western blotting with beta-Actin as a loading control. **(B)** Transfection of the miR-33a Mimic in LS174T cells revealed substantial downregulation of Pim-1 mRNA (~50%) as measured by qRT-PCR. As a control an unrelated siRNA was used. **(C)** Persistance of Pim-1 downregulation by miR-33a Mimic and a Pim-1 specific siRNA is comparable whereas siRNA-dependent downregulation of Pim-1 is more efficient. Again beta-Actin was used as an loading control.

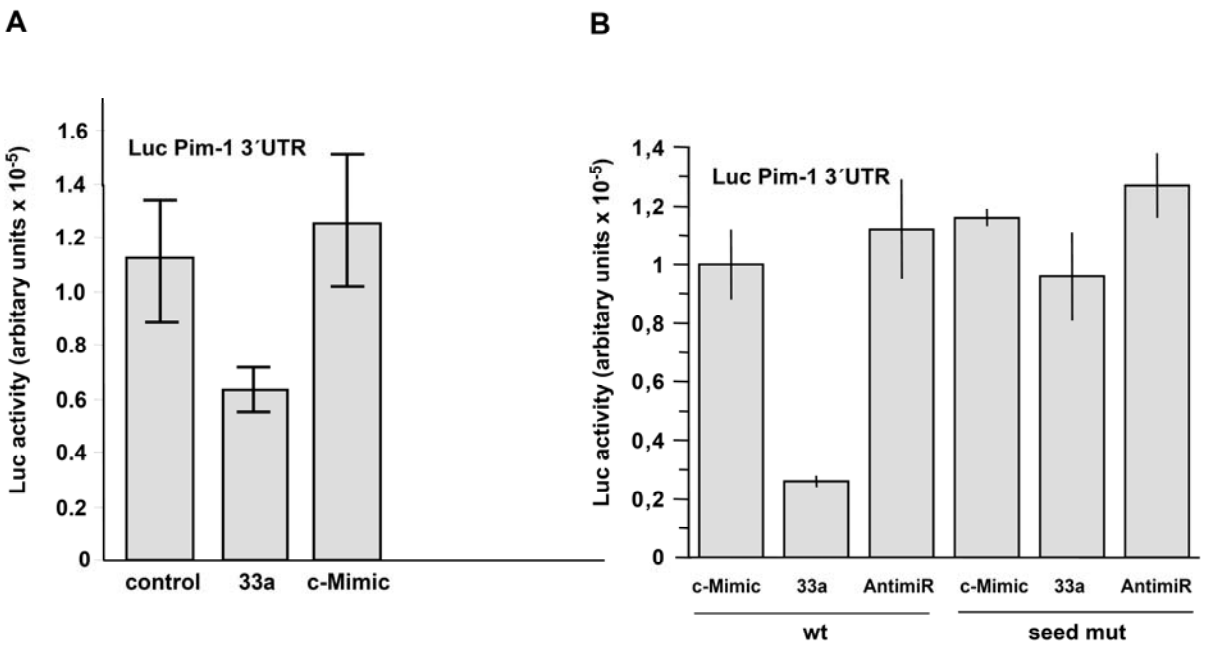

Figure 5

Figure 5: Pim-1 regulation by miR-33a is a direct effect as shown by seed mutagenesis. **(A)** Confirmation of the western blot data by using an luciferase reporter assay containing the 3´UTR of Pim-1. Quantification of the miR-33a Mimic effect on reporter expression reveals a downregulation of about 50%. The control Mimic has no effect on luciferase expression. **(B)** The seed region of the miR-33a binding site was mutated in the luciferase vector that contains the Pim-1 3´UTR. Luciferase assays were performed with wildtype and mutated Pim-1 3´UTRs. Again the repressive effect of a miR-33a Mimic under wildtype conditions is shown. Derepression of luciferase is shown for the mutated construct in the presence of a miR-33a Mimic compared to the wildtype. A slight additional derepression with a miR-33a specific LNA-AntimiR is observed for wildtype as well as mutated seed region. Data shown in panels A and B represent mean values derived from at least three independent experiments; errors bars, S.E.M.

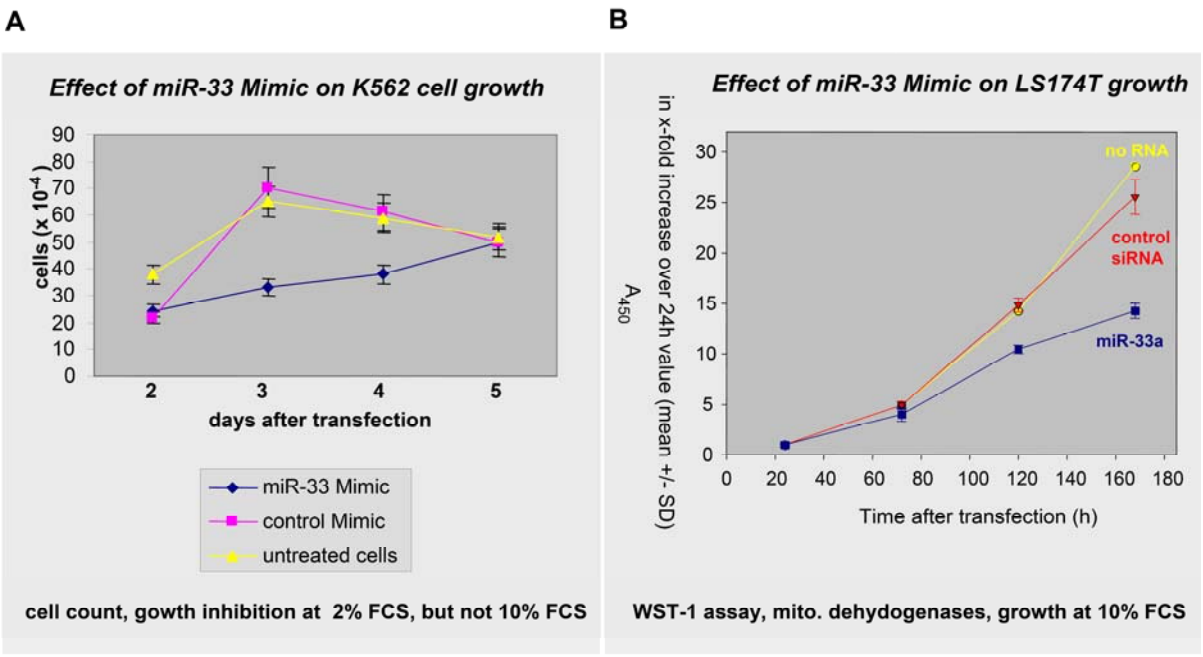

Figure 6

Figure 6: The miR-33a Mimic has an anti-prolliferative effect.

(A) Transfection of the miR-33a Mimic in K562 cells that were cultivated in the presence of 2% FCS shows reduced proliferation rate within three days after transfection. After three days untreated cells or cells transfected with a control Mimic stop their growth under the applied conditions. **(B)** The miR-33a Mimic impair growth of LS174T cells compared to untreated cells or cells transfected with an control siRNA. Data shown in panels A and B represent mean values derived from at least three independent experiments; errors bars, SD.

a,

```
Position 734-740 of PIM1 3' UTR  5'  ...CAAAAAAUGCACAAACAAUGCAA...
                                          ||||||     |||||||
hsa-miR-33b                      3'        CGUUACGUUGUCGUUACGUG

Position 734-740 of PIM1 3' UTR  5'  ...CAAAAAAUGCACAAACAAUGCAA...
                                          ||||||     |||||||
hsa-miR-33a                      3'       ACGUUACGUUGAUGUUACGUG
```

b,

```
Position 175-181 of CDK6 3' UTR  5'    ...UUACUGUUUUGAAAUCAAUGCAA...
                                                    |||||||
hsa-miR-33a                      3'         ACGUUACGUUGAUGUUACGUG

Position 175-181 of CDK6 3' UTR  5'    ...UUACUGUUUUGAAAUCAAUGCAA...
                                                    |||||||
hsa-miR-33b                      3'          CGUUACGUUGUCGUUACGUG

Position 7111-7117 of CDK6 3' UTR 5'  ...UCUUAAGUUUUAUGAAAUGCAAU...
                                                  ||||||
hsa-miR-33b                      3'       CGUUACGUUGUCGUUACGUG

Position 7111-7117 of CDK6 3' UTR 5'  ...UCUUAAGUUUUAUGAAAUGCAAU...
                                                  ||||||
hsa-miR-33a                      3'      ACGUUACGUUGAUGUUACGUG
```

c,

```
Position 6374-6380 of CDK6 3' UTR 5'   ...GAGGUCAGAGUGCCCUGCUGCUG...
                                                     |||||||
hsa-miR-16                       3'       GCGGUUAUAAAUGCACGACGAU

Position 266-272 of CDK6 3' UTR  5'  ...CCAGAAGAAGAGAAGCUGCUGAC...
                                                   ||||||
hsa-miR-214                      3'    UGACGGACAGACACGGACGACA

Position 6372-6378 of CDK6 3' UTR 5'   ...CCGAGGUCAGAGUGCCCUGCUGC...
                                                     |||||||
hsa-miR-214                      3'       UGACGGACAGACACGGACGACA
```

Figure S1: predicted miR-pairing in the Pim-1 and CDK6 3'-UTRs

(A) Pairing of miR-33a and miR-33b to the predicted target site in the Pim-1 3´-UTR. **(B)** Pairing of miR-33a and miR-33b to the respective binding sites in the CDK6 3´-UTR. **(C)** Binding of miR-16 and miR-214 to their predicted target sites in the CDK6 3'-UTR. The TargetScan alignment shows binding of respective miRs to their target sites. It can be seen that for Pim-1, the base-pairing involves two stretches, whereas in CDK6 only binding to the seed region is possible.

Contributions to this manuscript by the author of this thesis:

Construction of the luciferase reporter vector containing the Pim-1 3'-UTR was a collaborative effort with Dorothee Hartmann. Mutated derivatives were generated by the author; also, experiments for figure 2B, 3A, and 5 B including primer design; writing of parts of the materials and methods section; first proofreading of the manuscript and addition of figure S1.

Expression analysis of miR-17-92 cluster in K562 cells

Results

Promoter activity of elements 5´ to the miR-17-92 start site

To evaluate the role of DNA segments 5´ to the miR-17-92 cluster start site, containing a predicted promoter (Neural Network Promoter Prediction v2.2 software, Berkeley Drosophila Genome Project), several regions from this site were cloned from human leukemia cell line K562 into the pGL3 vector where the SV-40 promoter was replaced with those segments. A luciferase gene located 3´ to the segments in this vector allowed easy quantification of activity by luminescence read-out.

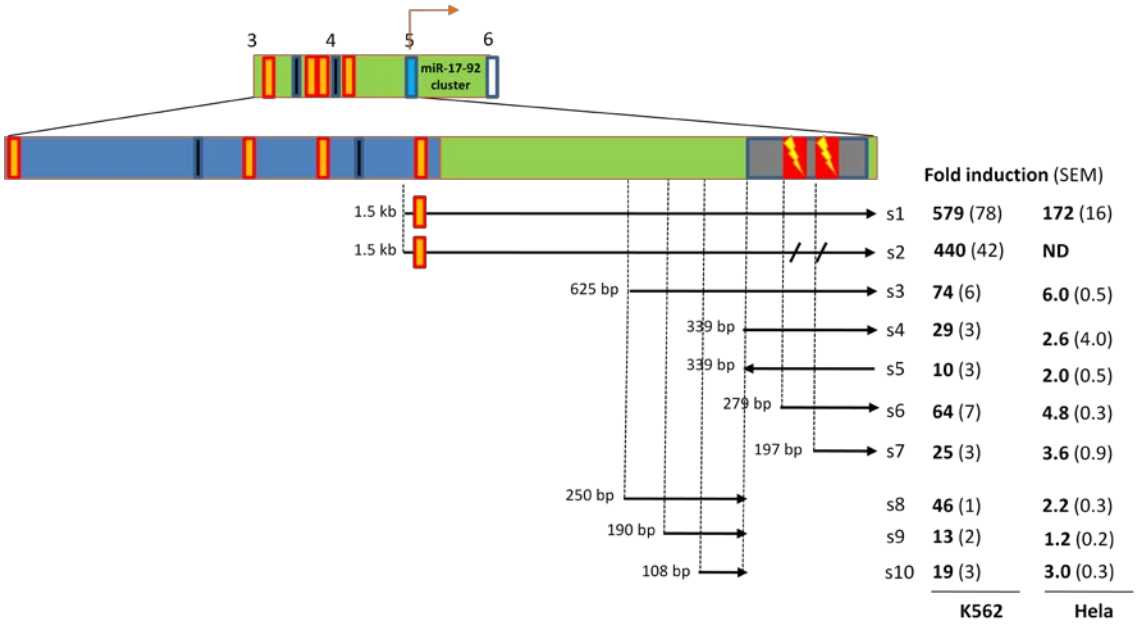

Figure 1. The miR-17-92 cluster is shown with a predicted promoter (light blue, indicated by an arrow) and a 2 kb region upstream of the cluster start site. 1 kb downstream of the cluster start site a polyadenylation site is located. Magnification of the 5´ region is shown below. The first part is constituted of a GC-rich region with a GC-content of more than 80% ending at 1.4 kb in front of the cluster start site (indicated in blue). Within this region 4 c-Myc binding sites can be found (orange boxes) as well as exons 2 and 3 of the MIRHG1 gene (black boxes). The following 1.4 kb are AT-rich (~ 70%) and contain the predicted promoter (grey box) harbouring two non-consensus TATA-boxes (red boxes). Lightning symbols within the TATA-boxes indicate that mutations were introduced at those sites to down-regulate promoter activity of the respective construct (s2). The sequence was changed from 5´-GGCATAAATACGTGTCTAAATGGACCT-3´ to 5´-GGCAGAAACACGTGT-CGAAACGGACCT-3´. The segments cloned are indicated as arrows (denominated s1-s10). Segment s5 is an inverted version of segment s4 to assess directionality of promoter

activity. Segments s1 and s2 contain a single c-Myc binding site. Induction level of each segment is shown on the right side for K562 and for Hela cells [ND, not determined].

For each experiment, 10 µg vector with the respective segment was transfected into K562 cells followed by luciferase read-out after 48 h. From figure 1 it can be seen that segments s1 and s2 containing a single c-Myc binding site show highest level of luciferase induction. In Hela cells, expression of s2-containing vector was not determined. A down-regulation by ~25% is observed for mutation of both TATA-boxes (s2) when analysed in K562 cells. We can see a clear reduction in activity of segments containing a c-Myc binding site (s1 and s2) relative to those not containing such a site (s3-s10). The overall difference between those two groups is about 10-fold. For segments s3–s7 we see a decrease in promoter activity when extending the 5' deletion, the only exception being segment s6, which shows ~2-fold higher activity than the longer segment s4. Segments without the predicted core promoter (s8-s10) show also promoter activity.
In Hela cells, the trends in activity for segments s1-s7 are similar to those observed in K562, although here we see a more pronounced effect of the c-Myc binding-site. That is, in K562 we find a 7.8 times higher induction comparing s1 with s3, and in Hela this factor is 29. Segments s8-s10 show also activity in Hela cells.

Dependency of promoter activity on Pim-1 expression

For determination of the influence Pim-1 exerts on the promoter segments, co-transfection experiments were performed by transfection of respective promoter constructs (10 µg) with siRNAs against Pim-1 (2 µg). As can be derived from figure 2, there is an increase of promoter activity under Pim-1 knockdown conditions. This effect is most prominent for the 1.5 kb segment s1 containing the c-Myc binding site. Here we can see an almost 2-fold increase of activity under Pim-1 knockdown conditions compared to control siRNA co-transfection of this segment. Comparing segment s3 for Pim-1 knockdown and control, we observe an increase of activity by 1.5-fold. The shortest segment shown in this assay is segment s4. Here, the difference in activity is lowest and we see only 1.3-fold induction in comparison with the control. We can clearly infer an upregulation of promoter activity in those cases. Interestingly, when comparing expression levels of the unchanged pGL3 vector harbouring the SV40 promoter, we observe a slight decrease in activity under Pim-1 knockdown conditions (figure 2b). The expression after knockdown is reduced by

approximately 30%. Fragment s6 is the only case where Pim-1 knockdown decreased the expression level.

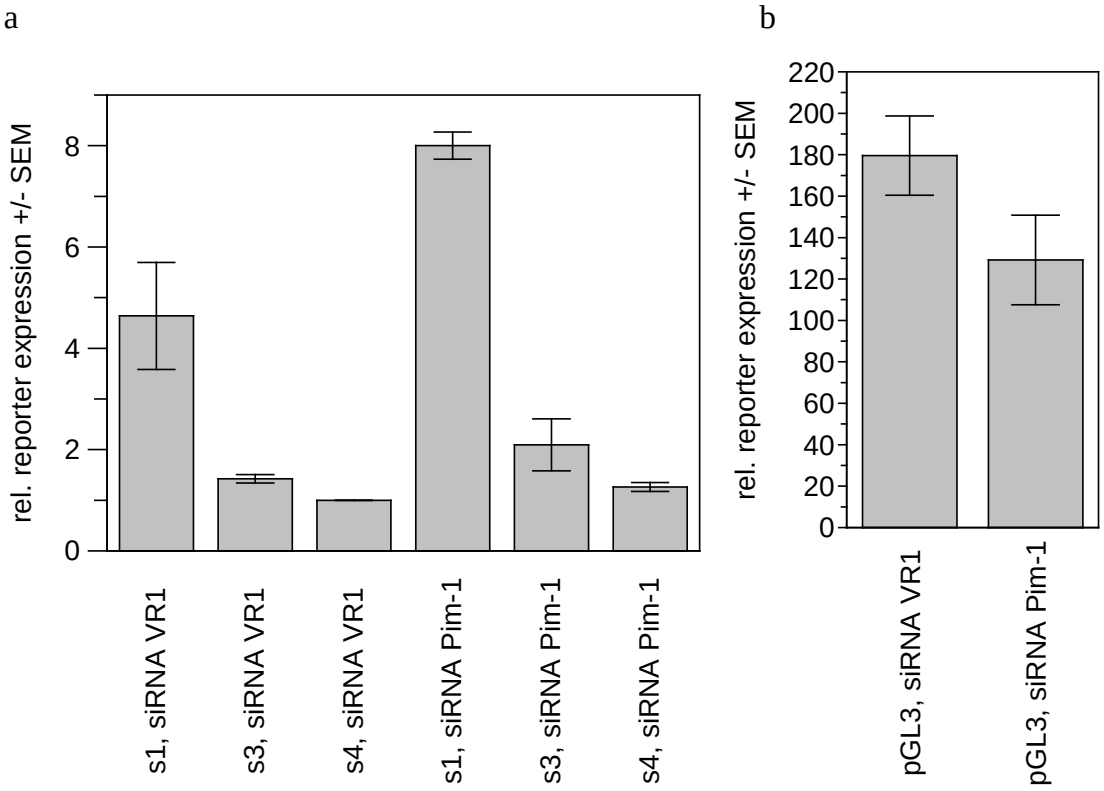

Figure 2. (**a**) Relative expression levels of reporter constructs containing segments s1, s3, and s4 are shown for conditions of Pim-1 knockdown. The 339 bp segment s4 under negative control conditions (VR1 siRNA) was set to 1. The first three bars indicate the activity under normal conditions, whereas the last three bars are the results for Pim-1 knockdown. An increase in promoter activity can be seen under Pim-1 knockdown conditions (for details see text). (**b**) A comparison of the standard pGL3 control vector (carrying the SV-40 promoter) under Pim-1 knockdown and normal conditions is shown. Here we see a decrease in reporter expression in the knockdown setting.

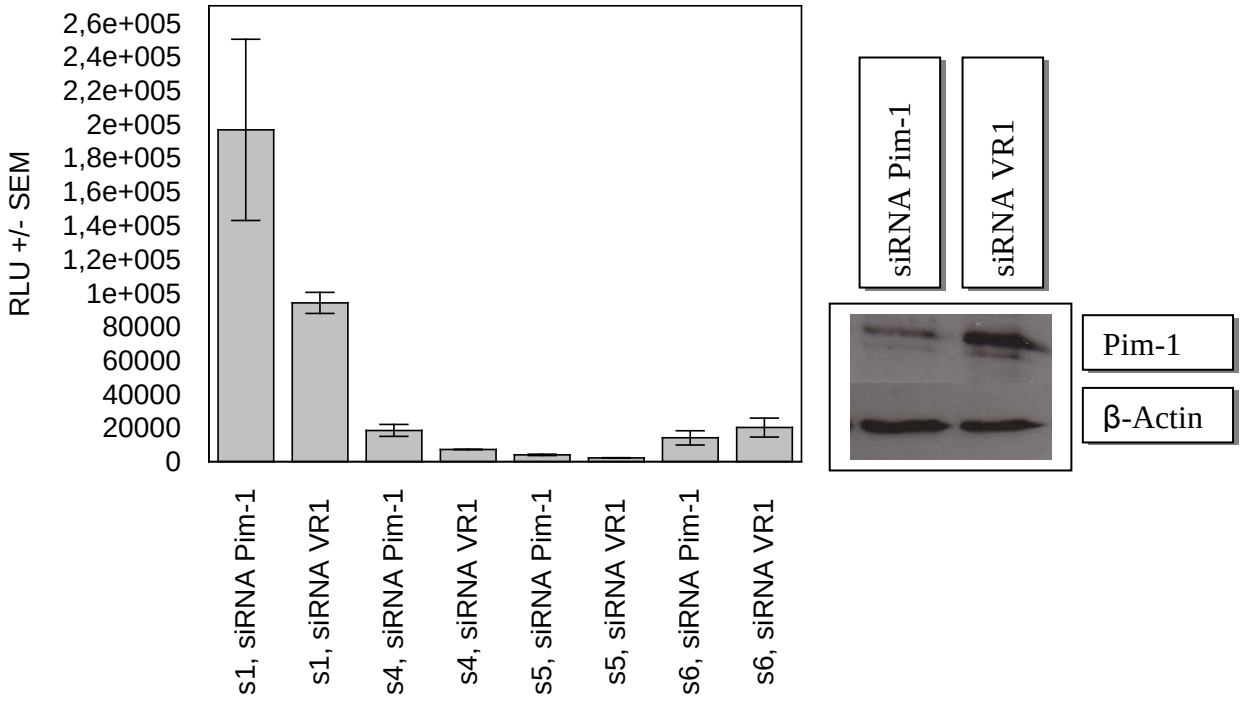

Figure 3. Expression of further miR-17-92 5´ segments is shown here for Pim-1 knockdown conditions. Again, for s1 a 2-fold increase in expression is seen compared to normal conditions. This effect is even higher (2.5-fold) for segment s4. For segment s5 the increase is 1.8-fold. Fragment s6 is the only case where Pim-1 knockdown decreased the expression level. Shown are measured RLUs (relative light units). On the right side, a representative Western blot for Pim-1 knockdown is shown.

Dependency of promoter activity on c-Myc expression

It is known that c-Myc plays a role in expression of the locus containing the miR-17-92 cluster (Chromosome 13, ORF 25; see discussion for details). Here the goal was to evaluate the importance of c-Myc for the cloned regions under consideration (s1-s10). As described above for the Pim-1 knockdowns, c-Myc was silenced in co-transfection experiments. These experiments demonstrate that c-Myc significantly influences the expression of the cloned segment s1 as shown in figure 4. The decrease after knockdown is 3.1-fold for this segment and only 1.5-fold for the 625 bp segment s3 which harbours no c-Myc binding site.

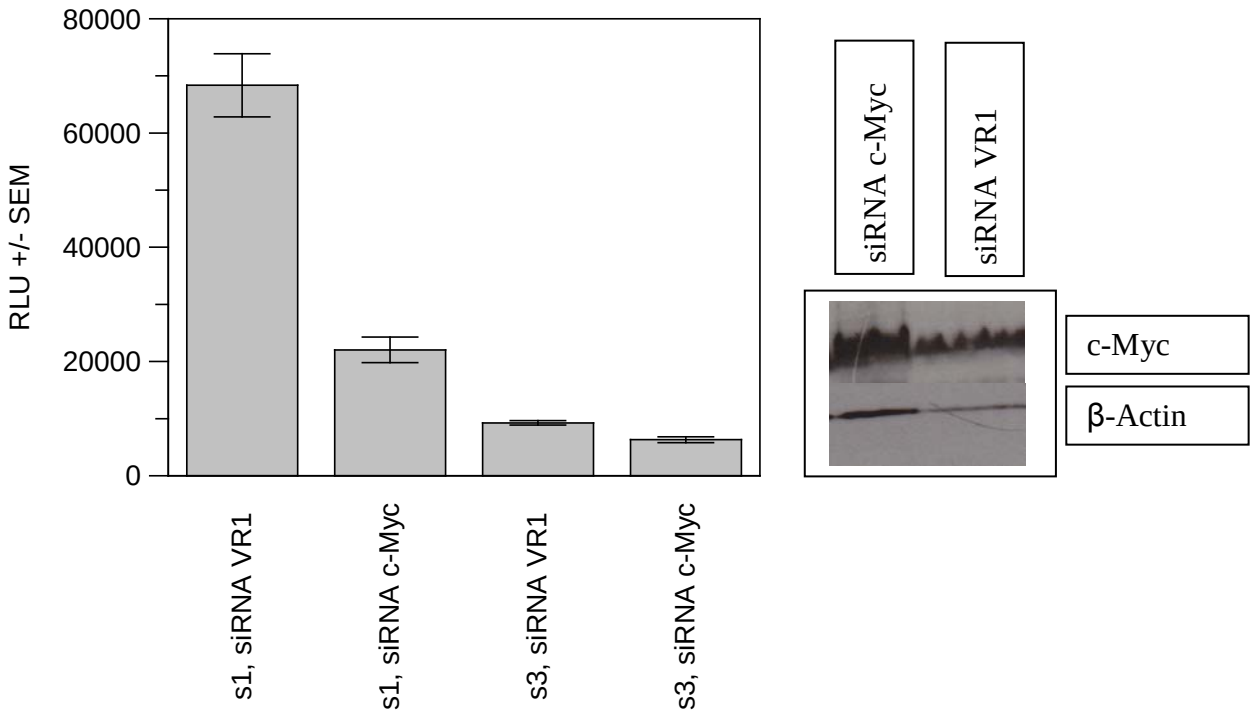

Figure 4. Effects of c-Myc on promoter activity of segments s1 and s3 are shown. The decrease in activity is prominent (3.1-fold) for segment s1 containing a c-Myc binding site, but less pronounced (1.5-fold) for segment s3 lacking the c-Myc site. In the right panel, a representative c-Myc Western blot is shown for respective knockdown experiments.

Effects of Pim-1 knockdown on miR-17-92 expression levels

Here we wanted to investigate the miR-17-92 expression levels after Pim-1 knockdown. For this purpose, K562 cells were transfected with 2 µg siRNA against Pim-1. RNA was prepared 8 h, 24 h, and 48 h after transfection and used for qRT-PCR assays. Those initial experiments were conducted using primers located in exon 4 of the MIRHG1 gene in the locus Chr13Orf25, the expression levels of which were shown to correlate with those of single miRNAs (see discussion). From the data we can infer that the cluster is up-regulated ~2-fold 48 h after Pim-1 knockdown (figure 5). The mild decrease after 8h seems not to be significant if one considers the error bars and also at time point 24 h after transfection the expression level remained essentially unchanged compared to the control.

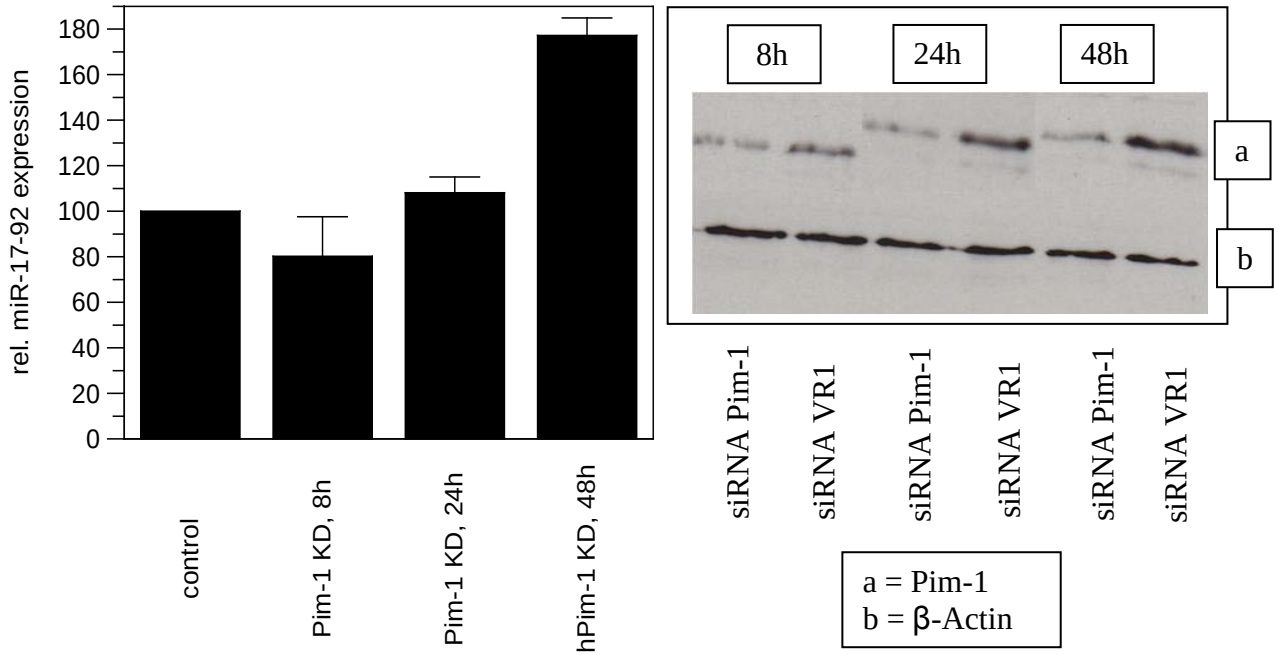

Figure 5. Expression of the miR-17-92 cluster after Pim-1 knockdown. Time points 8 h, 24 h, and 48 h are shown. In the right panel, respective Western blots for the knockdown experiments are depicted.

Chromatin immunoprecipitation against HP1γ

Heterochromatin Protein 1γ (HP1γ) is known to be recruited to sites of histone 3 methylation at lysine 9 (H3K9) due to interaction with its chromo-domain, and thus contributing to silenced states of chromatin. Nevertheless, it was also found that HP1γ associates with actively transcribed genomic regions [1]. Furthermore, evidence for a role of Hp1γ in differentiation and maintenance of cancerous phenotypes was presented by Takanashi et al. [2]. A connection to Pim-1 is evident as it was shown that this kinase phosphorylates HP1γ at its chromo shadow domain (located at the carboxy terminus) leading to an alteration of HP1γ ´s transcriptional repression capacity [3].

Here we wanted to see if such interactions might play a role in regulation of the miR-17-92 cluster. For this reason we tested HP1γ-binding to segments of the miR-17-92 cluster (figure 6a) and found that under Pim-1 knockdown conditions (48 h), binding of HP1γ is altered especially in regions A2-A5 (figure 6b, column "+AB", left and middle panels). Binding in region A1 is less affected. Figure 6b (right panel) shows the binding of Pim-1 to the regions investigated under normal growth conditions. In regions A1, A3, and A5

weak binding is observed, but no binding can be seen for region A2 containing the predicted promoter and part of the 5´ region of the miR-17-92 cluster.

a

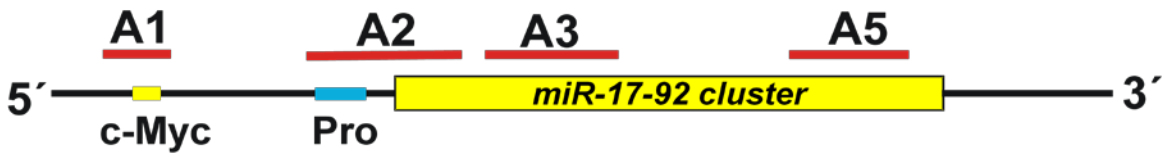

b

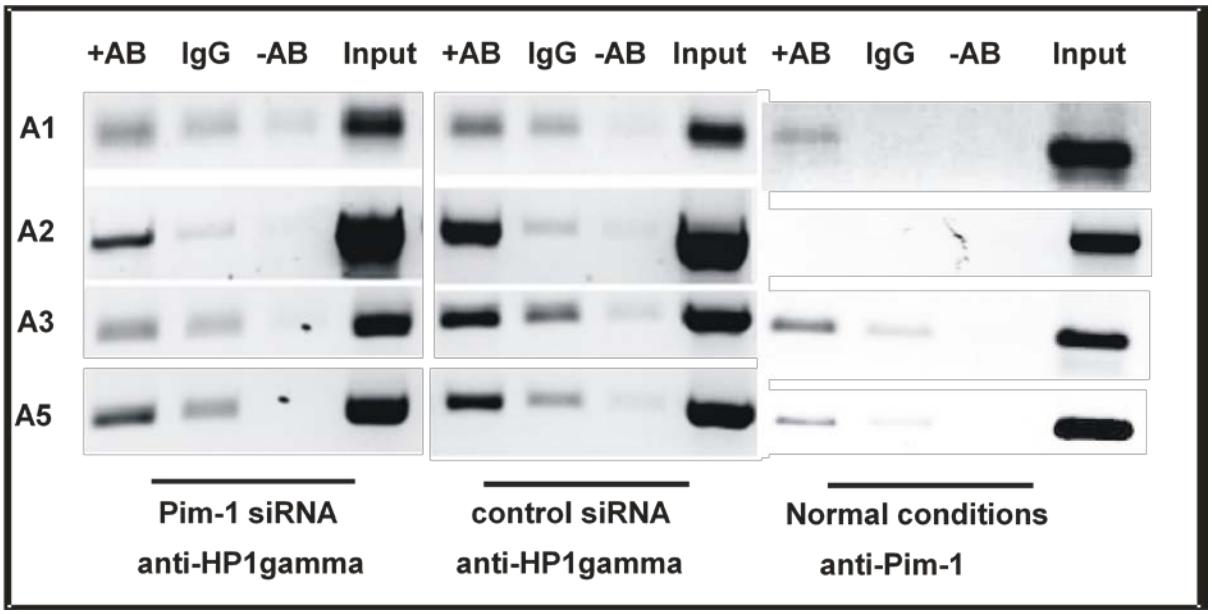

Figure 6. CHIP analysis of regions in front of and within the miR-17-92 cluster. (**a**) Primers for fragment A1 enclose a sequence containing a c-Myc binding site (the same site as in segments s1 and s2). A2 includes the predicted promoter. A3 and A5 include regions within and at the end of the miR-17-92 cluster, respectively. (**b**) Pim-1 knockdown experiments were performed as described and CHIP analysis was done 48h after transfection. In the left panel, effects of knockdown can be seen especially for region A2 (predicted promoter), but also within the cluster (A3 and A5) in terms of reduced HP1γ binding. At region A1 (~1.5 kb upstream of the cluster start site) little effect of Pim-1 knockdown on HP1γ binding is observed compared to controls (middle panel). In the right panel, Pim-1 binding to the respective regions is shown for normal cell culturing and growth conditions where Pim-1 localizes to region A1 and to a lesser extent to regions A3 and A5. It is not found in A2. [+AB: specific antibody; IgG: unspecific antibody; -AB: control without antibody; Input: total lysate before pre-clearing steps]

Discussion

Our interest in the miR-17-92 cluster concerns the relation of its high expression levels in K562 cells [4], and the finding that Pim-1 kinase is also highly expressed in this model system [5, 6]. The anti-apoptotic kinase Pim-1 is a proto-oncogene that promotes tumorigenesis due to synergism with c-Myc [7-9] and may play a role in regulation of this cluster since expression of the cluster is c-Myc-dependent [10-13]. A possibility how Pim-1 may influence cluster regulation is due to its interaction with HP1γ that is phosphorylated at its carboxy terminus (chromo shadow domain) by Pim-1, leading to altered association with heterochromatic genome regions and changes in transcriptional activity [3] (see also model in figure 7).

We have focused our efforts on regions 5´ the miR-17-92 start site, as little is known about it compared to the ORF25 promoter region (see introduction). The Berkeley Drosophila Genome Project offers a promoter prediction tool[1] that identified a putative promoter immediately 5´ to the cluster start site. Furthermore, the 1.4 kb region immediately upstream of the cluster has an AT-content of about 70% which is another clue to transcriptional activity. Matsubara et al. [14] found a polyadenylation site at the end of the miR-17-92 cluster, giving rise to the appealing assumption that the cluster may be transcribed as a transcription unit independent of the ORF25 locus. Our goal was to evaluate the promoter activity of this 5´ region. As seen in our luciferase promoter assays the segments 5´ to the cluster start site show such activity. From comparison of K562 and Hela cells we can conclude that in Hela cells, the c-Myc binding site is more important for regulation of the miR-17-92 cluster than in K562 cells. Also, the lower relative activity of segments s3-s10 in Hela indicates that in this cell line either fewer factors bind to those regions or inhibitory factors are responsible for this observation. Whatever the reason for these differences may be, our data clearly show that the region immediately upstream of the cluster start site harbors regulatory elements that are used in a context-dependent manner, i.e. they depend on cell type. Mutation of non-consensus TATA-boxes in the predicted promoter reduces activity of the respective construct (s2, figure 1) and underlines the importance of this region, albeit not to an extent as was shown for mutation of the locus promoter [15].

[1] Neural Network Promoter Prediction v2.2, http://fruitfly.org

The role of c-Myc on activity of constructs containing a c-Myc binding site is shown in figure 4 for K562 cells. c-Myc silencing strongly reduces activity of this segment (s1). Effects seen in a construct without a c-Myc site (s3) reflect the impact of c-Myc knockdown on cell proliferation and global transcription. It was shown by Venturini et al. [16] that c-Myc knockdown reduces miR-17-92 expression in K562 cells, which could be confirmed in our experiments (data not shown).

Pim-1 was shown to synergistically act with a dimer of the transcription factor c-Myc and its binding partner Max (Myc-associated factor X) leading to an increased transcription from 20% of the c-Myc bound promoters in the human genome. This is due to phosphorylation of histone H3 at serine 10 (H3S10) by Pim-1 [9]. Regarding our data on the segments we cloned and their response to Pim-1 knockdown, it appears unlikely that this mechanism is involved here. Because segment s1 contains a c-Myc binding site, one would expect a decrease in reporter activity but not an increase upon Pim-1 knockdown. Also, for segments s3 and s4 which are much shorter and harbor no c-Myc site, an increase in reporter expression is seen, thus implicating a second, rather inhibitory mechanism of Pim-1 on miR-17-92 expression (figure 2a, figure 3). The fact that expression of the luciferase reporter from the SV-40 promoter is down-regulated after Pim-1 knockdown (figure 2b) could be assigned to the general anti-proliferative effects of such a knockdown (Lange-Grünweller et al., manuscript 1). At the same time, this supports a specific role of Pim-1 in regulation of the miR-17-92 cluster, because the cloned 5´ segments show activation upon Pim-1 knockdown, either containing or not containing c-Myc binding sites. The mechanism of this is not clear, but it appears to be indirect as no binding of Pim-1 is seen in the promoter and start site region of the cluster under normal growth conditions (region A2, figure 6b). At the moment, no data are available on H3S10 phosphorylation for this region that could be assigned to a Pim-1/c-Myc interaction. Thus we focused on HP1γ, the phosphorylation state of which can be altered by Pim-1 and may thus influence its binding to the internal promoter region and expression levels at this site. In our CHIP analysis of HP1γ binding to the cluster region, we see a reduced binding under Pim-1 knockdown settings. This may point to a possible mechanism how Pim-1 may alter chromatin state and thus transcriptional activity at those sites, although we were not able to reveal the direct mediator molecule of Pim-1, i.e. if HP1γ phosphorylation is indeed responsible for the observed behavior, as

phosphorylation-specific antibodies failed to discriminate the bound HP1γ forms (data not shown). Also, as we could show that total HP1γ levels do not change under Pim-1 knockdown (Lange-Grünweller et al., manuscript 1). Quantitative CHIP on Chip may be a strategy to solve this question, if appropriate antibodies are used that can clearly discriminate phosphorylation states of HP1γ.

Under cellular stress conditions, the AT-rich region may be suited to integrate different regulatory signals as e.g. mediated by Pim-1. The miR-17-92 cluster is also upregulated upon growth factor depletion (data not shown). So, possibly conditions exist for which several regions get more important and are controlled by to date unknown mechanisms. For those reasons, we plan to analyze transcription under Pim-1 knockdown settings using qRT-PCR for several regions distributed over the whole locus (Chr13, ORF25; see figure 8).

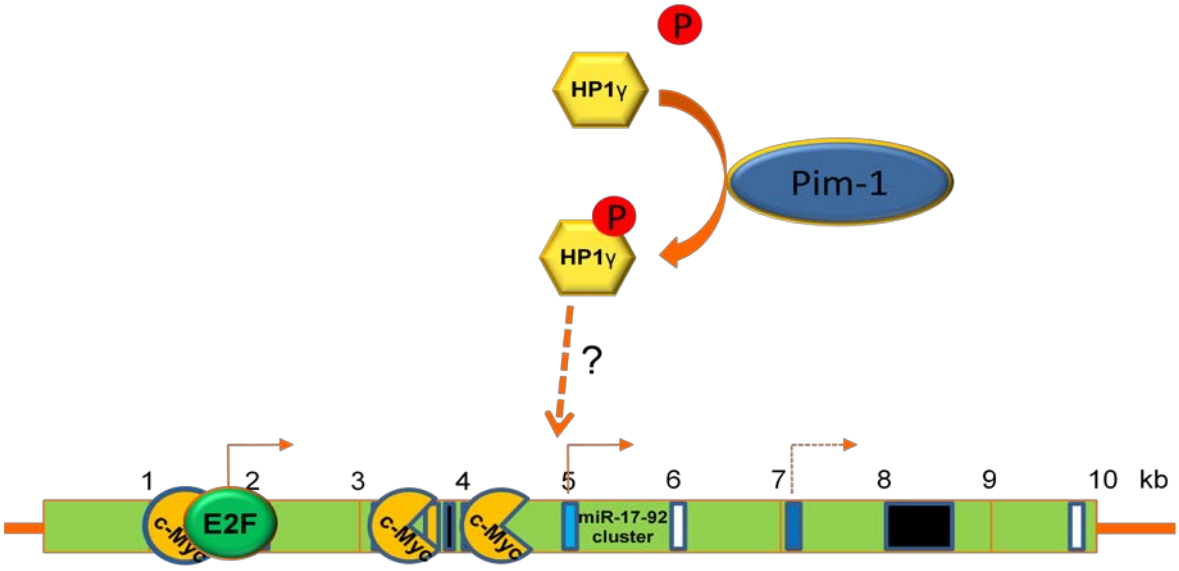

Figure 7. Model of miR-17-92 regulation using an internal promoter. A change in Pim-1 expression may cause alteration in HP1γ binding to regions located immediately 5´ to the miR-17-92 start site. Under Pim-1 knockdown conditions lack of HP1γ phosphorylation is proposed to lead to reduced binding of this chromatin protein, enabling higher efficiency of transcription, especially at the indicated site.

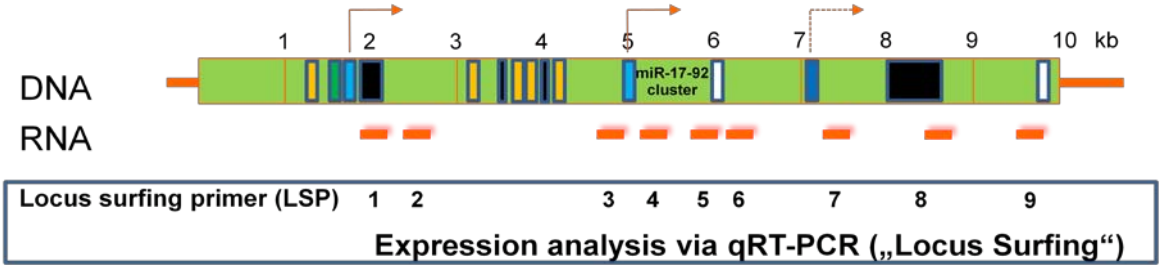

Figure 8. miR-17-92 cluster. RNA from regions indicated with orange boxes will be analyzed in terms of quantitative changes after Pim-1 knockdown. So far, this has only been done for region 8 (see also figure 5).

Conclusions

We showed that a kinase, Pim-1, influences the expression of the miR-17-92 cluster, thus providing another example how the microRNA "world" of the cell is interdigitated with factors and pathways regulating cell proliferation and apoptosis. Chromatin states and chromatin regulation appear to facilitate the expression of the miR-17-92 cluster. Evaluation of mechanisms facilitating stable inheritance of miRNA expression profiles [17] will probably yield new insights for intervention.

Really surprising is the fact that Pim-1 downregulation leads to an increased miR-17-92 expression which was shown to promote tumorigenesis (see introduction), despite the fact that cells proliferate less under such conditions (Lange-Grünweller et al., manuscript 1). An intricate cellular network may thus maintain the cancerous phenotype by anti-apoptosis due to miR-17-92 cluster expression and proliferation due to Pim-1 expression in K562 cells. The upregulation of the cluster under Pim-1 knockdown conditions can thus be seen as an anti-apoptotic response of the cells in case of missing proliferation signals provided by Pim-1. Under serum-deprived conditions, a similar cluster regulation was seen (data not shown). Biologically and especially in the context of a cancer cell this response makes sense as it offers a buffer or time delay until the cell finally commits to apoptosis and opens up the possibility to recover from such short-term deprivations of growth factors.

The connections between players involved in this anti-apoptotic program or delay of apoptosis remain largely unknown, but functional complementation of Pim-1 and miR-17-92 towards maintaining the cancer phenotype is supported by our data.

References

1. Vakoc, C.R., et al., *Histone H3 lysine 9 methylation and HP1gamma are associated with transcription elongation through mammalian chromatin.* Mol Cell, 2005. **19**(3): p. 381-91.
2. Takanashi, M., et al., *Heterochromatin protein 1gamma epigenetically regulates cell differentiation and exhibits potential as a therapeutic target for various types of cancers.* Am J Pathol, 2009. **174**(1): p. 309-16.
3. Koike, N., et al., *Identification of heterochromatin protein 1 (HP1) as a phosphorylation target by Pim-1 kinase and the effect of phosphorylation on the transcriptional repression function of HP1(1).* FEBS Lett, 2000. **467**(1): p. 17-21.
4. Ota, A., et al., *Identification and characterization of a novel gene, C13orf25, as a target for 13q31-q32 amplification in malignant lymphoma.* Cancer Res, 2004. **64**(9): p. 3087-95.
5. Chen, J.L., A. Limnander, and P.B. Rothman, *Pim-1 and Pim-2 kinases are required for efficient pre-B-cell transformation by v-Abl oncogene.* Blood, 2008. **111**(3): p. 1677-85.
6. Hammerman, P.S., et al., *Pim and Akt oncogenes are independent regulators of hematopoietic cell growth and survival.* Blood, 2005. **105**(11): p. 4477-83.
7. van Lohuizen, M., et al., *Predisposition to lymphomagenesis in pim-1 transgenic mice: cooperation with c-myc and N-myc in murine leukemia virus-induced tumors.* Cell, 1989. **56**(4): p. 673-82.
8. Verbeek, S., et al., *Mice bearing the E mu-myc and E mu-pim-1 transgenes develop pre-B-cell leukemia prenatally.* Mol Cell Biol, 1991. **11**(2): p. 1176-9.
9. Zippo, A., et al., *PIM1-dependent phosphorylation of histone H3 at serine 10 is required for MYC-dependent transcriptional activation and oncogenic transformation.* Nat Cell Biol, 2007. **9**(8): p. 932-44.
10. Diosdado, B., et al., *MiR-17-92 cluster is associated with 13q gain and c-myc expression during colorectal adenoma to adenocarcinoma progression.* Br J Cancer, 2009. **101**(4): p. 707-14.
11. Dews, M., et al., *Augmentation of tumor angiogenesis by a Myc-activated microRNA cluster.* Nat Genet, 2006. **38**(9): p. 1060-5.
12. Tagawa, H., et al., *Synergistic action of the microRNA-17 polycistron and Myc in aggressive cancer development.* Cancer Sci, 2007. **98**(9): p. 1482-90.
13. O'Donnell, K.A., et al., *c-Myc-regulated microRNAs modulate E2F1 expression.* Nature, 2005. **435**(7043): p. 839-43.
14. Matsubara, H., et al., *Apoptosis induction by antisense oligonucleotides against miR-17-5p and miR-20a in lung cancers overexpressing miR-17-92.* Oncogene, 2007. **26**(41): p. 6099-105.
15. Woods, K., J.M. Thomson, and S.M. Hammond, *Direct regulation of an oncogenic micro-RNA cluster by E2F transcription factors.* J Biol Chem, 2007. **282**(4): p. 2130-4.
16. Venturini, L., et al., *Expression of the miR-17-92 polycistron in chronic myeloid leukemia (CML) CD34+ cells.* Blood, 2007. **109**(10): p. 4399-405.
17. Lu, J., et al., *MicroRNA expression profiles classify human cancers.* Nature, 2005. **435**(7043): p. 834-8.

Contributions

Project design: **Arnold Grünweller, Roland K. Hartmann**

Experiments, results and cloning for figure 1: Dorothee Hartmann, except for segment s2. Cloning and primer design of s1-s4, Robert Prinz. Results for s1-s4 are in accordance with results generated by Robert Prinz. Primer design s5-s7: Robert Prinz. Primer design s8-s10: Arnold Grünweller.

Experiments for figure 2 and figure 5: Robert Prinz
Experiments for figure 3 and figure 4**:** Dorothee Hartmann.

Figure 6: Arnold Grünweller, (right panel added from another figure by Arnold Grünweller). Experiments by Nicole Bürger, Kerstin Lange-Grünweller. Moana Klein and Lisa Schemberger helped in establishing the CHIP assays.

Appendix

A1 Abbreviations

Abbreviation	Meaning
A	Adenosine
Amp	Ampicillin
APS	Ammonium peroxodisulfat
Bp	Base pair(s)
BPB	Bromophenol blue
BSA	Bovine serum albumine
C	cytosine
DNA	deoxyribonucleic acid
DNase	deoxyribonuclease
dNTP	deoxynucleoside triphosphates
DTT	dithiothreitol
EDTA	Ethylenediamine tetraacedic acid
Fig.	Figure
g	gram
G	guanosine
GNA	Glycol Nucleic Acid
h	hour(s)
HEPES	N-2-Hydroxyethylpiperazin-N'-2-ethane sulfonic acid
KD	Knock down
l	liter
LB	Luria-Bertani
LNA	Locked Nucleic Acid
M	molar [mol/l]
mA	milliampere
Min	Minute
miR	microRNA
miRNA	microRNA
MW	Molecular weight
nt(s)	Nucleotide(s)
NTP	Ribonucleosidtriphosphate
Orf	Open reading frame
p.a.	pro analysis
PAA	Polyacrylamide
PAGE	Polyacrylamid gel elektrophoresis
PCR	Polymerase chain reaction
pmol	Picomol
qRT-PCR	Quantitative Real time PCR
QT-PCR	Quantitative PCR
RISC	RNA-induced silencing complex
RNA	ribonucleic acid
RNAi	RNA interference
RNase	ribonuclease
rpm	rounds per minute
RT-PCR	Reverse transcription PCR

s	second
SDS	Sodium Dodecyl Sulfate
siRNA	Short interfering RNA
T	Thymine
TBE	Tris-Borat-EDTA Buffer
TEMED	N,N,N,N,-Tetramethylethylendiamin
Tm	melting temperature
Tris	Tris-hydroxymethylaminomethan
U	Uridine
XCB	Xylene cyanol blue

A2 Chemicals

All chemicals used are in accordance with p.a. standard.

Substance	**provider**
2- Mercaptoethanol	Roth
Acrylamid (Rotiphorese Gel 30; 37,5:1)	Roth
Agar Agar (high gel strength)	Serva
Agarose GTQ	Roth
Ammonium acetate	Fluka
Ampicillin	Roth
Bovine serum albumin (BSA)	Sigma
Bromophenol blue (BPB)	Merck
Chloramphenicol	Sigma
Chloroform	Merck
Crystal violet	Fluka
Deoxynucleosidtriphosphates (dNTPs)	Fermentas
Dithiothreitol (DTT)	Gerbu
Ethanol p.a. 99.8 %	Roth
Ethidiumbromide	Roth
Glycerol	Gerbu
Glycin	Roth
HEPES-b	Gerbu
Isopropanol p.a.	Roth
Methanol	Roth
Milk Powder blotting grade	Roth
N,N,N‘,N‘-Tetraethylmethylenediamin (TEMED)	Roth
Na Cl_2	Roth
Na SO_4	Roth
Nucleosidtriphosphates (NTPs)	Roche
Peptone	Roth
SDS running buffer (Rotiphorese 10x SDS PAGE)	Roth
SDS ultra pure	Roth
Sodiumacetate	Merck
Tris-(hydroxymethyl)aminomethane	Gerbu
Xylenecyanol blue (XCB)	Serva
Yeast extract (standard grad, low salt)	Gerbu

Tween 20	Roth

A3 Lab Equipment

Plastic consumables for cell culture, bacterial growth and general lab work (PCR tubes etc.) were from Sarstedt. Cell culture plates and plates for luminescence assays were from Greiner Bio-One.

Equipment	**Manufacturer**
Agarose gel chamber	Biorad
Autoclave	Systec V95
Balance	Sartorius
Centrifuge	Hettich universal 320
Centrifuge (cooling function)	Heraeus Fresco 17
Centrifuge (cooling function)	Eppendorf 5810R
Electroporator	Gene Pulser Xcell
Gel documentation system	Cybertech, CS1 with Mitsubishi Video Copy Processor; Biostep, GelSystem MINI
Incubater (humidified)	Nuaire, DHD Autoflow
Incubator Memmert BE400	Memmert
Incubator, shaking	GFL, Model 3033
Lab shaker	IKA, Vibrax-VXR
Lab shaker	Eppendorf Thermomixer 5436
LightCycler 2.0	Roche
Magnetic stirrers	Heidolph
Microscope	Motic AE20
PCR cycler	Biometra TGradient Thermocycler
Photospectrometer	Thermo Biomate 3
Platereader (multiformat)	Tecan, Safire II
Power supply	Bio-Rad Power Pac 3000
Protein Gel chamber	Bio-Rad Mini Protean 3 cell
Quartz cuvette	Hellma 104-QS, 105.202, 115B-QS, 105
Semi dry blotter	C.B.S. Scientific
Shaking incubator	GFL 3033
Sterile bench	Hera Safe KS 15
Thermoblock TB1	Biometra

A4 Software

Microsoft Office 2007, Grafit 3.04, NEBCutter 2.0, miRBase (http://www.mirbase.org/), Manipulate and Display a DNA Sequence (http://arbl.cvmbs.colostate.edu/molkit/manip/), Berkeley Drosophila Genome Project - Neural Network Promoter Prediction v2.2 (March 1999) (http://www.fruitfly.org/seq_tools/promoter.html), EMBOSS Pairwise Alignment Algorithms (http://www.ebi.ac.uk/Tools/emboss/align/index.html), Integrated DNA Technologies Oligo Analyzer 3.1 (http://eu.idtdna.com/analyzer/Applications/OligoAnalyzer/), TargetScanHuman 5.1 (http://www.targetscan.org/).

A5 Primer List

Primers for cloning Pim-1 3´-UTR

5´-GCTCTAGAGCTGTCAGATGCCCGAGGG-3
Name: Inv. hPim-1 3´UTR F CCE
5´-GCTCTAGAGCAATAAGATCTCTTTTATTCCCCTGT-3´
Name: Inv. hPim-1 3´UTR F CCE

GC pairs are introduced for more efficient restriction. This was done according to instructions from NEB.

Primer for mutagenesis of **Pim-1 3´-UTR** miR-15/16seed

5´-TTGCCTCTTTTACC*TGGTGGT*TCTCCAAAAATCTG-3´
Name: Pim1 mir-15a mut f1
5´-CAGATTTTTGGAGA*ACCACCA*GGTAAAAGAGGCAA-3´
Name: Pim1 mir-15a mut r1

Primer for mutagenesis of **Pim-1 3´-UTR** miR-33 seed

5´-AAAAAATGCACAAA*CAGTGCGA*TCAACAGAAAAGCT-3´
Name: Pim1 mir-33a mut f1
5´-AGCTTTTCTGTTGA*TCGCACTG*TTTGTGCATTTTTT-3´
Name: Pim1 mir-33a mut r1

Primers for cloning p21 3´-UTR

5´-GCTCTAGAGCCCTCAAAGGCCCGCTCTA-3´
Name: Invitrogen p21 3´UTR F (CCE)
5´-GCTCTAGAGCGGAGGAGCTGTGAAAGACACA-3´
Name: Invitrogen p21 3´UTR R (CCE)

Primer for mutagenesis of **p21 3´-UTR** miR-17/20a seeds

5´-GAAGTAAACAGATG*GGACTGT*GAAGGGGCCTCACC-3´
Name: mir17/20a mut F1
5´-GGTGAGGCCCCTTC*ACAGTCC*CATCTGTTTACTTC-3´
Name: mir17/20a mut R1

5´-CTCCCCAGTTCATT*GGACTGT*GATTAGCAGCGGAA-3´
Name: mir17/20a mut F2
5´-TTCCGCTGCTAATC*ACAGTCC*AATGAACTGGGGAG-3´
Name: mir17/20a mut R2

Primers for cloning of putative miR-17-92 promoter regions

5´-ATATAGATCTTGCCGCCGGGAAACGGGTT-3´ AGATCT BglII restr. site
5´-ATAT overhang for more efficient restriction
Name: miR-17-92 f1

5´-ATATAGATCTCTACGCGGAGAATCGCAG-3´ AGATCT BglII restr. site
5´-ATAT overhang for more efficient restriction
Name: miR-17-92 f2

5´-ATATAGATCTCTTTAGACAATGTACCTTTTCTG-3´ AGATCT BglII restr. site
5´-ATAT overhang for more efficient restriction
Name: miR-17-92 f3

5´-ATATAAGCTTCCATACAAATTCAGCATAATCCCTAATGG-3´
AAGCTT HindIII restr. Site 5´-ATAT overhang for more efficient restriction
Name: miR-17-92 r1

Primer for mutagenesis of putative TATA boxes in miR-17-92 promoter region

5´-TAAAGAATTCTTAAGGCAGAAACACGTGTCGAAACGGACCTCATA-TCTTTG-3´
Name: PROMO 17-92 MUT F

5´-CAAAGATATGAGGTCCGTTTCGACACGTGTTTCTGCCTTAA-GAATTCTTTAC-3´
Name: PROMO 17-92 MUT R

Mir-17-92 LOCUS Expression-Profile Analysis: LOCUS SURFING PRIMERS

5´-CTCCGGTCGTAGTAAAGCGCAGG-3´ Name: LSP 1 b F
5´-CAGGAGGAGTAGCCGCCACC-3´ Name: LSP 1 b R
FRAGMENT: 90 bp

5´-TGCCGCCGGGAAACGGGTT-3´ Name: LSP 2F
5´-GCAGTTTAGGAACAGAAGACC-3´ Name: LSP 2R
FRAGMENT: 198

5´-GTGTGGCAGCCGCATCTGGCTG-3´ Name: LSP 2 b F
5´-CTCGGGAGAAACTTTCCTACCCAGAG-3´ Name: LSP 2 b R
FRAGMENT: 269 bp

5´-GGAAGAGCCACCACTTCCAGT-3´ Name: LSP 3 F
5´-CCATACAAATTCAGCATAATCCCTAATGG-3´ Name: LSP 3 R
FRAGMENT: 160 bp

5´-GTTGTTAGAGTTTGAGGTGTTAATTCTAAT-3´ Name: LSP 4a F
5´-GGTCACAATCTTCAGTTTTACAAGGTG -3´ Name: LSP 4a R
FRAGMENT 93 bp

5´-ACTGCAGTGAAGGCACTTGT -3´ Name: LSP 4b F (A3)
5´-TGCCAGAAGGAGCACTTAGG-3´ Name: LSP 4b R (A3)
FRAGMENT: 167bp

5´-GATCGGTTGCAATGCTGTGTTTC-3´ Name: LSP 5 F
5´-TGTATCTTGTACATTTAACAGTGGAAGTCG-3´ Name: LSP 5 R
FRAGMENT: 140 bp

5´-*GCGTGTCAGATTTGGCAGTAT*-3´ Name: LSP 6 F
5´-CAGAGCGGCATTCTCTCTAAATT-3´ Name: LSP 6 R
FRAGMENT: 242 bp

5´-*CCTGAGAAAAAACAACTTTGACCCTTG*-3´ Name: LSP 7 F
5´-GAAAGTTGTACATGCAAACGCC -3´ Name: LSP 7 R
FRAGMENT: 160 bp

5´-CAGTAAAGGTAAGGAGAGCTCAATCTG-3´ Name: LSP 8 F (Scherr)
5´-TCAGATTATTCTTTAGCTTAGTGGTTGTATG -3´ Name: LSP 8 R (Scherr)
FRAGMENT: 115 bp

5´-*GGGTCATTAGGAAAATGCACATATTCCATG*-3´ Name: LSP 9 F
5´-CTCAAACAGCCAGACCAAACTG-3´ Name: LSP 9 R
FRAGMENT: 150 bp

Sequencing Primers

pGL3 vector: Sequences provided by the manufacturer were used. Longer constructs needed sequencing from within. Sequences can be found below.

Pim-1
5´-TCTCCAAAAATCTGCCTGGGTT-3´ Primer for sequencing of the 3´-UTR
Name: Pim-1 3rd

p21
5´-TCCTCTAAGGTTGGGCAGGG-3´ 3rd Primer for sequencing of the 3´-UTR
Name: p21 3´UTR 3rd seq primer

miR-17-92
For long constructs, sequences from cloning of shorter fragments were used for sequencing reaction.

Looped Primers for RT-PCR of mature miRNAs

Primers named “QT” are forward primers for the quantitative PCR that are equal to the mature miRNA sequence. Primers named “loop” are primers used in RT-PCR reactions.

5´-GTCGTATCCAGTGCAGGGTCCGAGGTATTCGCACTGGATACGACctacctg-3´
Name: mir-20a loop 01
5´-TAAAGTGCTTATAGTGCAGGTAG-3´
Name: mir-20a QT 01

5´-GTCGTATCCAGTGCAGGGTCCGAGGTATTCGCACTGGATACGACctacctg-3´
Name: mir-17 loop 01
5´-CAAAGTGCTTACAGTGCAGGTAG-3´
Name: mir-17 QT 01

5´-GTCGTATCCAGTGCAGGGTCCGAGGTATTCGCACTGGATACGACtgcaatg-3´
Name: mir-33a loop 01
5´-GTGCATTGTAGTTGCATTGCA-3´
Name: mir-33a QT 01

5´-GTCGTATCCAGTGCAGGGTCCGAGGTATTCGCACTGGATACGACcacaaac-3´
Name: mir-15a loop 01
5´-TAGCAGCACATAATGGTTTGTG-3´
Name: mir-15a QT 01

5´-GTCGTATCCAGTGCAGGGTCCGAGGTATTCGCACTGGATACGACcgccaat-3´
Name: mir-16-1 loop 01
5´-TAGCAGCACGTAAATATTGGCG-3´
Name: mir-16-1 QT 01

5´-GTCGTATCCAGTGCAGGGTCCGAGGTATTCGCACTGGATACGACagcctat-3´
Name: mir-26a loop 01
5´-TTCAAGTAATCCAGGATAGGCT-3´
Name: mir-26a QT 01

5´-GTCGTATCCAGTGCAGGGTCCGAGGTATTCGCACTGGATACGACggcattc-3´
Name: mir-124-1 loop 01
5´-TAAGGCACGCGGTGAATGCC-3´
Name: mir-124-1 QT 01

5´-GTCGTATCCAGTGCAGGGTCCGAGGTATTCGCACTGGATACGACaaagtct-3´
Name: mir-423 loop 01
5´-TGAGGGGCAGAGAGCGAGACTTT-3´
Name: mir-423 QT 01

5´-GTCGTATCCAGTGCAGGGTCCGAGGTATTCGCACTGGATACGACcacttat-3´
Name: mir-374a loop 01
5´-TTATAATACAACCTGATAAGTG-3´
Name: mir-374a QT 01

5´-GTCGTATCCAGTGCAGGGTCCGAGGTATTCGCACTGGATACGACggggctc-3´
Name: mir-486 loop 01
5´-TCCTGTACTGAGCTGCCCCGAG-3´
Name: mir-486 QT 01
5´-GTCGTATCCAGTGCAGGGTCCGAGGTATTCGCACTGGATACGACagtacat-3´
Name: mir-144 loop 01
5´-TACAGTATAGATGATGTACT-3´
Name: mir-144 QT 01

5´-GTCGTATCCAGTGCAGGGTCCGAGGTATTCGCACTGGATACGACatacata-3´
Name: mir-1-1 loop 01
5´-TGGAATGTAAAGAAGTATGTAT-3´
Name: mir-1-1 QT 01

5´-GTCGTATCCAGTGCAGGGTCCGAGGTATTCGCACTGGATACGACgccaata-3´
Name: miR-195 loop 01
5´-TAGCAGCACAGAAATATTGGC-3´
Name: miR-195 QT 01

5´-GTCGTATCCAGTGCAGGGTCCGAGGTATTCGCACTGGATACGACactgcct-3´
Name: miR-214 loop 01
5´-ACAGCAGGCACAGACAGGCAGT-3´
Name: miR-214 QT 01

5´-GTCGTATCCAGTGCAGGGTCCGAGGTATTCGCACTGGATACGACttcaaaa-3´
Name: miR-424 loop 01
5´-CAGCAGCAATTCATGTTTTGAA-3´
Name: miR-424 QT 01

5´-GTCGTATCCAGTGCAGGGTCCGAGGTATTCGCACTGGATACGACacaaacc-3´
Name: miR-497 loop 01
5´-CAGCAGCACACTGTGGTTTGT-3´
Name: miR-497 QT 01

5´-GTCGTATCCAGTGCAGGGTCCGAGGTATTCGCACTGGATACGACctgttc-3´
Name: miR-24-1 loop 01
5´-TGGCTCAGTTCAGCAGGAACAG-3´
Name: miR-24-1 QT 01

5´-GGACCCTGCACTGGATACGAC-3´ Reverse primer for all QT-PCR reactions.
Name: uni loop rev QT 01

A6 Map of pGL3control vector

Reproduced data sheet from Promega.

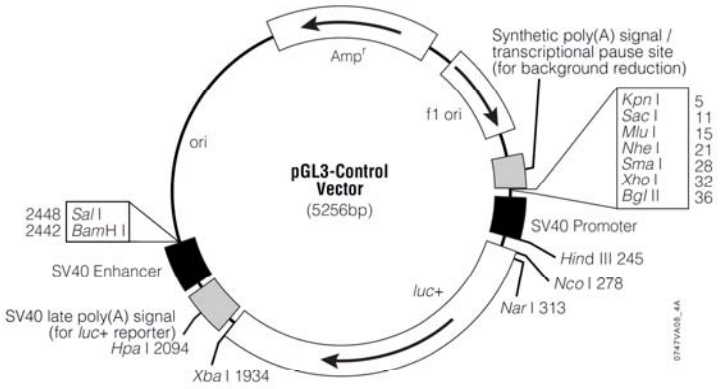

Figure 4. pGL3-Control Vector circle map. Additional description: *luc+*, cDNA encoding the modified firefly luciferase; Amp^r, gene conferring ampicillin resistance in *E. coli*; f1 ori, origin of replication derived from filamentous phage; ori, origin of replication in *E. coli*. Arrows within *luc+* and the Amp^r gene indicate the direction of transcription; the arrow in f1 ori indicates the direction of ssDNA strand synthesis.

pGL3-Control Vector Sequence Reference Points:

Multiple cloning region	1–41
SV40 Promoter	48–250
Luciferase gene (*luc+*)	280–1932
GLprimer2 binding site	281–303
SV40 late poly(A) signal	1964–2185
SV40 Enhancer	2205–2441
RVprimer4 binding site	2499–2518
*Col*E 1-derived plasmid replication origin	2756
β-lactamase gene (Amp^r)	3518–4378
f1 origin	4510–4965
Synthetic poly(A) signal	5096–5249
RVprimer3 binding site	5198–5217

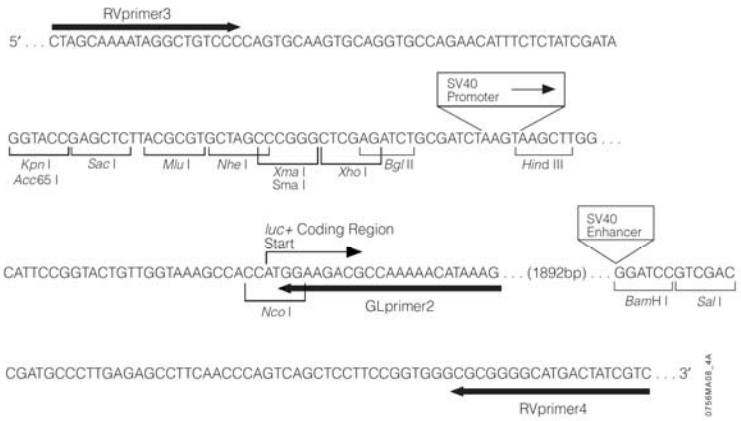

Figure 5. pGL3 Vector multiple cloning regions. The upstream and downstream cloning sites and the location of the sequencing primers, GLprimer2, RVprimer3 and RVprimer4 are shown. The large primer arrows indicate the direction of sequencing. The positions of the promoter (in the pGL3-Promoter and pGL3-Control Vectors) and the enhancer (in the pGL3-Enhancer and pGL3-Control Vectors) are shown as insertions into the sequence of the pGL3-Basic Vector. (Note that the promoter replaces four bases [AAGT] of the pGL3-Basic Vector.) The sequence shown is of the DNA strand generated from the f1 ori.

Promega Corporation · 2800 Woods Hollow Road · Madison, WI 53711-5399 USA · Toll Free in USA 800-356-9526 · Telephone 608-274-4330 · Fax 608-277-2516 · **www.promega.com**
Printed in USA. Part# TM033
Revised 4/02 Page 5

Acknowledgements

Thanks go to Prof. Dr. Roland K. Hartmann for support and making possible this work and carefully reading the manuscript, to Dr. Arnold Grünweller for moral and practical support over the time of this thesis. Both of them provided insightful discussions and project design of this work. I am grateful to Dr. Arnold Grünweller for preparation of manuscript 1 and manuscript 2. Furthermore, I want to thank Dr. Markus Gößringer, Dr. Dan Li, Dr. Michael Weber, and Benedikt Beckmann for tips and tricks. For good cooperation in the lab, I want to thank all current and former members of the group.

I am also grateful to our collaboration partner Prof. Dr. Achim Aigner for his valuable input and discussions.

Curriculum vitae

Robert Prinz

Born	1981, June, 19th Marburg, Germany

Studies, Biology

10/2001 – 08/2006	Philipps University Marburg, Faculty of Biology Main emphasis: Genetics, Pharmacology, Parasitology Diploma Thesis at the Philipps University School of Medicine, Marburg, Department of Pharmacology and Toxicology, Group Prof. F. Czubayko / Prof. A. Aigner Project: Polymer-based targeting approaches

Additional activities

12/2004 - 09/2005	Clinical Research Group Chronic Airway Diseases, Department of Internal Medicine (Respiratory Medicine) Philipps University, Group Prof. H. Fehrenbach Project: "TransMIT-Projektbereich für Experimentelle Histopathologie". Analysis of lung tissue using CAST-based microscopy.

PhD Student

10/2006 -12/2009	Philipps University Marburg, Faculty of Pharmacy, Department of Pharmaceutical Chemistry Group: Prof. R.K. Hartmann Projects: - Regulation of miR-17-92 cluster in K562 cells - Regulation of Pim-1 Kinase - LNA-based Targeting approaches

Additional activities

2007-	Rechenkraft.net e.V., Marburg, Germany Projects: - Supporting science via distributed computing (DC)

Marburg, December 2009

Publications

Theses

Diploma Theses

PEI-F25-LMW als Transfektionsreagenz für DNA und siRNA sowie seine Anwendung im Targeting von VEGF mittels siRNA in Prostatakarzinomzellen

Philipps University Marburg, 2006

Paper

- S. Höbel, R. Prinz, A. Malek, B. Urban-Klein, J. Sitterberg, U. Bakowsky, F. Czubayko, A. Aigner, Polyethylenimine PEI F25-LMW allows the long-term storage of frozen complexes as fully active reagents in siRNA-mediated gene targeting and DNA delivery, European Journal of Pharmaceutics and Biopharmaceutics (2008), doi: 10.1016/j.ejpb.2008.03.014

- Several manuscripts in preparation

Presentations

Voraussetzungen für Leben unter extremen Bedingungen
Volkssternwarte Marburg e.V., 2006

Zelluläre Kommunikation – Von Zeichen, Repräsentationsvorgängen und dem „Selbst einer Zelle“
Guest lecture „Vorlesung Bio-Kommunikation II - Krebs und Kommunikation”, University of Salzburg, 2009

Cells as semiotic systems – practical and quantitative implications
Biosemiotic Gatherings 2009, Prague

Misc

Preparatory board „Cancer and Communication” Conference 2009, *Salzburg*

Book review “Reviving the Living” *Angew. Chem. Int. Ed. 2009, 48, 5237 – 5238*

Book review “Reviving the Living” *Angew. Chem. 2009, 121, 5339 – 5340 (German)*

7 Selbstständigkeitserklärung

Ich versichere, dass ich meine Dissertation

Regulation of proto-oncogenic Pim-1 kinase and miR-17-92 microRNA cluster in the human leukemia cell line K562

selbstständig, ohne unerlaubte Hilfe angefertigt und mich dabei keiner anderen als der von mir ausdrücklich bezeichneten Quellen und Hilfen bedient habe.
Die Dissertation wurde in der jetzigen oder einer ähnlichen Form noch an keiner anderen Hochschule eingereicht und hat noch keinen sonstigen Prüfungszwecken gedient.

Marburg, 16.12.2009